from "Investigation of Rates and Mechanisms of Reactions", 4th edition, C. F. Bernasconi, Ed., John Wiley & Sons, New York, 1986, Part 1, p. 13.

OFFPRINTS FROM INVESTIGATIONS OF RATES AND MECHANISMS OF REACTIONS, VOLUME 6, PART 1, 4/e
Edited by Dr. Bernasconi

Chapter I

TRANSITION STATE THEORY

Maurice M. Kreevoy and Donald G. Truhlar

1 INTRODUCTION

Transition state theory [1] provides a basic conceptual framework for the interpretation of chemical reaction rates, and this chapter presents an introduction to this theory and its applications. Transition state theory is also sometimes called activated complex theory; we use the former name consistently without implying any distinction. We also use the convenient label transition state theory (TST) to refer to various generalized transition state theories, such as variational transition state theory, when it is unnecessary to make the distinction.

Transition state theory is an inherently approximate theory. It is an object of this chapter to show what the approximations are, what are their possible consequences for conclusions that may be drawn from the theory, and how the concepts of the theory may be used both for detailed calculations and for semiempirical modeling. We hope to show that TST (and its generalizations), despite its approximations, is useful for illuminating the main features of the pathways by which chemical reactions occur. Indeed, for most such purposes, TST is the only available approach that provides useful information.

2 ASSUMPTIONS AND DERIVATIONS

Transition state theory was first advanced historically for bimolecular reactions, and this class of reactions presents the most straightforward application of the theory. In order to focus most clearly on the assumptions of the theory we first consider its application to gas phase bimolecular reactions.

2.1 Definition of a Transition State

If the reactants have N atoms, that is, the number of atoms in reactant A plus the number in reactant B is N, then the system AB may be described in terms of $3N$ coordinates and $3N$ conjugate momenta; the $6N$-dimensional space of these variables is called phase space. A transition state is a hypothetical system localized to a phase-space hypersurface that divides the reactant region of phase space from the product region. The transition state is described by a $(6N - 2)$-dimensional subspace of the full phase space; the two missing dimensions are the reaction coordinate and its conjugate momentum.

The above definition encompasses both conventional and generalized transition states. A conventional transition state hypersurface is independent of momenta and may be defined by a $(3N-1)$-dimensional hypersurface in the $3N$-dimensional coordinate space. Furthermore, a conventional transition state hypersurface passes through a saddle point on the potential energy surface of the AB system. In the usual case a normal mode analysis at the saddle point for a gas phase reaction yields $(3N-7)$ real frequencies for internal vibrational motions, one imaginary frequency corresponding to the reaction coordinate, and six zero frequencies that correspond to translation and rotation of the whole system. The conventional choice of the transition state is obtained by omitting the normal mode associated with the imaginary frequency. Since normal modes are orthogonal in mass-weighted or mass-scaled atomic cartesians, where the weight or scale factor for each atomic cartesian is proportional to the square root of the mass of the atom, the missing coordinate is orthogonal to the transition state hypersurface in a mass-weighted or mass-scaled cartesian coordinate system at the saddle point. The missing coordinate is called the reaction coordinate s and its conjugate momentum is called p_s. Except at the saddle point, the definition of the reaction coordinate is not unique. It will be considered further in Sections 2.2.3 and 4.1.

In later discussions it is often convenient to refer to the transition state hypersurface in phase space as simply the transition state dividing surface or the transition state (TS).

2.2 Gas Phase Bimolecular Reactions

Transition state theory may be presented in terms of macroscopic quasithermodynamic quantities like the concentration of activated complexes and the free energy of activation and then translated to the molecular level by the methods of statistical thermodynamics. Alternatively, it may be derived at the molecular level by considering phase-space bottlenecks to the flow of phase points from reactants to products. At the detailed dynamical level, TST may be derived from two assumptions, an equilibrium assumption and a dynamical bottleneck assumption. The equilibrium assumption is discussed in detail in Section 2.2.1. The bottleneck assumption is fundamentally classical so we restrict our discussion to classical mechanics in Sections 2.2.2 and 2.2.3, where we discuss transition state theory in terms of the concepts mentioned above. The molecular level derivation leads to a variational criterion that may be used

to improve the accuracy of the dynamical bottleneck assumption, and this is presented in Section 2.2.3. Although the fundamental assumption of transition state theory is a classical mechanical one, quantum effects are very important and must be included for qualitatively correct results. This is done in Sections 2.2.4 and 2.2.5. Section 2.2.6 discusses TST activation parameters.

2.2.1 Equilibrium Assumption

The equilibrium assumption of TST, sometimes called the quasi-equilibrium assumption, is that TS species which originated in the reactant region of phase space are assumed to be present in equilibrium with reactants, not just in total amount but also in the way they are distributed in the transition state hypersurface in phase space (or, in quantum mechanical language, in their distribution of internal state populations). To clarify this, consider a reaction

$$A + B \rightarrow C + D \tag{R1}$$

where A, B, C, and D denote atoms or molecules and where we assume that the temperature of the system is maintained constant throughout the reaction. For the forward reaction we can distinguish several different rate constants. The most common is the phenomenological rate constant k_1 defined by the following equation

$$-\frac{d[A]}{dt} = +\frac{d[C]}{dt} = k_1[A][B] - \frac{k_1}{K}[C][D] \tag{1}$$

where [A], [B], ... denote concentrations and K is the equilibrium constant for reaction (R1). (The distinction between concentrations and activities is not of concern here.) It is an almost universal fact that, after a transient period which is usually too short to be studied, the simple kinetic order rate law Eq. (1) is observed to hold for any elementary reaction (R1). In fact, when Eq. (1) does not hold, one typically postulates a more detailed mechanism involving intermediates or excited state species and analyzes the experimental data by a complex rate law derived by assuming simple kinetic order rate laws for the individual steps. This is reasonable and has been empirically very successful. As pointed out by Denbigh [2] though;

> there is no specifically thermodynamic reason why the measured rate law must be expressible as a difference of two terms.... The existence of the two terms must therefore be given an interpretation which is *kinetic*, and it has become customary to regard the observed reaction rate as being equal to the difference of the rates in the forward and backward directions, these processes taking place simultaneously at the molecular level. This interpretation is entirely in harmony with a collisional picture of the mechanism; at the same time there is clearly an element of convention in identifying the two terms with the forward and backward rates.

In fact, this identification is an oversimplification [3–5]. We can define one-way flux coefficients by

$$k_1^f \equiv \sum_\alpha \sum_\beta P_\alpha^A P_\beta^B k_{\alpha\beta} \tag{2}$$

$$k_{-1}^f \equiv \sum_\gamma \sum_\delta P_\gamma^C P_\delta^D k_{\gamma\delta} \tag{3}$$

where P_α^A is the probability that A is in state α, defined by a complete set of quantum numbers; $k_{\alpha\beta}$ is the reaction rate constant for collisions of A in state α with B in state β; and so forth. Note that $k_{\alpha\beta}$ is well defined in terms of reaction cross sections [5]. Then we can also write

$$-\frac{d[A]}{dt} = +\frac{d[C]}{dt} = k_1^f[A][B] - k_{-1}^f[C][D] \tag{4}$$

which superficially resembles Eq. (1). However, the essence of Eq. (1) is that k_1 is independent of extent of reaction, that is, of time. In contrast, even during the period where Eq. (1) holds, k_1^f and k_{-1}^f may change dramatically (because P_α^A, P_β^B, P_γ^C, and P_δ^D are not constants). Thus k_1^f and k_{-1}^f are not the quantities extracted from a phenomenological analysis using Eq. (1). Note also that the ratio k_1^f/k_{-1}^f is also in general a function of extent of reaction, tending to K only as the system approaches chemical equilibrium.

A common assumption in collision theory [6–14] is that the rate constant may be calculated from Eq. (2) with P_α^A and P_β^B replaced by their Boltzmann equilibrium values $P_\alpha^{A,eq}$ and $P_\beta^{B,eq}$. This is called the local equilibrium assumption [4]. If the internal energy transfer rates in A and B are very fast compared to the reaction rate (because nonreactive inelastic collisions of A and B with each other or third bodies are much more probable than reactive collisions of A with B), then P_α^A and P_β^B will approximately equal their equilibrium values at the given temperature and k_1^f will be constant with the value

$$k_1^e = \sum_\alpha \sum_\beta P_\alpha^{A,eq} P_\beta^{B,eq} k_{\alpha\beta} \tag{5}$$

This will be called the local equilibrium approximation to the rate constant or the equilibrium flux coefficient, or, for short, the equilibrium rate constant. There are two possible sets of circumstances under which we can be sure that k_1^e is a good approximation to the phenomonological rate constant k_1; both sets of circumstances require that reaction is slow compared to internal relaxation so that k_1^f is also equal to k_1^e. Then k_1 equals k_1^e if also [5] either (1) the transients decay [so that Eq. (1) holds with constant k_1] before back reaction is appreciable, or (2) back reaction is slow compared to internal relaxation of products so that k_{-1}^f also equals k_{-1}^e. Note that it is possible for k_{-1}^f to be constant and equal k_{-1}^e but k_1^f not to be constant and k_1 not to equal k_1^e. Note also that the local equilibrium assumption of transition state theory is expected to be most valid for slow reactions for which the reaction process cannot deplete the Boltzmann distribution of reactive states faster than internal relaxation processes can reestablish it.

As stated at the beginning of this section, in transition state theory we assume an equilibrium distribution of those transition states that originated as reactants. What is often not appreciated is that this is entirely equivalent to the local equilibrium assumption of collision theory. In classical mechanics the equivalence of these assumptions may be considered to be a straightforward consequence [15, 16] of Liouville's theorem [17–20] by which a system in thermal equilibrium in one region of phase space will evolve into a thermal equilibrium system in other regions of phase space. Thus if reactants are at equilibrium, transition state species originating as reactants will be in equilibrium; transition state species originating as products may be at equilibrium too, or they may be in nonequilibrium or even missing. The equivalence of the collision-theory and transition-state-theory equilibrium assumptions has been argued clearly by Anderson [21, 22] and Miller [11], and the reader is referred to their contributions for further discussion.

In summary, the equilibrium assumption of transition state theory is equally as valid as that of collision theory. Both are most valid if reaction is slow compared to the internal relaxation processes that repopulate reactive states.

Quantitative estimates of the error caused by the equilibrium assumption for fast reactions are not as readily available as one would wish. For translational equilibrium there have been several studies. A typical result is that of Present and Morris [23] who estimated an error of 8% or less for cases where the translational threshold energy is $5RT$ or more, where R is the gas constant and T is temperature. Reliable estimates for faster reactions are harder to obtain. For vibrational and rotational equilibrium, the extent and effect of nonequilibrium in the reactants can in principle be ascertained by solving the set of coupled state-to-state rate equations (commonly known as the master equation) involving all reactant and product state-to-state energy transfer and reaction rates, but the only attempt known to us to make a realistic estimate for a reasonably fast reaction is the study of $Cl + HBr \rightarrow HCl + Br$ at room temperature, a case for which the activation energy is about $1.3RT$ [24]. That study yielded one regime of phenomenological kinetics for which the local equilibrium assumption holds very well and another for which there is a correction factor of a factor of three.

2.2.2 Conventional Transition State Theory

In the previous section we discussed the fact that collision theory, as usually applied, and transition state theory involve the same equilibrium assumption. But they yield different results because they involve different assumptions for the dynamics. Collision theory attempts to calculate [12] or approximate [9, 13, 14] the global dynamics from reactant to product by numerically following the evolution of specific collisions, either by individual trajectories [9, 13] or quantum mechanical wave functions [12, 14]. Transition state theory, in contrast, avoids the calculation of global dynamics by making a dynamic bottleneck assumption. The dynamic bottleneck assumption has been called the fundamental assumption of transition state theory [11, 25, 26]. As should be

clear from the discussion in this section, another good name for it is the no-recrossing assumption.

The transition state theory approximation to the rate constant of reaction (R1) will be called $k_1^{\ddagger}$. The simplest derivations of transition state theory, which are readily available in textbooks [1], begin with the equation

$$-\frac{d[\mathrm{A}]}{dt} = \tfrac{1}{2}\nu[\delta]_e \tag{6}$$

where δ denotes an extended transition state species, $[\delta]_e$ the equilibrium concentration of this species, the factor of one half yields the equilibrium concentration of this species with reaction-coordinate momentum directed toward products, and ν is the probability that a single δ with reaction-coordinate momentum directed toward products does proceed to products in unit time. In terms of the reaction coordinate s introduced in Section 2.1, the extended transition state species δ is defined to include a finite range of s as corresponding to the transition state, and one calculates $[\delta]_e$ by the equilibrium assumption as

$$[\delta]_e = K_1^{\delta}[\mathrm{A}][\mathrm{B}] \tag{7}$$

where K_1^{δ} is an equilibrium constant corresponding to this definition of δ. Calculating ν and K_1^{δ} with a consistent transition state definition yields the standard result [which will be presented below, Eq. (9) or (13)]. This derivation makes the dynamic bottleneck assumption clear: The assumption is that all transition state species with their reaction-coordinate momentum directed toward products do convert to products and represent portions of trajectories that start as reactants, pass through the transition state only once, and proceed to products. If these trajectories did not start as reactants and end as products, they do not contribute to k_1^e and transition state theory will err when it counts them. Since transition state theory only counts transition state species with reaction-coordinate momenta directed toward products, it will not count any trajectories that start as products, cross the transition state once, and proceed to reactants, but it will incorrectly count or overcount trajectories that start as reactants, cross the transition state toward products, but later recross, or those that start as products, cross the transition state, and then recross toward products. Now consider the trajectories that do start as reactants and end as products. Since the transition state has been defined to divide reactants from products in phase space, these trajectories must cross it an odd number of times. If, however, the same trajectory crosses three or more times, transition state theory will err by counting the two or more forward crossings, whereas the whole trajectory clearly contributes only one net forward crossing to the equilibrium flux coefficient k_1^e. Putting all these considerations together we see that in classical mechanics, transition state theory is exact if the local equilibrium assumption is valid and if no trajectory recrosses the transition state, but it errs otherwise. In fact, we note for use in Section 2.2.3 that if the local equilibrium

assumption and classical mechanics are valid, transition state theory always overestimates the rate constant because it overcounts the reactive trajectories, that is, it counts all forward-crossing trajectories so it does not miss any contributions to the equilibrium flux coefficient k_1^e, but if recrossing occurs, it counts some trajectories that do not contribute to k_1^e, and/or it overcounts some trajectories that do. Thus, classical mechanical transition state theory provides an upper bound to the classical mechanical equilibrium rate constant [27–31].

The above method of derivation of $k_1^\ddagger$ is simple and correct, but the consistent calculation of ν and K_1^δ involves manipulations that may appear approximate. For example, many derivations involve the assumption that the potential is approximately constant or parabolic over a finite width δ of the reaction coordinate. Since δ cancels out in the final answer, one suspects that the derivation could be made more manifestly rigorous by carefully taking limits as $\delta \to ds$. This is indeed the case. In that limit the transition state becomes infinitesimally narrow, that is, it becomes a hypersurface in phase space as we have defined it here. (Mathematically one can restrict a system to a hypersurface by using Dirac delta functions.) Derivations [10a, 11, 28–33] that do not involve a fictitious formal partition function for the reaction coordinate treated as a free translation or motion over a parabolic barrier are preferable. Such derivations make it clearer that the equilibrium one-way flux from reactants to products through a transition state dividing surface is given precisely by

$$R_1^f = k_1^\ddagger[\mathrm{A}][\mathrm{B}] \tag{8}$$

where $k_1^\ddagger$ is the standard transition-state-theory rate expression. This dynamic interpretation of $k_1^\ddagger$ as the flux through a surface [25] is more suitable for discussing the validity and breakdown of transition state theory than is the quasi-equilibrium interpretation implicit in Eqs. (6) and (7), but the latter is valuable for suggesting the quasi-thermodynamic activation parameters (discussed in more detail in Section 2.2.6) that are very useful for interpreting and correlating reaction rates in solution. Both interpretations are valid; in fact, they are equivalent. Both interpretations lead to the following standard result [now we drop the subscripts denoting reaction (R1)]:

$$k^\ddagger = \frac{\tilde{k}T}{h}\frac{\Phi^\ddagger}{\Phi^{\mathrm{A}}\Phi^{\mathrm{B}}}\exp\frac{-V^\ddagger}{RT} \tag{9a}$$

$$= \frac{\tilde{k}T}{h}\frac{Q^\ddagger}{\Phi^{\mathrm{R}}_{\mathrm{rel}}Q^{\mathrm{A}}Q^{\mathrm{B}}}\exp\frac{-V^\ddagger}{RT} \tag{9b}$$

where $\tilde{k}$ is the Boltzmann constant, h is Planck's constant, Φ^{X} is the partition function per unit volume of X (where X = A, B, or ‡, and ‡ excludes the reaction coordinate), $Q^\ddagger$ is the internal partition function of the transition state (excluding overall translation and the reaction coordinate), $\Phi^{\mathrm{R}}_{\mathrm{rel}}$ is the translational parti-

tion function per unit volume [2a, 34] for reactant relative motion, Q^A and Q^B are internal partition functions of individual reactants, and $V^\ddagger$ is the potential energy (per mole) of the saddle point. Equation (9b) is obtained from Eq. (9a) by canceling out the partition function for overall translation of the whole system in the numerator and denominator. In Eq. (9) and elsewhere in this chapter the zero of potential energy is chosen as that of the reactants in their classical equilibrium position, and symmetry factors are omitted.

Another useful form of the TST rate constant is

$$k^\ddagger = (\tilde{k}T/h)K^\ddagger \tag{10}$$

Here we should note the difference between K^δ in Eq. (7), which includes a finite region of s in the transition state, and $K^\ddagger$, which excludes the reaction coordinate. Equation (10) may be obtained from the derivation based on Eqs. (6) and (7) by noting that the reaction-coordinate part of the statistical mechanical expression for $\frac{1}{2}K^\delta$ combines with ν to yield $\tilde{k}T/h$. Alternatively, Eq. (10) may be considered a definition of $K^\ddagger$. Since $Q^\ddagger$ excludes one internal degree of freedom, it is not the internal partition function for any real species, and $K^\ddagger$ is correspondingly not the equilibrium constant for any real reaction; $K^\ddagger$ may be called a quasi-equilibrium constant. The quasi-thermodynamic activation parameters, such as free energy of activation and enthalpy of activation, are derived from $K^\ddagger$ by analogy to the relation between changes in real thermodynamic variables and real equilibrium constants. The fact that this is merely a convention should always be kept in mind lest too much reality be attributed to these quasi-thermodynamic parameters. Nevertheless, with this caveat, they can often be usefully related to structural and/or mechanistic features of reactions. By analogy of $K^\ddagger$ to a real equilibrium constant, we define the (standard state) free energy of activation as

$$\Delta G^{\ddagger,0} = -RT \ln(K^\ddagger/K^{\ddagger,0}) \tag{11}$$

where $K^{\ddagger,0}$ is the transition state reaction quotient evaluated at the standard state. For reaction (R1) the transition state reaction quotient is $[\ddagger]/[A][B]$, and K^0 is therefore the reciprocal of the standard state concentration (see Sect. 2.2.6 for an explicit formula). Combining Eqs. (10) and (11) yields

$$k^\ddagger = (\tilde{k}T/h)K^{\ddagger,0} \exp(-\Delta G^{\ddagger,0}/RT) \tag{12}$$

2.2.3 Generalized Free Energy of Activation; Variational Theory

We have seen that in classical mechanics $k^\ddagger$ is always greater than or equal to the local equilibrium rate constant k^e. If the local equilibrium approximation is valid, the best approximation to the phenomenological rate constant k can be obtained by choosing the transition state to minimize $k^\ddagger$; this is called the variational theory of reaction rates or variational transition theory [11, 26, 29–31, 33]. It is equivalent to maximizing the free energy of activation in the

quasi-equilibrium version of TST, rather than making the transition state assumption at the dividing surface of maximum potential energy, as in conventional TST. To take advantage of the variational bound principle, we could introduce arbitrary definitions of the transition state dividing surface in phase space, calculate the equilibrium flux coefficient through each, and choose the smallest value as the best approximation to the true rate constant. A more practical procedure is to introduce a one-parameter sequence of generalized transition states and minimize the calculated rate constant with respect to this parameter [26, 31].

In the variational-transition-state-theory procedures employed by Garrett, Truhlar, and co-workers [26, 31, 35–48], the first step is a global choice for the reaction coordinate. Usually we choose this as the union of the paths of steepest descent (also called the minimum energy path or MEP) in mass-scaled coordinates from the saddle point towards reactants and products. We label the saddle point as $s = 0$, the range of s on the reactants' side as negative, and the range of s on the products' side as positive. The MEP in mass-scaled coordinates has the convenient properties that it matches the usual choice of s as the unbound normal coordinate at the saddle point, its effective reduced mass is a constant, and it tends to properly scaled A–B and C–D relative translational coordinates in the $s = -\infty$ and $s = +\infty$ limits, respectively [49]. Also, it has a simple physical interpretation as the path followed by a classical trajectory that starts at the saddlepoint but is continuously damped so as to always have only an infinitesimal velocity ("trajectory in heavy molasses") [50–53]; for this reason Fukui introduced the name intrinsic reaction path for the MEP in mass-scaled coordinates [50–52]. (For this choice of reaction path, s becomes the intrinsic reaction coordinate.) The damped-trajectory interpretation of the MEP in mass-scaled coordinates explains why this quantity is invariant to arbitrary orthogonal transformations of the coordinates [37]. Furthermore, it makes this reaction coordinate particularly relevant in the limit of slow reaction-coordinate motion, which is the important limit for most reactions with significant activation energy since the rate constants for such reactions tend to be dominated by contributions from energies near the threshold energy [54]. The choice of s as the MEP in mass-scaled coordinates is also convenient for generalized transition state theory, and we shall assume in what follows that this is the choice which has been made.

For each value of s we define the generalized transition state divided surface as the hypersurface locally perpendicular to the MEP in mass-scaled coordinates but globally curved in such a way as to assure that it does divide reactants from products. Again the result may be written in the form of Eq. (9) or (11), but now the transition state quantities are replaced by generalized transition state (GT) quantities that depend on the location s of the generalized transition state along the reaction coordinate. We obtain the generalized transition state theory rate constant expressions

$$k^{GT}(s) = \frac{\tilde{k}T}{h} \frac{\Phi^{GT}(s)}{\Phi^{A}\Phi^{B}} \exp \frac{-V_{MEP}(s)}{RT} \tag{13a}$$

$$= \frac{\tilde{k}T}{h} \frac{Q^{\ddagger}(s)}{\Phi^{R}_{rel} Q^{A} Q^{B}} \exp \frac{-V_{MEP}(s)}{RT} \tag{13b}$$

and

$$k^{GT}(s) = \frac{\tilde{k}T}{h} K^{\ddagger,0} \exp \frac{-\Delta G^{GT,0}(s)}{RT} \tag{14}$$

Canonical variational theory (CVT) is obtained by minimizing any of these equivalent expressions with respect to s for a given temperature, that is, for a given canonical ensemble. The resulting value of s is called s_*, and it depends on T. The resulting approximate rate constant is

$$k^{CVT} = \min_s k^{GT}(s) \tag{15a}$$

$$= k^{GT}(s_*) \tag{15b}$$

where $\min_s$ is an operator that takes the minimum of the following function over all possible s; Equation (15b) defines s_* as the location of this minimum. As noted in the first paragraph of this section, the variational procedure may also be thought of as maximizing the generalized free energy of activation. Thus,

$$k^{CVT} = (\tilde{k}T/h)K^{\ddagger,0} \exp\{-[\max_s \Delta G^{GT,0}(s)]/RT\} \tag{16c}$$

$$= (\tilde{k}T/h)K^{\ddagger,0} \exp[-\Delta G^{GT,0}(s_*)/RT] \tag{16b}$$

$$= (\tilde{k}T/h)K^{\ddagger,0} \exp(-\Delta G^{CVT,0}/RT) \tag{16c}$$

Since total energy is conserved, we can rigorously consider the contributions of each total energy to the thermal rate constant separately. Then a better variational result can be obtained by optimizing the generalized transition state dividing surface separately for each total energy, that is, for each microcanonical ensemble. Having done this, one can calculate the fixed-temperature rate constant by averaging the fixed-total-energy results over a canonical distribution of total energies. This is called [26, 31] microcanonical variational theory (μVT). One would expect that if the best transition state is a strong function of total energy, it will also be a strong function of temperature. Thus, if one performs CVT calculations as a function of T and does not find a strong temperature dependence of s_*, then one may probably assume that μVT calculations are unnecessary. This has been found to be the usual case.

It is interesting to note that, with a different choice of reaction coordinate, variational transition state theory can also be applied to barrierless reactions without saddle points. The above formalism has so far been applied to only one bimolecular case without a barrier, and s_* was found to be a strong function of T [46]. Furthermore, μVT calculations gave significantly lower rate constants than CVT calculations in this case [46]. This result suggests the intuitively

plausible conclusion that μVT also is likely to be called for by nearly barrierless reactions, such as solution reactions whose rate approaches the diffusion limit, and it suggests caution in the application of TST to such reactions.

2.2.4 Nonclassical Treatment of the Generalized Transition States and Vibrational Adiabaticity

In the preceding sections we assumed classical mechanics for all internuclear degrees of freedom. This is useful in developing the theory because the dynamic bottleneck assumption, which is responsible for the useful result that generalized transition state theory provides an upper bound on the equilibrium rate constant, is intrinsically classical, that is, it violates the uncertainty principle [25]. Any attempt to translate this assumption into quantum mechanics suffers from the ambiguity of noncommuting operators [11]. Thus the theory is usually quantized in an approximate fashion that takes advantage of the separation of the reaction coordinate. First the motion in the reactants and the transition state hypersurface is quantized. This affects $Q^{\ddagger}$, Q^{A}, and Q^{B} in conventional transition state theory or $Q^{GT}(s)$, Q^{A}, and Q^{B} in generalized transition state theory. In classical mechanics these internal partition functions are phase-space integrals; in quantum mechanics they are sums over states. Since the unbound reaction-coordinate motion is excluded from the transition state, the transition state has discrete energy levels and its sum over states may be calculated using the same methods as are standard for bound systems. This yields a hybrid approximate rate constant in which the bound degrees of freedom are treated as quantized, but the reaction coordinate is still treated as classical. There is no rigorous variational theorem for this quantity, but since reaction-coordinate motion is ultimately responsible for motion through the dynamical bottleneck, it seems reasonable to minimize the hybrid rate constant with respect to the location of the generalized transition state. This is called quantized or hybrid variational transition state theory. It may provide a good approximation when quantal effects on the reaction-coordinate motion are small, but otherwise one should include reaction-coordinate quantal effects as discussed in Section 2.2.5.

It is interesting to consider the absolute-zero-of-temperature limit of the generalized free energy of activation $\Delta G^{GT,0}(s)$ of Eq. (14) in the hybrid theory. At zero temperature all degrees of freedom are in their ground states and, aside from contributions of symmetry numbers and electronic degeneracies, which are small, $\Delta G^{GT,0}(s)$ approaches a simple limiting value:

$$\Delta G^{GT,0}(s) \widetilde{_{T\to 0}} \Delta V_a^G(s) \tag{17}$$

where we have defined

$$\Delta V_a^G(s) = V_{MEP}(s) + \varepsilon_{int}^G(s) - \varepsilon_{int}^{RG} \tag{18}$$

in terms of the ground state energy $\varepsilon_{int}^G(s)$ of the generalized transition state and

the zero point vibrational energy ε_{int}^{RG} of the reactants. [The ground state abbreviation G denotes the zero point state for vibrational motion and zero angular momentum for rotational and orbital motions. When the relative translational orbital motion is important, it is preferable to call $\varepsilon_{int}^{G}(s)$ the ground state, s-wave energy to emphasize this.] The quantity $\Delta V_a^G(s)$ has a simple interpretation. At zero temperature all reactant modes are in their ground states. If a zero temperature system were artificially advanced slowly along the reaction coordinate and the other modes remained in the ground state, that is, adjusted adiabatically, their energy requirement for any position s along the reaction coordinate would be $V_{MEP}(s) + \varepsilon_{int}^{G}(s)$. Thus ΔV_a^G is the change in the ground state adiabatic potential curve for reaction-coordinate motion as the system proceeds from reactants to the generalized transition state. The determination of the variational transition state by Eq. (15a) is often dominated by the s dependence of high frequency modes. When this is the case, since these modes tend to remain predominantly in their ground states up to temperatures quite a bit higher than room temperature, $\Delta V_a^G(s)$ provides a useful interpretive guide to the location of the variational transition state even at room temperature and above.

Adiabaticity of the internal modes with respect to the reaction coordinate has an even more quantitative connection to variational transition state theory [31, 37, 47]. In the adiabatic theory of reactions [8, 49, 54–61], one assumes that all internal modes adjust adiabatically to motion along the reaction coordinate, that is, as the system progresses from $s = -\infty$, all internal modes stay in the same state. If we then treat the energy states $\varepsilon_{int}(\alpha, s)$ of the generalized transition state for quantum numbers α as real, even though transition states are artificially defined by the excluding one coordinate, the energy requirement for the internal modes at location s along the reaction coordinate is

$$\Delta V_a(\alpha, s) = V_{MEP}(s) + \varepsilon_{int}(\alpha, s) - \varepsilon_{int}(\alpha, s = -\infty) \tag{19}$$

If we assume that all states react for which the relative translational energy [i.e., the initial ($s = -\infty$) energy in the reaction coordinate] exceeds

$$\Delta V_a^{\ddagger}(\alpha) = V_{MEP}(s = 0) + \varepsilon_{int}(\alpha, s = 0) - \varepsilon_{int}(\alpha, s = -\infty) \tag{20}$$

we obtain conventional transition state theory. If, alternatively, we assume adiabaticity of all other motions with respect to reaction-coordinate motion, which is itself assumed classical, then the relative translational energy for collisions beginning with the set of quantum numbers α must exceed

$$\Delta V^{A}(\alpha) = \max_s \Delta V_a^G(s) \tag{21}$$

and it can be shown [31, 37] that this is equivalent to microcanonical variational theory. This is a very interesting relationship between two different kinds of theory since the adiabatic theory involves a different barrier location for

each internal state, independent of total energy, and microcanonical variational theory involves a best dynamical bottleneck for each total energy, independent of internal state.

2.2.5 Nonclassical Treatment of the Reaction Coordinate; Tunneling

Quantal effects on reaction-coordinate motion are expected to be especially large at low energy because the average reaction-coordinate momentum is small, small momentum implies a large deBroglie wavelength, and classical mechanics becomes inaccurate when the potential energy changes significantly over the course of a single deBroglie wavelength. Also at low energies only a small fraction of systems have enough energy to surmount potential energy barriers, so small probabilities of tunneling through barriers can make significant or dominant contributions. The conventional way to account for this effect is to include a transmission coefficient, that is, one approximates the rate constant as

$$k^{\ddagger/Y} = \kappa^{\ddagger/Y} k^{\ddagger} \tag{22}$$

where Y denotes the method used for the transmission coefficient $\kappa^{\ddagger/Y}$, and $k^{\ddagger}$ is the hybrid rate constant expression of the previous section. Alternatively, we may correct the hybrid CVT rate constant expression by

$$k^{CVT/Y} = \kappa^{CVT/Y} k^{CVT} \tag{23}$$

where the transmission coefficient is again based on a method denoted Y for illustration purposes. Note that for a given method of treating tunneling effects the transmission coefficient should be different for the different hybrid rate constant expressions, and so we have used different symbols, $\kappa^{\ddagger/Y}$ and $\kappa^{CVT/Y}$.

In quantum mechanics it is difficult to calculate thermally averaged rate constants directly [33]. In general, definitive quantum mechanical treatment of thermal rate constants requires calculating rate coefficients for all important state-selected processes as a function of energy, then performing a thermal average. Since quantal effects on reaction-coordinate motion become most important in the low temperature limit, it is most important to estimate the quantal effects on the ground state reaction probability at low relative translational energy. At low relative translational energy the reaction probability is dominated by head-on collisions, which are represented in quantal collision theory by s waves, since they have zero orbital angular momentum of relative translational motion. Thus, in the low temperature limit the transmission coefficient can be calculated from ground state, s-wave transmission probabilities, which are here denoted P^G.

In the low temperature limit, CVT becomes equivalent to μVT and hence to the adiabatic theory of reactions. In this theory, as discussed in Section 2.2.4, the effective barrier for reaction-coordinate motion is given by Eq. (18). Thus the implicit ground state, s-wave reaction probability of canonical variational

theory becomes the classical reaction probability P_C^{AG} for the ground state, s-wave adiabatic potential curve; this is a unit step function at the energy of the barrier maximum,

$$P_C^{AG} = \theta[E_{rel} - \max_s \Delta V_a^G(s)] \tag{24}$$

where θ is the unit step function defined by

$$\theta(x) = \begin{cases} 1, & x > 0 \\ 0, & x < 0 \end{cases} \tag{25}$$

The transmission coefficient of μVT, and hence of CVT in the low temperature limit, may then be approximated by the ratio of the thermal average of P^G to the thermal average of P_C^{AG}. At nonzero temperatures CVT is no longer exactly equivalent to μ^{VT}, and the ground state reaction probability implied at nonzero temperature is

$$P_C^{CVT,G} = \theta[E_{rel} - \Delta V_a^G(s_*)] \tag{26}$$

The ground state transmission coefficient $\kappa^{CVT/G}$ for CVT is the ratio of the thermally averaged ground state quantal reaction probability to the thermally averaged ground state classical one implied by the hybrid CVT calculation, that is,

$$\kappa^{CVT/G} = I \Big/ \int_0^\infty P^{CVT,G} \exp(-E_{rel}/RT)\, dE_{rel} \tag{27a}$$

$$= \exp[\Delta V_a^G(s_*)] I/RT \tag{27b}$$

where

$$I = \int_0^\infty P^G \exp(-E_{rel}/RT)\, dE_{rel} \tag{28}$$

Similarly the ground state transmission coefficient $\kappa^{\ddagger/G}$ for conventional TST is

$$\kappa^{\ddagger/G} = I \Big/ \int_0^\infty \Theta[E_{rel} - \Delta V_a^G(s=0)] \exp(-E_{rel}/RT)\, dE_{rel} \tag{29a}$$

$$= \exp[\Delta V_a^G(s=0)] I/RT \tag{29b}$$

Notice that $\Delta V_a^G(s=0)$ is the classical barrier height $[\max_s V_{MEP}(s)]$ plus the zero point energy of the conventional transition state minus the zero point energy of reactants. The importance of using the correct denominators in Eqs. (27a) and (29a) has been emphasized previously [41].

In the high temperature limit the quantal effects on reaction-coordinate motion should become unimportant, that is, the transmission coefficient should tend to unity. (Note: In some treatments the transmission coefficient is defined formally to include classical recrossing corrections, which are omitted here; if these are included then the previous statement is not true. No practical yet accurate methods, short of full dynamics calculations, are available to estimate classical recrossing effects.) If we approximate P^G by an accurate method at low energy, then $\kappa^{\ddagger/G}$ and $\kappa^{CVT/G}$ will be accurate at low temperature; if we approximate P^G such that it tends to unity at high energy, then $\kappa^{\ddagger/G}$ and $\kappa^{CVT/G}$ will tend to unity at high temperature. Approximate ground state transmission coefficients obtained from such approximate P^G functions therefore have the correct behavior in both limits, and they may actually provide reasonable approximations over the whole temperature range. The difficulty is obtaining accurate P^G functions at low energy, and this will be discussed next.

The formalism presented in Sections 2.2.1 to 2.2.4 is greatly simplified by the dynamical bottleneck assumption. It is this assumption that allows one to focus on the localized hypersurface defined as the transition state and to avoid global dynamics calculations. Stated another way, it is this assumption that reduces TST theory to a quasi-equilibrium theory involving standard methods of statistical mechanics or molecular thermodynamics. The ground state reaction probability reintroduces the global dynamics, and since we will consider the estimation of P^G by calculations in a reaction-coordinate formalism, the global definition of the reaction coordinate is necessary. As discussed in Section 2.2.3, we define s as the path of steepest descent on the Born–Oppenheimer potential surface as expressed in mass-scaled coordinates. The use of mass-scaled coordinates is very important for developing physical approximations. In mass-scaled cartesian coordinates, or any orthogonal transformation thereof, the many-particle kinetic energy expression in the Hamiltonian has no cross terms and every square term is preceded by the same reduced-mass expression. Thus the many-particle problem with the many-atom potential energy function V has a one-to-one correspondence to a single mass point moving in $3N$ dimensions under the same potential function, now considered as a one-body many-dimensional potential function V. This means that the effect of the potential may be estimated using one's real world intuition. In a mass-scaled coordinate system, for example, if the steepest descent reaction path (along which the reaction coordinate is measured) is curved, it will cause internal centrifugal effects like bobsled effects. In other coordinate systems a large curvature of the reaction path may simply be an artifact of the coordinate definition with no physical consequences. We will consider the curvature of the reaction path in more detail since it is now clear that it plays a very important role in tunneling processes in chemical reactions [37, 39, 41, 43–45, 48, 62–70].

For atom transfer reactions involving a light atom transfer, the relative masses of the acceptor (Ac), the donor (Do), and the atom transferred (At) place a particularly strong constraint on reaction-path curvature. For such a reaction the angle between the intrinsic-reaction-coordinate directions in the entrance

and exit channels is

$$\beta = \arctan\left(\frac{m_{At}m_{total}}{m_{Ac}m_{Do}}\right)^{1/2} \tag{30}$$

where m_X is the mass of X and m_{total} is the sum of the masses. For m_{At} much smaller than the donor and the acceptor masses, β is very small, that is, the intrinsic reaction coordinate almost turns completely around in mass-scaled coordinates. Thus, the intrinsic reaction coordinate must be very curved in such cases, and the curvature is expected to be reasonably localized near the distance of closest approach of the acceptor and the donor. If the tunneling region is symmetrical or almost symmetrical, as expected for a thermoneutral or almost thermoneutral reaction, then the reaction-path curvature will be large in the highest part of the MEP. Other things being equal, the relevant reaction-path curvature is expected to be smaller for less extreme mass combinations and less symmetrical reactions.

It is useful to consider two extreme cases, the small curvature and large curvature limits. For cases where the reaction path has large curvature in the tunneling region so that the entrance and exit portions of the intrinsic reaction path are almost antiparallel, the system is expected to tunnel directly across from the entrance portion to the exit portion without necessarily following the minimum energy path all the way to the large curvature region [45, 71–75]. Such a treatment may be visualized as a sudden (or Franck–Condon) transition. For small curvature cases the motions transverse to the intrinsic reaction coordinate are often better represented by an adiabatic model than a sudden model. The Marcus–Coltrin path approximation [37, 39, 41, 62, 63, 65] and small curvature approximation of Skodje et al. [43, 68, 69] both incorporate such vibrationally adiabatic approximations. Because of the adiabatic and ground state approximations, the effective barrier in these methods is $\Delta V_a^G(s)$. However in the Marcus–Coltrin method the distance s is replaced by a shorter distance ξ which measures distance along an assumed tunneling path that is shorter than the intrinsic reaction path. In the similar but more general small curvature approximation, one retains s but accounts for an effective path shortening by using a smaller, s-dependent reduced mass. Both methods show that even relatively small reaction-path curvature can have a large effect on the transmission coefficient, and it is important to model reaction-path-curvature effects accurately.

In both the small and large curvature cases the effect of reaction-path curvature is a negative internal centrifugal effect. A positive or classical internal centrifugal effect is a bobsled effect, that is, in classically allowed regions a nonzero kinetic energy along a curved reaction path will force the system to the convex side of the path. For classically forbidden tunneling the kinetic energy along the reaction path is negative and so is the internal centrifugal effect, that is, the system cuts the corner [56, 76, 77]. By cutting the corner, the system effectively decreases the tunneling distance and so the corner-cutting path is a

higher probability tunneling path than one along the intrinsic reaction coordinate. The system wave function is actually largest along the path that represents the best compromise between short tunneling distance and low effective barrier. For small curvature the tunneling is dominated by a path near the concave-side vibrational turning points of the transverse modes [37, 62]. For large curvature the dominant tunneling paths may be much farther from the intrinsic reaction coordinate. An approximate variational principle (based on least imaginary action and *not* related to the classical variational principle for the location of the generalized transition state dividing surface) has been used to automatically locate the optimum tunneling path or paths for systems with arbitrary reaction-path curvature [47, 75]. For small and large reaction-path curvature, this method yields very similar results to the small curvature and large curvature methods, respectively; but for intermediate reaction-path curvature it leads to better results than either of these limiting approximations.

A few additional comments may be useful before ending this section. First, it is very common to see transmission coefficients based on one-dimensional tunneling calculations for $V_{MEP}(s)$. This procedure can be derived from the small curvature approximation by neglecting the s dependence of $\varepsilon^G_{int}(s)$, which is called the conservation-of-vibrational-energy approximation [49], and by neglecting reaction-path curvature. Usually these are both poor approximations; they need not even give the correct order of magnitude [37, 49, 54, 60].

Another point worthy of comment concerns Eq. (22). If the effective potential curve for tunneling is $\Delta V^G_a(s)$, and if this peaks other than at $s = 0$, then as tunneling effects decrease in importance (because the temperature is raised), $\kappa^{\ddagger/Y}$ tends to a Boltzmann factor, unlike $\kappa^{CVT/Y}$, which tends more directly to unity. This occurs because $\kappa^{\ddagger/Y}$ includes a classical correction for reflection at the maximum of $\Delta V^G_a(s)$ of trajectories that are counted as successful in $k^{\ddagger}$. Thus, consistent transmission coefficients for conventional transition state theory include some classical reaction coordinate variational-transition-state-theory effects as well as including tunneling.

Finally, we note that the best tunneling path for a given system is not necessarily independent of energy, and at a given energy the dominant tunneling region need not be well localized. In the small curvature limit the dominant tunneling path does appear to be reasonably independent of energy and well localized, but these convenient properties tend to be lost as the curvature gets larger [75]. Thus in the large curvature limit we need to consider a tunneling probability as a function of approach coordinate even at a single energy [47, 71–75].

2.2.6 Quasi-Thermodynamic Activation Parameters

We have seen in Section 2.2.5 that the final rate expression of conventional transition state theory with a transmission coefficient $\kappa^{\ddagger/Y}$ is

$$k^{\ddagger/Y} = \kappa^{\ddagger/Y}(\tilde{k}T/h)K^{\ddagger,0} \exp[-\Delta G^{\ddagger,0}/RT] \tag{31}$$

and the final rate expression of canonical variational theory with a ground state transmission coefficient $\kappa^{CVT/G}$ is

$$k^{CVT/G} = \kappa^{CVT/G}(\tilde{k}T/h)K^{\ddagger,0} \exp[-\Delta G^{CVT,0}/RT] \tag{32}$$

If we define Γ as the nonequilibrium correction factor,

$$\Gamma = k/k^e \tag{33}$$

where k is the phenomenological rate constant and k^e is its local equilibrium flux coefficient, and if we let $\gamma^{\ddagger/Y}$ and $\gamma^{CVT/G}$ be the ratio of the exact local equilibrium flux coefficient k^e to the estimates of Eqs. (31) and (32), we see that the true measured rate constant can be written as

$$k = \gamma^{\ddagger/Y}\Gamma\kappa^{\ddagger/Y}(\tilde{k}T/h)K^{\ddagger,0} \exp[-\Delta G^{\ddagger,0}/RT] \tag{34a}$$

$$= \gamma^{CVT/G}\Gamma\kappa^{CVT/G}(\tilde{k}T/h)K^{\ddagger,0} \exp[-\Delta G^{CVT,0}/RT] \tag{34b}$$

It is interesting to write Eq. (34b) as

$$k = \gamma^{CVT/G}\Gamma\kappa^{CVT/G} \exp[-\Delta G^{V,0}/RT]k^{\ddagger} \tag{35}$$

where we have defined

$$\Delta G^{V,0} = \Delta G^{CVT,0} - \Delta G^{\ddagger,0} \tag{36}$$

Equation (34b) provides an exact factorization of the observable rate constant into several precisely defined factors. These factors may all be considered as corrections to the conventional TST rate and they account for variational-transition-state-theory optimization effects [i.e., classical entropic effects, the exponential in Eq. (35)], quantum effects on the reaction coordinate ($\kappa^{CVT/G}$), nonequilibrium effects (as given by Γ, which includes solvent friction effects), and the breakdown of the no-recrossing assumption ($\gamma^{CVT/G}$). We emphasize that the factors are defined precisely by the equations; the word descriptions are approximate. Thus, $\kappa^{CVT/G}$ includes a small classical part, and Γ accounts for all the errors in incorporating quantum effects in the theory, as well as for the breakdown of the no-recrossing assumption.

The quasi-thermodynamic activation parameters are obtained by replacing Eqs. (34) by

$$k = (\tilde{k}T/h)K^{\ddagger,0} \exp[-\Delta G^{a,0}/RT] \tag{37}$$

where $\Delta G^{a,0}$ is defined as the empirical (standard state) free energy of activation, and then treating $\Delta G^{a,0}$ by methods of thermodynamics.

For gas phase reactions the standard state is usually chosen to be 1 atm. Hence, the standard state reaction quotient of Eq. (11) may be written

$$K^{\ddagger,0} = N_A^u \tilde{k} T / P^0 \tag{38}$$

where P^0 denotes 1 atm, N_A is Avogadro's number, the exponent u is zero if the concentration units in k are molecules per unit volume, and u is one if they are moles per unit volume. Substituting this into Eq. (37) yields

$$k = (\tilde{k}T)^2 N_A^u / hP^0) \exp(-\Delta G^{a,0}/RT) \tag{39}$$

or

$$\Delta G^{a,0} = -RT \ln \frac{hP^0 k}{(\tilde{k}T)^2 N_a^u} \tag{40}$$

Substituting the factorized expression Eq. (35) into Eq. (40) provides an exact expression for the observable free energy of activation as a sum of a conventional TST contribution and several precisely defined corrections,

$$\Delta G^{a,0} = \Delta G^{\ddagger,0} + \Delta G^{V,0} + \Delta G^{\kappa,CVT} + \Delta G^{\Gamma} + \Delta G^{\gamma,CVT} \tag{41}$$

in an obvious notation.

Alternative partitions are provided by Eqs. (34a) and (34b) which yield

$$\Delta G^{a,0} = \Delta G^{\ddagger,0} + \Delta G^{\kappa,\ddagger} + \Delta G^{\Gamma} + \Delta G^{\gamma,\ddagger} \tag{42}$$

and

$$\Delta G^{a,0} = \Delta G^{CVT,0} + \Delta G^{\kappa,CVT} + \Delta G^{\Gamma} + \Delta G^{\gamma,CVT} \tag{43}$$

By analogy to standard thermodynamics equations, the molar entropy, enthalpy, and volume of activation are given by

$$\Delta S^{a,0} = -\left(\frac{\partial \Delta G^{a,0}}{\partial T}\right)_P \tag{44}$$

$$\Delta H^{a,0} = \Delta G^{a,0} + T\Delta S^{a,0} \tag{45}$$

$$\Delta V^{a,0} = RT\left(\frac{\partial(\Delta G^{a,0}/RT)}{\partial P}\right)_T \tag{46}$$

Using Eqs. (44)–(46), any of the quasi-thermodynamic activation parameters may be partitioned as in Eqs. (41)–(43). Since, as discussed in Section 2.2.5,

$\kappa^{\ddagger/Y}$ may contain a significant mixture of variational transition state optimization effects along with tunneling effects, and since, as discussed in Section 3, $\gamma^{CVT/G}$ is expected to usually be closer to unity than $\gamma^{\ddagger/Y}$ is, Eqs. (41) and (43) provide a better basis for the approximate interpretation of the quasi-thermodynamic activation parameters than does Eq. (42). In particular, if we approximate $\gamma^{CVT/G}$, which primarily accounts for multidimensional recrossing effects and the inadequacy of the tunneling calculations, as unity, we obtain

$$\Delta G^{a,0} = G^{CVT,0} - RT \ln \Gamma - RT \ln \kappa^{CVT/G} \tag{47}$$

Substituting Eq. (47) into any of Eqs. (44)–(46) yields three contributions to any of the quasi-thermodynamic activation parameters, and one can use models or other information to try to sort these out. It is unfortunately very common to see interpretations based on the implicit equation of $\Delta G^{a,0}$ to $\Delta G^{\ddagger,0}$. This neglects $-k_B T \ln \Gamma$ and $-k_B T \ln \kappa^{\ddagger/Y}$, as well as $-k_B T \ln \gamma^{\ddagger/Y}$, some of which could be significant or have significant derivatives with respect to temperature or pressure.

If the observed rate constant is represented as

$$k = B_1 T^{B_2} \exp(-E_a/RT) \tag{48}$$

which fits almost all available data within experimental error, then Eqs. (44)–(46) and (48) yield

$$\Delta S^{a,0} = R\left[B_2 - 2 + \ln \frac{hP^0 B_1 T^{B_2}}{(kT)^2 N_A^u}\right] \tag{49}$$

$$\Delta H^{a,0} = E_a + (B_2 - 2)RT \tag{50}$$

$$\Delta V^{a,0} = \frac{\partial E_a}{\partial P} - RT \frac{\partial}{\partial P} \ln B_1 T^{B_2} \tag{51a}$$

$$= -RT \frac{\partial \ln k}{\partial P} \tag{51b}$$

Setting $B_1 = A$ and $B_2 = 0$ yields the more usual results for an Arrhenius fit to the rate data.

2.3 Gas Phase Unimolecular Reactions

Consider a reaction

$$A \underset{-2}{\overset{2}{\rightleftharpoons}} \text{product(s)} \tag{R2}$$

Superficially the theory of Section 2.2 would need very little change. Equation (9) becomes

$$k^{\ddagger} = \frac{\tilde{k}T}{h}\frac{\Phi^{\ddagger}}{\Phi^{A}}\exp\frac{-V^{\ddagger}}{RT} \tag{52a}$$

$$= \frac{\tilde{k}T}{h}\frac{Q^{\ddagger}}{Q^{A}}\exp\frac{-V^{\ddagger}}{RT} \tag{52b}$$

and $K^{\ddagger,0}$ becomes unity, so Eq. (12) becomes

$$k^{\ddagger} = (\tilde{k}T/h)\exp(-\Delta G^{\ddagger,0}/RT) \tag{53}$$

Similarly, Eqs. (13), (14), and (16) become

$$k^{GT}(s) = \frac{\tilde{k}T}{h}\frac{\Phi^{GT}(s)}{\Phi^{A}}\exp\frac{-V_{MEP}(s)}{RT} \tag{54a}$$

$$= \frac{\tilde{k}T}{h}\frac{Q^{\ddagger}(s)}{Q^{A}}\exp\frac{-V_{MEP}(s)}{RT} \tag{54b}$$

$$k^{GT}(s) = (\tilde{k}T/h)\exp[-\Delta G^{GT,0}(s)/RT] \tag{55}$$

and

$$k^{CVT}(s) = (\tilde{k}T/h)\exp(-\Delta G^{CVT,0}/RT) \tag{56}$$

Then Section 2.2.4 is applicable except that reactant B is excluded.

The additional complication is that the nonequilibrium correction factor can be very large for gas phase unimolecular reactions. The reaction rate is often dominated by highly excited states that react more rapidly than their populations can be replenished by energy transfer collisions. This leads to nonequilibrium factors Γ that may be one or more orders of magnitude less than unity and that are strong functions of temperature and pressure. The procedure, often so successful for bimolecular reactions, of estimating the equilibrium rate constant k^e and assuming that it represents a good first approximation to the phenomenological rate constant, is often useless for gas phase unimolecular reactions. The more appropriate procedure is well known and dates back to early work by Lindemann, Hinshelwood, Rice, Ramsperger, and Kassel. An excellent review of the early theories has been given by Robinson and Holbrook [78]. The simplest theory which yields qualitatively correct results involves a mechanism in which energetic molecules of various total energies E are considered separately. Let E_0 denote the threshold energy for reaction (R2) and let molecules with energies E in excess of E_0 be denoted A*(E). Then the mechanism is

$$A + M \underset{k_{-1}}{\overset{k_1(E)}{\rightleftarrows}} A^*(E) + M \tag{R1*}$$

$$A^*(E) \xrightarrow{k_2(E)} \text{product(s)} \tag{R2*}$$

and it is essential that $k_1(E)$ and $k_2(E)$ decrease and increase, respectively, as functions of E. The observable rate constant is a consequence of the scheme (R1*)–(R2*), and it is not possible to calculate it directly. Instead one must calculate the fixed-energy rate constants $k_1(E)$ and $k_2(E)$ and the deactivation rate constant k_{-1} and insert them in the scheme (R1*) – (R2*). When this is done the results show that in typical cases the important species A*(E) are not in local equilibrium with A; instead the important states with energies above E_0 are underpopulated. We mentioned in Section 2.2.3 that it is sometimes necessary to calculate fixed-energy, that is, microcanonical, rate constants in order to find good enough dynamical bottlenecks for transition state theory to be quantitatively accurate. For unimolecular reactions we must calculate microcanonical rate constants for a different reason, namely because it is necessary to distinguish different energy states in the mechanism. Transition state theory as applied to the calculation of $k_2(E)$ for unimolecular reactions is called Rice–Ramsperger–Kassel–Marcus (RRKM) theory. It has been treated thoroughly in two excellent monographs [78, 79], and advances in unimolecular rate theory since then have been extensively reviewed elsewhere [80–86].

As the pressure is raised, the local equilibrium assumption becomes valid and equations (52)–(56) may be applied directly. At lower pressures we must use the microcanonical analogues.

The fixed-energy analogue of Eq. (54) is [31, 37]

$$k^{GT}(E, S) = \frac{N^{GT}(E, s)}{h\phi^{R}(E)} \tag{57}$$

where $N^{GT}(E, s)$ is the total number of internal states, excluding overall translation and the reaction coordinate, of the generalized transition state at s with internal energy less than or equal to E, and $\phi^{R}(E)$ is the density of reactant states per unit energy. Equation (57) is the generalized-transition-state-theory analogue of the conventional transition-state-theory result [87–89].

As discussed elsewhere [46, 86, 90], the variational transition state location, that is, the value $s_*(E)$ that minimizes $k^{GT}(E, s)$, may have a significant dependence on E, especially when the reaction in the exothermic direction shows no barrier. Since s_* is the same for the reverse as for the forward reaction, this is reasonable by comparison to the case of barrierless bimolecular reactions discussed above.

For unimolecular reactions $K^{\ddagger,0}$ is unity. This means that Eqs. (49) and (50) are replaced by

$$\Delta S^{a,0} = R\left[B_2 - 1 + \ln\frac{hB_1T^{B_2-1}}{\tilde{k}}\right] \tag{58}$$

and

$$\Delta H^{a,0} = E_a + (B_2 - 1)RT \tag{59}$$

There is no change in Eq. (51). The quasi-thermodynamic activation parameters are most useful for interpretative purposes when $\Delta G^{\ddagger,0}$ or $\Delta G^{CVT,0}$ dominates $\Delta G^{a,0}$. Thus, except in the high pressure limit, the quasi-thermodynamic activation parameters are less useful for gas phase unimolecular reactions than for bimolecular reactions.

2.4 Reactions in Solution

The basic ideas discussed above with regard to the transition state theory of reactions in the gas phase are also applicable to reactions in solution. The two main assumptions of TST, local equilibrium and a dividing surface that is not recrossed, are formally the same in solution, but their validity must be re-examined for the new context. In addition, the presence of the solvent changes the effective potential energy surface representing the mutual interaction of solutes. Sections 2.4.1 and 2.4.2 discuss the effect of solvent on the potential energy surface and the no-recrossing assumption. Section 2.4.3 discusses the validity of the local equilibrium assumption in solution. Section 2.4.4 examines the meaning of the quasi-thermodynamic activation parameters in the context of Sections 2.4.1 to 2.4.3. Section 2.4.5 considers the mechanistic complication, for fast reactions, of the distinction between rearrangement-controlled and diffusion-controlled reactions.

2.4.1 Static Solvent Effects

Two approaches that include the solvent in the theoretical description of a reaction in solution may be illustrated by considering the gas phase equations (9) and (12). To include solvent in Eq. (9) we would replace the partition functions and potential energy of the isolated reacting particles by those of the solvated particles. In statistical mechanical language this involves the concept of a potential of mean force [20b, 34a]. The potential of mean force for particles in a solvent is *defined* so that if it is manipulated just like the Born–Oppenheimer potential for gas phase species, one obtains the correct statistical and thermodynamic functions for dissolved particles. The potential of mean force is an explicit function of the coordinates of the solute particles, but it is an equilibrium quantity with respect to the solvent. In other words, the solvent contribution to the potential of mean force is the free energy of the solvent for fixed positions of the solute particles. This means that, in solution, the equilibrium thermodynamic properties of interacting solutes may be computed by including two contributions in their intermolecular force function: their intrinsic interaction and a force representing the work they must perform against the adiabatic solvent reorganization.

An important question to be adressed in a theoretical approach to reactions in solution is the primary system–bath separation. The traditional approach is to include as a primary system those atoms and molecules, charged or uncharged, appearing explicitly in the reaction as written, for example, (R1) or (R2). The remainder of the solution is the "bath". In a more detailed treatment, one or more solvent molecules are involved in the primary system. These two

approaches may be contrasted by writing, for example,

$$NH_4^+(aq) + H_2O(aq) \rightarrow NH_3(aq) + H_3O^+(aq) \qquad (R3a)$$

or

$$NH_4^+(H_2O)(aq) + 2H_2O(aq) \rightarrow NH_3(H_2O)(aq) + H_5O_2^+(aq) \qquad (R3b)$$

In (R3a) the primary system contains 8 particles; in (R3b) it contains 14. While (R3b) allows for a more detailed model, it also requires considerably more information and effort. In general we try to reduce the number of solvent molecules considered explicitly to the minimum (often zero) that will permit the observables to be mimicked. However, solvent motions that play a significant role in the reaction coordinate must always be treated explicitly. The treatment of solvent molecules as a bath, as discussed above, assumes that solvent molecules adjust statistically to changes in the primary system coordinates. In some cases the solvent cannot adjust to rapid primary system motion. This is sometimes called nonequilibrium solvation. The conceptually simplest way to treat this is to include the most strongly interacting solvent molecules as additional primary system constituents. If, however, many degrees of freedom of the solvent are nonequilibrating with the solute, then it may be possible, and practically simpler, to treat them by a collective coordinate, such as a polarization vector. The choice of which coordinates, individual and possibly also collective, to include in the primary system affects the accuracy of the subsequent theoretical development at every stage.

As mentioned above we can base TST for solution phase reactions on partition functions corresponding to the primary system in an adiabatic bath. This may involve important changes from the gas phase in the nature of the normal modes. For example, free rotation is usually missing in solution and is replaced by hindered rotations, librations, or even tight vibrations; these may be called pseudo-lattice vibrations or phonon modes. Free translation is also replaced by vibrational motions in a harmonic approximation [91]. Thus, Eqs. (9b), (13b), (52b), and (54b) are more convenient than Eqs. (9a), (13a), (52a), and (54a) for reactions in solution. Note that despite the solvent hindrance of translational motions, the partition function of the transition state and each chemical species is still proportional to the entire volume of the solution, and one still needs the partition function per unit volume in Eqs. (9a) and (13a).

If a calculation such as just described is actually carried out, one expects to get more accurate results if one uses variational transition state theory than if the transition state is simply placed at the saddle point of the potential-of-mean-force surface.

Since liquid phase partition functions are difficult to calculate, it is much more common to base solution phase transition state theory on the solution phase analogues of Eq. (12) or (53), and the associated Eqs. (40)–(51), (58), and (59) than on Eq. (9) or (52). In this approach one deals directly with the quasi-thermodynamic activation parameters.

The most common approach is to write

$$\Delta G^{\ddagger,0} = \Delta G_f^{\ddagger,0} - \Delta G_f^{\text{reactants},0} \tag{60}$$

thereby defining the free energy of formation of the transition state $\Delta G_f^{\ddagger,0}$. One can obtain $\Delta G_f^{\text{reactants},0}$ from experimental quantities like enthalpies of solvation, and one can try to estimate $\Delta G_f^{\ddagger,0}$ by analogy. The study of structural and solvent effects on quasi-thermodynamic activation parameters is well advanced, and it involves the consistent use of various thermodynamic and quasi-thermodynamic cycles [92–96]. The interpretation of quasi-thermodynamic activation parameters is discussed further in Section 2.4.4.

One kind of solvent effect is easily treated in general terms by transition state theory, namely, solution nonideality. As an example of how nonideality enters, consider Eq. (6) for a bimolecular reaction. In continuing the derivation we used the relation

$$K_1^{\delta} = \frac{[\delta]_e}{[A][B]} \tag{61}$$

for the equilibrium constant of the forward-crossing δ transition state species. But equilibrium constants may be expressed in terms of concentrations only in dilute gases and ideal solutions. In general, Eq. (61) must be replaced by

$$K_1^{\delta} = \frac{a_{\delta}}{a_A a_B} \tag{62a}$$

$$= \frac{[\delta]_e}{[A][B]} \frac{\gamma_{\delta}}{\gamma_A \gamma_B} \tag{62b}$$

where a_X and γ_X are the activity and activity coefficient of X, respectively. Use of Eq. (62b) instead of Eq. (61) yields

$$[\delta]_e = K_1^{\delta} \frac{\gamma_A \gamma_B}{\gamma_{\delta}} [A][B] \tag{63}$$

Instead of Eq. (7) and

$$k^{\ddagger} = \frac{\tilde{k}T}{h} K^{\ddagger,0} \exp\left(\frac{-\Delta G^{\ddagger,0}}{RT}\right) \frac{\gamma_A \gamma_B}{\gamma_{\delta}} \tag{64}$$

instead of Eq. (12). Since the standard state free energy of activation refers to an ideal solution, nonideality effects are included in the ratio of activity coefficients. When the nonideality involved is the effect of salts on the activities of ionic reactants, this is called the primary salt effect [97]. (A secondary salt

effect involves not the effect of salts on γ_X but the effect of salts on the concentrations of species entering into the phenomenological rate equation.) Since the transition state includes only an infinitesimal range of the reaction coordinate, γ_δ is not quite the same kind of quantity as a real activity coefficient.

In the rest of this chapter, "potential surface" implies potential energy surface for gas phase reactions and potential-of-mean-force surface for solution reactions.

2.4.2 Effect of Solvent on Rate of Conversion of Transition States

As discussed in Section 2.2.1, transition state theory provides an approximation to the equilibrium rate constant. In the gas phase, if classical mechanics were exact, transition state theory would always overestimate the equilibrium rate constant because of recrossing effects. When quantum effects are included, additional errors in either direction are possible, but the quantum correction for tunneling is often uncertain, and underestimation of the tunneling contribution may cause transition state theory to underestimate the equilibrium rate constant. In solution there are additional effects caused by the interactions with a solvent. The dominant dynamical effect of solvent interactions on the equilibrium rate constant is to decrease the rate constant by inducing further recrossing effects. Of course the solvent may also have a large static effect associated with the free energy of solvation of the reactants and the transition state, as discussed in Section 2.4.1. The static solvent effect may be included in transition state theory with no change in the formalism. The dynamic solvent effect, however, requires a generalized theory, such as the Brownian-motion, one-dimensional, transition state theory of Kramers [98–100]. Kramers generalized transition state theory to the case where the motion along the reaction coordinate is interrupted by a series of frequent but weak outside perturbations. The mathematical framework he used is that appropriate to Brownian motion, that is, the motion of a heavy, slow-moving solute in a light, fast-moving solvent, and thus the resulting theory corresponds to diffusion through the bottleneck region of phase space, as compared to Liouvillean flow in phase space for the gas phase theory. The diffusive flow is characterized by a new parameter, the friction coefficient for the reaction coordinate. To be useful for quantitative calculations, Kramers theory would require several improvements, among them: (1) generalization to multidimensional systems [101–104], (2) a realistic incorporation of quantum effects [100a, 105], (3) a more realistic treatment of system–solvent interactions, applicable to arbitrary masses and molecular sizes [106–110], and (4) a detailed prescription for the friction coefficient in terms of a molecular level characterization of the solute–solvent interactions [108–110]. Nevertheless, the simple Kramers treatment is very instructive, and it provides useful guidance to the nature of the dominant effect of dynamic solute–solvent interactions. We will present here a very slightly generalized version of Kramers theory, incorporating improvement (1) in an independent mode framework but presenting only qualitative discussions of improvements (2)–(4).

We should also mention an alternative approach to treating dynamic solvent effects, which might be considered when the effect of solvent is dominated by strong and specific interactions of the reacting system with a few solvent molecules. In such cases, just as for the static solvent effects discussed in Section 2.4.1, those molecules could just be considered part of the primary reaction system. This makes the system much larger and harder to treat; for example, the phase space has a higher dimensionality and the reaction coordinate must have components in solvent coordinates as well as in the coordinates of the original system, but it transforms dynamic solvent effects into effects that are includable in a gas phase formalism [111]. Even when solvent effects really are many-body phenomena, one can attempt this approach by using generalized solvent coordinates such as degree of polarization. In the rest of this section it is assumed that the system includes all reactants and possibly some specifically coupled solvent molecules, such as a solvent molecule making an important hydrogen bond at or near the reaction center, and that the bath includes the rest of the solvent.

The original derivation of Kramers [98] was based on the Fokker–Planck equation [20c, 112]; the theory can also be derived [113] from the equivalent Langevin equation [20d]. Here we present a much simpler derivation, similar to one of Helfand [114], which yields the high friction limit (often called the Smoluchowski limit) of Kramers' result as a consequence of simple dimensional considerations for a pseudo-one-dimensional unimolecular reaction of a reactant A. Assume that the potential of mean force along the reaction coordinate has the harmonic shape

$$V(s) \cong \tfrac{1}{2} f_A (s - s_A)^2, \qquad s \cong s_A \tag{65}$$

in the reactants' region (centered at s_A, assumed negative) and the parabolic shape

$$V(s) = V^\ddagger + \tfrac{1}{2} f_\ddagger s^2, \qquad s \cong 0 \tag{66}$$

in the vicinity of the transition state (at $s = 0$), where f_A and $f_\ddagger$ are positive and negative force constants, respectively. The root-mean-square displacement of the reactant from its equilibrium separation is

$$d_A = (\langle (s - s_A)^2 \rangle_A)^{1/2} \tag{67a}$$

$$= [\langle V \rangle_A / (\tfrac{1}{2} f_A)]^{1/2} \tag{67b}$$

$$= (\tilde{k}T / f_A)^{1/2} \tag{67c}$$

where we used the fact that the average potential energy of a harmonic oscillator is [17a, 20e] $\frac{1}{2}\tilde{k}T$. The quantity d_R provides a characteristic length scale for

reactants and a similar quantity

$$d_{\ddagger} = (\tilde{k}T/|f_{\ddagger}|)^{\frac{1}{2}} \tag{68}$$

provides a characteristic length scale in the vicinity of the parabolic maximum. Consider a case where phenomenological kinetics holds even in the absence of back reaction. Then the phenomenological rate constant reduces to the one-way flux coefficient calculated in the absence of products, that is,

$$k^S = j(s = 0)/N_A \tag{69}$$

where k^S is the Smoluchowski high friction limiting rate constant to be derived, $j(s = 0)$ is the current of particles passing the barrier at $s = 0$ per unit time, and N_A is the number of reactants. In the limit of high friction, the motion across the barrier satisfies Fick's first law of diffusion [10b, 20f]:

$$j(s = 0) = -D \left.\frac{dn}{ds}\right|_{s=0} \tag{70}$$

where D is the diffusion coefficient (with units of length squared per time) and $n(s)$ is the local concentration of reacting species at point s along the reaction coordinate. For this one-dimensional example concentration has units of particles per length, and the concentration in the reactants' region may be approximated by dividing N_A by twice the characteristic reactant length d_A, that is,

$$n_A(s = -s_A) = N_A/(2d_A) \tag{71}$$

Substituting Eqs. (70) and (71) into Eq. (69) yields

$$k^S = -\frac{D}{2d_A} \left.\frac{dn}{ds}\right|_{s=0} \Big/ n_A(s = -s_A) \tag{72}$$

Since products are missing, $n(s)$ must fall to zero within a few, say π, characteristic lengths beyond the barrier. Then

$$\left.\frac{dn}{ds}\right|_{s=0} \cong \frac{n(s = \pi d_{\ddagger}) - n(s = 0)}{\pi d_{\ddagger}} \tag{73a}$$

$$\cong -\frac{n(s = 0)}{\pi d_{\ddagger}} \tag{73b}$$

But for this one-dimensional example

$$n(s = 0) = n(s = -s_A) \exp(-V_{\ddagger}/RT) \tag{74}$$

Putting Eqs. (73b) and (74) into Eq. (72) yields

$$k^S = \frac{D}{2\pi d_A d_\ddagger} \exp \frac{-V^\ddagger}{RT} \tag{75}$$

and using Eqs. (67c) and (68) converts this to

$$k^S = \frac{D f_A^{1/2} |f_\ddagger|^{1/2}}{2\pi \tilde{k} T} \exp \frac{-V^\ddagger}{RT} \tag{76}$$

which is exactly the high friction limit of Kramers' result. Of course a dimensional analysis such as we have just presented is not guaranteed to yield the correct proportionality constant, but the precise value of the factor 2 and π in Eqs. (71) and (73) were chosen with the correct result in mind to make the answer exact.

For later discussion it is useful to rewrite Eq. (76) in a different notation. First, the usual notation for the reactant oscillator frequency is introduced:

$$\omega_A = (f_A/\mu)^{1/2} \tag{77}$$

where μ is the reduced mass for motion along s, and we introduce the usual imaginary frequency for the vicinity of the parabolic maximum

$$\omega_\ddagger = (f_\ddagger/\mu)^{1/2} \tag{78}$$

Also we introduce the friction constant ζ defined such that the frictional retarding force along the reaction coordinate is

$$F_{\text{fric}} = -\mu\zeta \frac{ds}{dt} \tag{79}$$

where ds/dt is the speed. (Thus, the units of ζ are inverse time.) By Einstein's relations, the diffusion coefficient for reaction-coordinate motion is related to the friction constant by [20d, 99]

$$\zeta = \frac{\tilde{k}T}{\mu D} \tag{80}$$

Substituting Eqs. (77), (78) and (80) into Eq. (76) yields

$$k^S = \frac{\omega_A \omega_\ddagger}{2\pi\zeta} \exp \frac{-V^\ddagger}{RT} \tag{81}$$

which is another form of the high friction limit of Kramers' result.

In the diffusive limit the system zigzags back and forth across the transition state ($s = 0$) many times during its motion from $s \cong s_A$ to $s \gg 0$. We can estimate the recrossing correction to transition state theory by comparing Eq. (76) to the conventional transition-state-theory result for the same unimolecular pseudo-one-dimensional model. The usual result is obtained as the pseudo-one-dimensional limit of Eq. (52). In the present case, $Q^\ddagger$ is replaced by unity since the system has only one coordinate, which is the reaction coordinate and is excluded from the transition state. Furthermore, the classical result for harmonic oscillator partition function is [2b, 10c, 19a, 34b]

$$Q^A = \frac{2\pi\tilde{k}T}{h\omega_A} \tag{82}$$

Then Eq. (52) becomes

$$k^\ddagger = \frac{\omega_A}{2\pi} \exp \frac{-V^\ddagger}{RT} \tag{83}$$

We define a frictional transmission coefficient by

$$\gamma^S = k^S/k^\ddagger \tag{84}$$

and, using Eqs. (81) and (83), we obtain

$$\gamma^S = \frac{\omega_\ddagger}{\zeta} \tag{85}$$

which is properly unitless and in the high friction limit is small. Thus the prediction of this analysis is that TST overestimates the rate constant in the high friction limit.

One can give an interesting microscopic interpretation to Eq. (85) by rewriting it in terms of characteristic times. In terms of the friction coefficient, the characteristic time for relaxation of momentum along the reaction coordinate is [99]

$$\tau_p = 1/\zeta \tag{86}$$

Furthermore, the time scale for crossing the energy barrier, given enough energy and the absence of friction, is

$$\tau_s = 1/\omega_\ddagger \tag{87}$$

Comparing Eqs. (85)–(87) shows that

$$\gamma^S = \tau_p/\tau_s \tag{88}$$

that is, the high friction limit of the transmission coefficient is the ratio of the relaxation time for momentum along the reaction coordinate to the time scale for frictionless traversal of the energy barrier.

So far we have considered the high friction limiting form. The result actually derived by Kramers [98] for the diffusion regime may be written

$$\gamma^{\zeta} = [(\tau_s/2\tau_p)^2 + 1]^{1/2} - (\tau_s/2\tau_p) \tag{89}$$

The limits of Kramers' result are

$$\gamma^{\zeta} \underset{\tau_p \to \infty}{\sim} 1 - \frac{\tau_s}{2\tau_p} + \frac{1}{8}\left(\frac{\tau_s}{\tau_p}\right)^2 \tag{90}$$

in the limit of very small friction and

$$\gamma^{\zeta} \underset{\tau_p \to 0}{\sim} \frac{\tau_p}{\tau_s} - \left(\frac{\tau_p}{\tau_s}\right)^3 \tag{91}$$

in the high friction limit. Equation (91) verifies that Kramers' result agrees with the result derived here in the high friction limit, as claimed above. The limiting form, Eq. (81), (85), or (88), is called the Smoluchowski limit because it can be derived from the Smoluchowski diffusion equation [99].

The simplest generalization of Kramers' treatment is to consider a multidimensional reaction but neglect the effect of solvent friction on all coordinates except the reaction coordinate [101, 115–118]. This yields a friction-influenced rate constant given by

$$k^{\zeta} = \gamma^{\zeta} k^{\ddagger} \tag{92}$$

where $k^{\ddagger}$ is now the standard multidimensional result. In this model τ_p is independent of s so, with a proper interpretation of τ_s, the correction of Eq. (89) could be applied to a hybrid variational transition state theory rate constant with as good a justification as it can be applied to a classical conventional transition-state-theory result.

In order for Eq. (88) or (89) to be useful for practical applications, we must be able to estimate τ_p, or equivalently ζ, for real systems. One model that is often used is Stokes' law. Stokes' law states that the frictional force on a sphere of radius a, moving with velocity $\vec{v}$, through a solvent of viscosity η, is

$$\vec{F}_{\text{fric}} = -(6 \text{ or } 4)\pi\eta a\vec{v} \tag{93}$$

where the 6 applies if the solvent sticks to the sphere and 4 applies if it slips over the sphere [119–121]. Comparison to Eq. (79) yields

$$\zeta = (6 \text{ or } 4)\pi\eta a/\mu \tag{94}$$

There is always a potential problem in determining atomic and molecular parameters like ζ from macroscopic observations, and the present example provides a prime example. Even aside from the difficulty of estimating an effective value for a, Stokes' law yields a friction coefficient appropriate for the time scale of viscosity, which is a long time scale compared to the relevant time scale τ_s for barrier crossing. One way to introduce the relevant time scales is to use a generalized Langevin approach [106–110, 119]. In this approach the frictional force of Eq. (79) is replaced by

$$F_{\text{fric}} = -\mu \int_0^\infty \zeta(\tau) \left.\frac{ds}{dt'}\right|_{t'=t-\tau} d\tau \tag{95}$$

where $\zeta(\tau)$ is the generalized friction coefficient and the frictional force now involves a memory of the whole past history of the particle. Grote and Hynes [118] reconsidered the Kramers' problem with this generalization, and they derived a transmission coefficient given by

$$\gamma^{\text{GH}} = \{1 + [\hat{\zeta}(\lambda_r)/2\omega_t]^2\}^{1/2} - \hat{\zeta}(\lambda_r)/2\omega_t \tag{96}$$

where λ_r is the reactive frequency, and $\hat{\zeta}(\lambda)$ is the Laplace transform of $\zeta(\tau)$ at frequency λ:

$$\hat{\zeta}(\lambda) = \int_0^\infty \exp(-\lambda\tau)\zeta(\tau)\, d\tau \tag{97}$$

Equation (96) is identical to Eq. (89) except that the Brownian friction coefficient ζ is replaced by $\hat{\zeta}(\lambda_r)$. In principle, λ_r should be obtained self-consistently, that is, it depends on $\hat{\zeta}(\lambda_r)$, but in zero order it equals ω_t.

Realistic models [122, 123] of the generalized friction show that $\hat{\zeta}(\omega_t)$ is often small because ω_t is typically faster than the collective solvent relaxation time which controls η. Thus $\hat{\zeta}(\omega_t)$ is dominated by infrequent hard collisions, and the frictional retardation of chemical reaction rates is expected to be considerably smaller than would be predicted by using Eqs. (86), (89), and (94), that is, by assuming the adiabatic solvent response of the Brownian dynamics model.

Other models of solute–solvent interaction can also be used, and in general these agree with the generalized Langevin result that the effect of friction is smaller than predicted by using Kramers' theory with a friction coefficient based on the viscosity [124, 125].

The models of solvent friction discussed above are classical and one-dimensional. Quantal effects [100a, 126–130], shielding of the reaction-coordinate motion from solvent interactions by other parts of the primary reaction system [102], and other multiatomic and multidimensional effects [101–104] have also been studied but are beyond the scope of the present chapter.

In the next section we consider the low friction limit where the local equilibrium assumption breaks down, and this has an easily recognized analogy to the low pressure falloff regime for gas phase unimolecular reactions. The high friction effects discussed in the present section also have analogies to high pressure effects on gas phase unimolecular reactions, but these are not so widely studied since one must consider pressures on the order of 10^2 atm to observe them in the gas phase [131–133].

2.4.3 Effect of Solvent on Rate of Creation of Transition States

The treatment of Section 2.4.2 still assumes that the reactants' phase space is populated at equilibrium and hence that those points in the phase space of the transition state that would eventually evolve to reactants if time were reversed are also populated at equilibrium. Since reaction rates are not measured at chemical equilibrium though, this is not a completely valid assumption. At chemical equilibrium the most reactive regions of reactant phase space are depleted by forward reaction faster than they can be repopulated by nonreactive processes but, by microscopic reversibility, these reactive phase-space regions are preferentially replenished by the reverse reaction. By the very definition of equilibrium the depopulation and replenishment occur at exactly the same rate and there is no net change in the phase-space distribution function. However, in any actual case where there is net forward reaction, even very close to equilibrium, the depopulation and replenishment do not balance. In general, the depopulation of the most reactive states dominates, and the actual rate is less than the (unmeasurable but in principle calculable) equilibrium rate constant. Phenomenologically it is generally found that, after a short transient period, the observed rate constant is, within experimental error, independent of the extent of reaction. If the transient period is shorter than the time necessary to build up appreciable back reaction, then the phenomenological, that is, observed, rate constant may be calculated as if products are absent, but this same rate constant will apply to any situation involving net reaction, even if the system is infinitesimally removed from chemical equilibrium. To prove this would require proof that there is only one slow time scale in the problem, and that the fast time scales are indeed fast enough that the phenomenological kinetic rate law holds before back reaction is appreciable. Instead, we accept this as an experimental fact for many systems. Then the consequences above may be inferred. In this section we discuss the deviation of the observed rate constant from the hypothetical equilibrium one.

Consider a reaction system A (for unimolecular reactions) or A + B (for bimolecular cases) in a solvent bath S, and assume that the reactants are dilute enough that we may neglect A–A, A–B, and B–B interactions. Also, on the basis of the previous paragraph, assume that the back reaction is negligible. If the interaction between reactants and the bath were very weak, the reactive states (i.e., regions of phase space) of A and B would be completely depleted and reaction would stop. Thus, after the transient period, the observed reaction rate would be zero. As we consider a sequence of artificial systems in which the

reactant–bath coupling is increased, the repopulation of reactive states occurs more readily, and the observed rate constant increases. If the strength of the reactant–bath coupling is measured by the friction constant ζ or $\hat{\zeta}(\lambda_r)$ of Section 2.4.2, then the observed rate constant k should be a monotonically increasing function of ζ until ζ is large enough so that repopulation is very fast compared to reaction even for the most reactive states. Then k may become independent of ζ. As ζ is increased still further, k should begin to decrease for the reasons discussed in Section 2.4.2. In this case, a plot of k versus ζ should have the shape shown in Fig. 1, part A, and labeled Kramers. This curve is labeled this way because this actually is the result predicted more quantitatively by Kramers' full treatment [98]. For the case he considered, there are no intrinsic recrossing effects; that is, transition state theory would be exact in the gas phase if reactant equilibrium could be maintained. Furthermore, the reaction was implicitly assumed to be slow enough that a plateau could be achieved where friction is strong enough to repopulate reactive states but weak enough not to cause diffusive slow down of transition state conversion to products. For other models of the reaction system and the reactant–bath coupling, one might obtain the other curve, simply (in fact, oversimply) labeled non-Brownian, in part A. Such a result was obtained, for example, by Skinner and Wolynes [124], who studied non-Brownian models for the reactant–bath coupling. They introduced a new parameter γ which is analogous to the ratio of solvent to solute masses for hard-sphere interactions. Thus the Brownian limit corresponds to $\gamma \to 0$, and in this limit they found that k is proportional to the first power of ζ. For high γ, however, this becomes ζ/γ. Thus at high γ, we are less likely to have a regime of system–bath coupling strength where equilibrium is maintained at the barrier

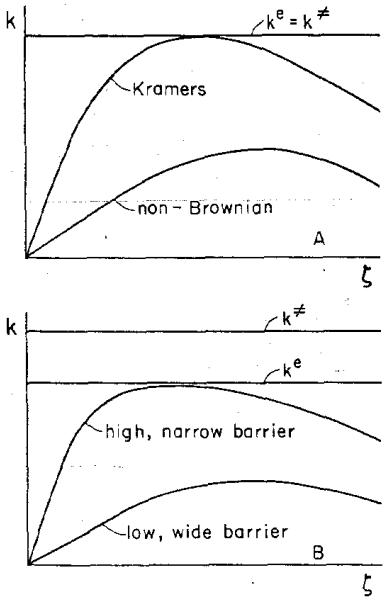

Fig. 1 Schematic illustration of the dependence of the rate constant on the solute–solvent coupling constant. Case A is a case where the equilibrium rate constant is given correctly by transition state theory and Case B is a case where it is not. The two curves shown for Case A represent typical results that would be calculated by Kramers' theory, with a Brownian treatment of the solvent coupling and by a more realistic stochastic treatment of the solvent coupling. The two curves shown for Case B illustrate two possible results that might be obtained by a stochastic treatment for different barrier shapes ▲.

but no effective system–bath collisions occur during passage over the barrier.

For some cases, the Liouvillian phase-space flow already includes recrossing, and the possible situations one may observe are illustrated in part B. The labels "high, narrow barrier" and "low, wide barrier" are oversimplified; the competition of reactive-state repopulation, reaction, and solvent interference with product conversion depends on the details of the nonreactive degrees of freedom and the frequency spectrum of the reaction coordinate motion. Nevertheless, slow reactions allow for faster rise of the low-ζ part of the curve and narrow barriers make it harder for solvent interactions to impede the barrier crossing, delaying the onset of the high-ζ behavior [124, 134].

In an isomerization or in some bimolecular reactions the repopulation of depleted reactive states of reactants is controlled by energy transfer from the solvent. In other bimolecular reactions the depopulation by reaction competes well even with the process of bringing reactants together. Since the reactive transition states are not present at equilibrium this looks superficially like a low friction case. A better analysis, however, is to use the following two-step mechanism:

$$\mathrm{A} + \mathrm{B} \underset{k_{-1}}{\overset{k_1}{\rightleftharpoons}} \mathrm{A}\cdots\mathrm{B} \underset{k_{-2}}{\overset{k_2}{\rightleftharpoons}} \mathrm{C} \qquad \text{(R1**)}$$

where $\mathrm{A}\cdots\mathrm{B}$ is an encounter complex, and we suppose that Step 1 is the rate limiting step. If we then consider the reaction $\mathrm{A}\cdots\mathrm{B} \rightarrow \mathrm{C}$, we will find a nonequilibrium distribution of reactants; that is, depopulation of reactive states of the encounter complex is faster than their repopulation by diffusion-controlled creation of new complexes. The transition state, $\mathrm{A}\cdots\mathrm{B}^{\ddagger}$, in $\mathrm{A}\cdots\mathrm{B} \rightarrow \mathrm{C}$ is thus also not in equilibrium with A + B, but this transition state is not the important one in this case, and we should not attempt to explain the friction dependence of the observed rate by applying generalized transition state theory to Step 2. Rather we should consider the transition states for the nonreactive process of diffusion. The observed rate constant will be proportional to the binary diffusion constant D_{AB}, which is inversely proportional to the friction coefficient. This familiar example illustrates the high friction limit for a transport process but the general theory of Section 2.4.2 shows that inverse dependence of a rate on the friction coefficient can also occur for a reactive transition state. In general parlance, the term diffusion-controlled reaction is generally applied only to reactions where the effect of friction occurs on the long-range spatial diffusion of reactants to form a short-lived reactive complex. This kind of diffusion-controlled reaction will be discussed further in Section 2.4.4. To avoid confusion with this generally accepted use of the term diffusion-controlled reaction, it may be preferable to use the term friction-controlled reaction to describe short-range diffusive effects at reactive transition states, as treated in Section 2.4.2.

The low friction limit in solution is very analogous to the low pressure unimolecular gas phase case discussed in Section 2.3. At low pressure or solute–solvent coupling, the number of activating collisions is insufficient to maintain the more reactive states of the molecule at equilibrium. The nonequilibrium

correction factor Γ depends on the frequency and the nature of these activating collisions. Rather than using a detailed theory [135] of these nonreactive collisions, it is often more appropriate to consider simple formulas [132, 134, 136, 137] for combining low-friction and high-friction corrections to transition state theory. The simplest procedure is to multiply the low-friction and high-friction corrections [132, 136, 137]. For the low-friction result we may use a strong collision result for the pseudo-one-dimensional parabolic case [137]:

$$\Gamma^{S} = 1 - \exp(-2\pi\zeta/\omega_{\ddagger}) \tag{98}$$

and for high friction we may use the Smoluchowski limit Eq. (85). The product approximation is particularly convenient for the analysis of Section 2.4.4. Skinner and Wolynes [137] suggested using a Padé approximant:

$$(\Gamma\gamma)^{SW} = \frac{2\pi\zeta}{\omega_{\ddagger}}\left[1 + \frac{2\pi\zeta}{\omega_{\ddagger}} + 2\pi\left(\frac{\zeta}{\omega_{\ddagger}}\right)^{2}\right]^{-1} \tag{99}$$

to interpolate between Γ^{S} and γ^{S}, and they obtained excellent agreement with the product of Γ^{S} times γ^{S}. Garrity and Skinner [130] suggested the even simpler Padé approximant:

$$(\Gamma\gamma)^{GS} = \frac{\zeta/\omega_{\ddagger}}{(2\pi)^{-1} + (\zeta/\omega_{\ddagger})^{2}} \tag{100}$$

Skinner and co-workers have also constructed higher-order Padé approximants for other collision models and other barrier shapes [124, 134].

2.4.4 Quasi-Thermodynamic Activation Parameters

In solution the standard state is ordinarily taken as $1M$. Then

$$K^{\ddagger,0} = V^{0}/N_{A}^{u} \tag{101}$$

where V^{0} is $10^{3}\,\mathrm{cm}^{3}$, and N_{A} is Avogadro's number. Following the same procedures as in Section 2.2.6 now yields

$$\Delta S^{a,0} = R\left(B_{2} - 1 + \ln\frac{hN_{A}^{u}B_{1}T^{B_{2}}}{V_{0}\tilde{k}T}\right) \tag{102}$$

and

$$\Delta H^{a,0} = E_{a} + (B_{2} - 1)RT \tag{103}$$

For unimolecular reactions $K^{\ddagger,0}$ is unity. Then Eq. (102) is replaced by

$$\Delta S^{a,0} = R\left(B_{2} - 1 + \ln\frac{hB_{1}T^{B_{2}}}{\tilde{k}T}\right) \tag{104}$$

but Eq. (103) is unchanged. For either molecularity $\Delta V^{a,0}$ is still given by Eqs. (51a) and (51b).

In solution we expect that both Γ and γ may be important, and we have given models for these two corrections in Sections 2.4.2 and 2.4.3. Then we have

$$\Delta G^{a,0} = \Delta G^{\ddagger,0} - RT \ln \Gamma^{\ddagger} - RT \ln \gamma^{\ddagger} - RT \ln \kappa^{\ddagger} \tag{105}$$

or

$$\Delta G^{a,0} = \Delta G^{CVT,0} - RT \ln \Gamma^{CVT} - RT \ln \gamma^{CVT} - RT \ln \kappa^{CVT} \tag{106}$$

where $\Gamma^{\ddagger}$ and Γ^{CVT} are the nonequilibrium correction factors for conventional transition state theory and canonical variational theory, respectively, $\gamma^{\ddagger}$ and γ^{CVT} are the recrossing factors, and $\kappa^{\ddagger}$ and κ^{CVT} are the tunneling corrections factors. We should include the effect of these quantities when interpreting quasi-thermodynamic activation parameters, although they are often neglected. Note that to a first approximation we may assume that γ^{CVT} is given by the formulas of Section 2.4.2, but $\gamma^{\ddagger}$ also includes recrossing of the conventional transition state by trajectories reflected at the CVT dynamical bottleneck. Thus, Eq. (106) may be more useful than Eq. (105).

2.4.5 Diffusion Control and Nearly Diffusion-Limited Reactions

In viscous media the rates of fast processes may be limited by the rate of encounter of pairs of reactants. The rate constant of encounter-controlled reactions, k_1 in reaction scheme (R1**), may be estimated from a steady state solution of the diffusion equation [10d, 138–140]. If k_2 in (R1**) is small, then $k_{-1} \gg k_2$. In this case it may be useful to ignore the encounter complex and consider the reactants in transition state theory to be A and B, as we have done above. Alternatively, in this limit, we can approximate k as $K_1 k_2$ where K_1 is k_1/k_{-1} in (R1**). The choice is based on computational convenience and does not reflect any change in the chemistry. For a fast rearrangement step or a slow diffusional step, as at high viscosity, the mechanism changes and we find that k equals k_1.

It is important to distinguish the two different high friction limits that have now been discussed in this chapter. In Section 2.4.2 we considered a high friction limit where the mechanism does not change; the rate constant is controlled by passage across an energetic or entropic barrier to rearrangement on a vibrational length scale, retarded by frequent interactions with a slowly relaxing solvent. In this section we have considered a system where the mechanism changes in the limit of high friction and/or fast covalency changes. The rate is then controlled by the diffusional approach of reactants over a much longer length scale of one or many solvation-shell radii.

3 TESTS OF TRANSITION STATE THEORY

Transition state theory has clearly passed one of the most difficult of all tests, the test of time, in that it has been found useful for about 50 years. TST

has many uses, ranging from *ab initio* prediction of rates to extrapolation and correlation of rates or qualitative interpretation of rates in terms of force field concepts. All the uses of TST can be tested by their internal consistency or their agreement with other approaches to the same problem. In this section, however, we will discuss only on a few attempts to most directly test the basic assumptions of TST by applications to very well-defined prototype systems. A more extensive review of this kind of test of TST has recently been published elsewhere [129]. We are concerned with the absolute accuracy of various versions of TST and also with their relative accuracy as compared to each other.

3.1 Tests for Gas Phase Reactions

Going as far back as 1930 or earlier, the $H + H_2$ reaction and its isotopic analogues have provided a key focus for theories of chemical kinetics [141]. The reason for this is that the reaction involves only three electrons and attempts to actually calculate the Born–Oppenheimer potential energy surface have always been more accurate for $H + H_2$ than for any other reaction [142]. At the present time the $H + H_2$ surface is believed known to a chemical accuracy of better than 1 kcal/mol [142–146]. Transition-state-theory calculations employing this potential energy surface and including tunneling calculations calculated by the Marcus–Coltrin path or small curvature approximations, are in good agreement with experiment (probably within experimental error) for $H + H_2$, $D + D_2$, $D + H_2$, $H + D_2$, and $Mu + H_2$ [43, 146–148]. (Note that Mu is an isotope of hydrogen in which the proton is replaced by a positive muon, which is only one ninth as massive.) The $Mu + H_2$ comparison is particularly noteworthy because the theoretical prediction, which is totally *ab initio*, was published [149] prior to the experiment, and because the quantum mechanical effects are very large for this system. The $D + H_2$ reaction is of special interest because experimental results [150, 151] are available down to the lowest temperature for this case. At 200 K the prediction of conventional transition state theory is too low by a factor of 45 for this reaction, and canonical variational calculations without tunneling are too low by a factor of 74. Including tunneling along the minimum energy path decreases the error to a factor of 13, but including the effect of reaction-path curvature in the tunneling calculation decreases the error to a factor of 1.2, which is within experimental error. The $H + H_2$ reaction is also noteworthy for being the easiest reaction to attack by accurate quantum mechanical scattering theory. Schatz and Kuppermann [152] have reported reasonably well-converged quantal dynamics calculations of the equilibrium rate constants of this reaction for a realistic potential energy surface (but not the most accurate available surface). Transition-state-theory calculations, including reaction-path curvature in the tunneling correction, agree with these calculations within a factor of 1.2 at 300–600 K, but are too low by a factor of 2 at 200 K [150]. This case involves very large tunneling corrections at low temperature, and that makes it hard to treat with high quantitative accuracy. There are two additional three-dimensional reactions for which reasonably accurate quantal equilibrium rate constants for a given potential energy surface are available [153]; such tests against accurate quantal results

provide the most definitive tests of approximate dynamical calculations like transition state theory because the same potential surface can be used. In contrast, comparison to experiment suffers the disadvantage that errors in the potential energy surface may either augment or partially cancel against errors in the approximate dynamics, and to an unknown extent. The two additional reactions for which comparison to quantal calculations is possible are H + BrH and H + BrD, and in these cases transition-state-theory calculations, again with a tunneling correction including reaction-path curvature, agree with the quantal results within a factor of 1.2 over the temperature range 150–500 K [153]. For H + BrH the tunneling correction is a factor of 1.6×10^2 at 150 K. There are also a large number of comparisons of conventional and variational transition-state-theory results to accurate quantal equilibrium rate constants for a purely collinear world; these are reviewed elsewhere [26, 43, 129]. The conclusion of these studies is that, in general, transition state theory is able to account adequately for quantum mechanical effects. When the conventional and variational results differ significantly, and sometimes they do, variational theory is systematically more accurate.

Several systematic surveys of the differences of conventional and variational transition-state-theory rate constants for three-dimensional atom transfer reactions with model potential energy surfaces have been reported [38, 154–158]. The largest differences between the two theoretical predictions occur for symmetric or nearly symmetric reactions in which the transferred atom is much lighter than either the atom donor or the atom acceptor. The large effect, which is due to a small zero point requirement in the vicinity of the saddle point, has been confirmed with an *ab initio* potential energy surface for the reaction $^{37}Cl + H^{35}Cl \rightarrow H^{37}Cl + {}^{35}Cl$ [45] and also, to a lesser extent, for the reaction $OH + H_2 \rightarrow H_2O + H$ [43, 44], which has a less extreme mass combination. For a temperature of 200 K, the ratio of the conventional transition-state-theory rate constant to the canonical variational theory one at 200 K is 110 for the $^{37}Cl + H^{35}Cl$ reaction and 2.7 for the $OH + H_2$ reaction. These ratios decrease to 28 and 1.9, respectively, at 300 K; the temperature dependence of this ratio is an indication that conventional transition state theory underestimates the energy of activation for the nontunneling contribution to the rate constants because of a higher internal-energy requirement at the least-recrossed dividing surface as compared to the saddle point dividing surface. Both reactions also show large tunneling corrections which exhibit large reaction-path curvature effects. Thus the tunneling corrections at 300 K are calculated to be 2 and 5, respectively, when reaction-path curvature is neglected, but 28 and 17, respectively, when it is included.

The comparisons of transition-state-theory results to accurate quantal equilibrium rate constants test the accuracy of the no-recrossing assumption and the incorporation of quantal effects. The validity of transition state theory also requires the satisfaction of the local equilibrium hypothesis, as discussed in Section 2.2.1.

3.2 Tests for Solution Phase Reactions

The fundamental questions of where or whether transition state theory applies to reactions in liquid solutions, and how to calculate the corrections when it does not, have received very much attention in the last five years. Most of this work is reviewed in a recent article on the current status of transition state theory [129]. Recent advances in the theory of reactions in solution have also been reviewed by Hynes [123]. In this section we provide a discussion of some principal issues.

An important source of knowledge of the validity of transition state theory in the gas phase is provided by comparisons to quantal-collision-theory calculations of equilibrium rate constants. This tests the dynamical bottleneck assumption and the incorporation of quantal effects, but it does not test the equilibrium assumption. The closest solution phase analogue is the comparison of transition-state-theory predictions to the results of many-body classical dynamics simulations. This tests the equilibrium and dynamical bottleneck assumptions but not the incorporation of quantal effects.

An important ingredient in classical dynamics simulations of rate processes in solution is the time-correlation-function approach [118, 159–166] to solution phase rate constants; this represents a generalization of the use of time correlation functions [20g, 167] for transport processes.

Two examples where full molecular dynamics calculations have been compared to transition-state-theory calculations for reactions in solution are the work of Allen and Schofield [168, 169] and Chandler, Berne, and co-workers [164, 165]. Allen and Schofield studied a low barrier, atom transfer reaction in the regime in which the rate constant increases with solute–solvent coupling; Chandler, Berne, and co-workers studied a conformational isomerization. They made stochastic simulations for both in the low and high friction regimes, and they performed two molecular dynamics simulations, one for a viscous solvent and one for a random, rigid lattice environment. The rate constant in the rigid environment was only 23% lower than that in the fluid, but a factor of 3.7 lower than transition state theory; they concluded that viscous continuum effects do not account for the main part of the solvent effect. A simple interpretation of the solvent correction factor is that collisions with individual solvent molecules are effective in transferring momentum to and from the reaction coordinate, thereby causing trajectories to recross the transition state. Further studies of these effects would be valuable.

4 SEMIEMPIRICAL CORRELATION: RATES, EQUILIBRIA, AND TRANSITION STATE STRUCTURES

In this section the emphasis is shifted from transition state *calculations* of reaction rates from known or assumed potential energy (or potential of mean force) surfaces to *correlation* of rates, using equilibrium data and transition state concepts to replace the missing potential surface information. For this we use

the term semiempirical theory. The semiempirical theories considered here involve simultaneous approximation of the internuclear dynamics and the governing electronic-structure-based potentials, in contrast to transition state theory per se, which is a statistical mechanical theory of the dynamics that presupposes the potential surface. The semiempirical models involve transition state concepts, but strictly speaking they are not transition state theory. A primary object of using such semiempirical models is the testing of the physical bases of the models and the characterization of TS structure.

Much of the work discussed in the following sections involves the numerical evaluation or estimation of standard-state-dependent quantities. In all these cases the standard state is a Raoult's law solution with a concentration of 1 *M*.

4.1 The Concept of a Variable Transition State Structure

4.1.1 Structure Maps and Parallel and Perpendicular Effects

Even among stable molecules, the electron distribution and sometimes the structure of a functional group shows systematic variation as attached substituents are varied. For example, the NMR chemical shift of F for meta-substituted fluorobenzenes, which reflects the electron density, varies systematically and significantly with the inductive parameter, σ_I, of the attached aromatic residue [170]. Transition states, which are less rigid structures than stable molecules, should be even more sensitive to such perturbations. Two-dimensional maps, showing the bond orders of two bonds for a set of transition states in a series of related reactions, have been introduced and used fruitfully to discuss these effects [171–173]. An example is given in Fig. 2.

The map shown in Fig. 2 is for a nucleophilic displacement reaction

$$A_i^- + BA_j \rightarrow A_iB + A_j^- \qquad \text{(R4)}$$

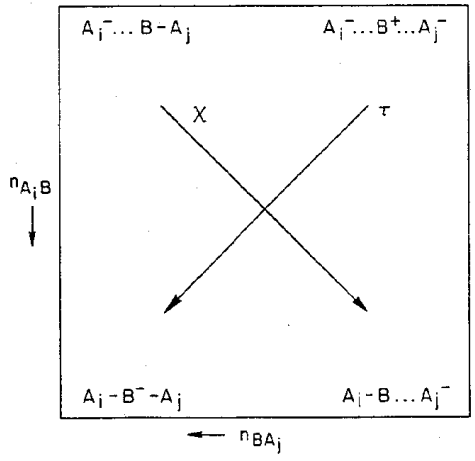

Fig. 2 A two-dimensional map for locating the transition state for the nucleophilic displacement, $A_i^- + BA_j \rightarrow A_iB + A_j^-$. The coordinates represent bond orders.

In the map we use the formal designations

$$A_i^- \cdots B^+ \cdots A_j^- \qquad \text{and} \qquad (A_i\text{–}B\text{–}A_j)^-$$

to denote noncovalent dissociative and hypervalent associative structures, respectively. The upper left corner of the map corresponds to a system for which the transition state has the reagents, still with their original covalency, correctly positioned for the covalency changes to begin. The diagonal from upper left to lower right is the locus of TSs for concerted displacement reactions in which the sum of the two bond orders remains constant and, approximately, so does the A_i–A_j distance and the total electron density of B. The upper right corner of the map corresponds to dissociative TSs, and the lower left corner to associative TSs. As compared to concerted TSs, the A_j–A_i distance should be larger for dissociative TSs and smaller for associative ones. At least in a qualitative sense, the sum of the bond orders, the A_j–A_i distance, and the formal charge on B (positive for dissociative cases and negative for associative ones) are all correlated. Two parameters have been defined to locate the TS on the map experimentally [174]. The first parameter, τ, is a measure of the tightness of the transition state [175]. It is zero in the upper right corner, 2 in the lower left, and 1 along the upper-left-to-lower-right diagonal. Thus it is formally equal to the total bond order to B. The second parameter, χ, is orthogonal to τ and increases from upper left to lower right; for a fixed total bond order of B, it measures the A_i–B bond order. The parameter χ, which we call the Leffler–Hammond parameter, has previously been represented by α [175], but α is also used to represent the slope of a Brønsted plot, and we will see that χ and this slope are not the same, except along the upper-left-to-lower-right diagonal of the map. For historical reasons, and because of its relation to the Brønsted parameter, χ is given the value 0.0 at the upper left corner, 0.5 at the center, and 1.0 in the lower right corner of the map [175]. For a three-atom, collinear reaction, specification of the τ and χ values of the TS would be formally sufficient to specify its structure.

Transition state maps such as Fig. 2 are convenient for illustrating the changes that the conventional TS structure undergoes when reaction conditions or the reactants themselves are changed. To some extent these rules may be extended to apply to variational transition states, and thus these maps are relevant to trends in $\Delta G^{\ddagger,0}$ or $\Delta G^{\mathrm{CVT},0}$.

In the TS for (R4) the reacting bonds, A_i–B and B–A_j, are partly ionic, and we may consider the transition state to be a resonance hybrid with four valence structures: $A_i\text{–}B^-\text{–}A_j \leftrightarrow A_i^- \cdot B^+ \cdot A_j^- \leftrightarrow A_i^- \cdot B\text{–}A_j \leftrightarrow A_i\text{–}B \cdot A_j^-$. First, we consider a case where $i = j$ and the contributions of the third and fourth structures are equal. If the energy of the second resonance structure is lowered, for example by making the solvent more polar, then, because of the character of the variation method for quantum mechanical energy and wave function calculations [176], the contribution of the second structure to the resonance hybrid is increased. An important point is that the change in the composition of the resonance hybrid

and the resultant change in the bond lengths are mutually reinforcing, that is, if the change in the resonance hybrid favors longer bonds, then longer bonds further favor the increased component of the resonance hybrid. Such electronic factors are reflected in the locations of the saddle points on the potential energy surface. For this kind of change the potential energy factors are also reinforced by partition function changes. Consider, for example, a low frequency spectator vibration whose force constant is lowered by the change in the resonance hybrid. This will promote a greater relative population of states with a large amplitude for this vibration, and in turn systems at a large amplitude extension of this vibration will favor the increased component of the resonance hybrid even more. All these changes affect τ in the same way; they lower it. These effects are special cases of the general rule that, in any coordinate that is orthogonal to the reaction coordinate, the transition state is expected to respond to perturbations in the same way as a stable molecule—it becomes more similar to any structure in its hybrid manifold that is stabilized; this is called Thornton's rule or the perpendicular effect [177, 178].

Next consider a case where $i = j$ and the electronegativity of A_j is increased so that the hybrid structure is stabilized by increasing the contribution of the fourth valence structure. Since geometries in which the fourth valence structure is favored can only be reached by passing through structures in which the $B–A_j$ bond is shorter, which therefore benefit less from the increase in electronegativity of A_j, such an arrangement of the system now becomes the conventional transition state. Thus, in the reaction coordinate, the *geometry* of a conventional TS responds to a perturbation by shifting *away* from the stabilized structure; this is called the Leffler–Hammond principle or the parallel effect [178–181]. The final outcome for the electron density depends on the nature of the perturbation, but, in the example given, the ionic character of A_j in the perturbed TS would still be somewhat larger than that in the unperturbed. Such a change in the structure of A_j will make (R4) faster rather than slower.

In more complicated systems more than two coordinates may need to be considered explicitly, but the same principles apply.

A source of problems in complex cases is the difficulty in identifying the TS reaction coordinate. The reaction coordinate is a normal mode of the conventional TS; at a generalized TS it may be identified with the minimum-energy path [37, 44, 47]. It is orthogonal to all other normal modes, including the molecular rotations and translations of the center of mass; a small displacement along the reaction coordinate should not induce a reaction in some other dimension. The reaction coordinate must be identified in order to decide to which perturbations the parallel effect applies and to which the perpendicular effect applies.

We should emphasize the distinction between Fig. 2 and a potential surface map. The points on Fig. 2 all correspond to tradition states, but for different reactions. In contrast, a conventional potential energy [182] contour or perspective map shows the potential energy as a function of bond coordinates or bond orders for a single reaction. A variable transition state map can be used to

discuss $\Delta G^{\ddagger,0}$ or $\Delta G^{CVT,0}$, but not $\Delta G^{a,0}$ except approximately when it is dominated by $\Delta G^{\ddagger,0}$ or $\Delta G^{CVT,0}$. However, a potential surface map for a single reaction cannot be generalized to show free energy of activation since $\Delta G^{GT,0}$ is a function of the location of a dividing surface, not of the location of a configuration point.

4.1.2 Marcus Formalism

Many of the ideas in Section 4.1.1 can be given simple and convenient quantitative expression in the Marcus formalism [10e, 183–190], which is summarized by

$$\Delta G^{a,0} = W^{r,0} + \Delta G^* \tag{107}$$

$$\Delta G^* = (1 + \Delta G^{0\prime}/\lambda)^2 \lambda/4 \tag{108}$$

Equation (107) purports to partition the phenomenological $\Delta G^{a,0}$ into one part, ΔG^*, which arises from the covalency† and structural changes during the actual rearrangement, called the $*$ step, and which correlates with $\Delta G^{0\prime}$ and λ, which are explained below, and another part, $W^{r,0}$, which represents the free energy (work) necessary to reach the configuration in which the $*$ step can take place. For bimolecular reactions in solution, this configuration corresponds to a specialized encounter complex, perhaps with a particular orientation and a certain degree of desolvation that must precede any covalency change. In cases where the unchanged reactants have an affinity for each other, for example have opposite charges or form a charge transfer complex, $W^{r,0}$ may be negative. The configuration immediately preceding the $*$ step may be called a reaction complex [191], or, more aptly, a precursor configuration, PC, and the analogous quantity on the product side may be called a successor configuration, SC; these terms are more suitable than encounter complex, which appears to imply the necessity for a potential minimum or that the reactants only need to be in contact. The numerical value of $W^{r,0}$, like $\Delta G^{a,0}$, depends on the standard states chosen. The overall free energy change for the $*$ step is $\Delta G^{0\prime}$. The quantity $\lambda/4$ is called the intrinsic barrier, and it is ΔG^* for the special case that $\Delta G'$ is zero. The standard free energy for making the final, separated products into the SC is $W^{p,0}$ and

$$\Delta G^{0\prime} = \Delta G^0 - W^{r,0} + W^{p,0} \tag{109}$$

where ΔG^0 is the overall standard state free energy difference of products from reactants.

Note that the PC and SC are introduced into the theory for two possible reasons: (1) in some cases they are actual local minima in the potential surfaces,

†In electron transfers, covalency changes are understood to include the transfer of an electron from one atomic center to another. In that case the adiabatic location of the electron may be strongly coupled to several varieties of interatomic distances and angles.

that is, intermediates, and better semiempirical correlations can be obtained by considering the unimolecular transformation between these species than by considering the whole reaction; (2) even when intermediates do not exist, certain contributions to $\Delta G^{a,0}$ are not expected to correlate with ΔG^0; these contributions include gas-phase steric factors, orientation effects in a solution-phase encounter complex, or specific desolvation effects such as desolvation of a hydrogen bond for reaction to a non-hydrogen-bonding substrate [192]. In case (2) the separation of the two kinds of contributions is somewhat arbitrary but may still be useful.

The PC is not necessarily a metastable complex. In order for the PC to serve the role discussed above, it may be necessary to define it as corresponding to a restricted range of values for one or more coordinates. With this definition one could then, in principle, calculate its partition functions and hence $W^{r,0}$.

Marcus theory was originally developed as a model for $\Delta G^{\ddagger,0}$ of outer-sphere electron transfer processes [183, 184, 193]. It was assumed that the actual movement of the electron in such processes is an electronically adiabatic Franck–Condon process. The structural changes required to produce a critical configuration, in which the diabatic electronic energy is the same with the electron in either the donor or the acceptor parts, are regarded as producing ΔG^*. A possible derivation proceeds as follows. If the force fields of reactants and products are harmonic, and the structural changes leading to the rearrangement are regarded as linear combinations of displacements in orthogonal coordinates x_n of the donor and acceptor, then the energy required for a structural change beginning at the PC is

$$V = \tfrac{1}{2}\sum_n f_n^{PC}(x_n - x_{n,0}^{PC})^2 \tag{110}$$

where f_n^{PC} is a force constant and $x_{n,0}^{PC}$ is the PC equilibrium value of x_n. Since the coordinates are orthogonal the displacements may be written in terms of their projections on a reaction coordinate x as

$$(x_n - x_{n,0}^{PC}) = c_n^{PC}x \tag{111}$$

Combining these equations shows that the energy required to reach the critical configuration is a parabolic function of the reaction coordinate with an effective force constant f_{eff} which is a weighted average of the force constants of the coordinates involved. That is,

$$V = \tfrac{1}{2}f_{eff}^{PC}(x - x_0^{PC})^2 \tag{112}$$

where

$$f_{eff}^{PC} = \sum_n f_n^{PC}(c_n^{PC})^2 \tag{113}$$

After the electron has been transferred, relaxation to the SC is governed by

similar equations, in the same coordinates, but with $x_{n,0}^{SC}$ replacing $x_{n,0}^{PC}$. In principle, f_{eff} is different for the precursor and successor complex, because the individual f_n are different, and the differences may be largest for those coordinates with the largest weights in Eq. (113). Marcus theory assumes nevertheless that f_{eff}^{SC} equals f_{eff}^{PC}. This is better justified for symmetric reactions than for nonsymmetric ones. In terms of Eq. (113) and its analogue for deviations from the SC, the reaction model becomes that shown in Fig. 3. λ is defined as the energy required to distort the structure of the PC to that of the SC, without the electron transfer or other covalency change; therefore

$$\lambda = \tfrac{1}{2} f_{eff}^{PC} \Delta x^2 \tag{114}$$

where

$$\Delta x = x_0^{SC} - x_0^{PC} \tag{115}$$

for the particular case that $\Delta G' = 0$. Further algebraic manipulation yields the following expression for the potential at the intersection of the parabolas

$$V_0^{\ddagger} = (1 + V'/\lambda)^2(\lambda/4) \tag{116}$$

where V' is the potential difference between SC and PC. A special case for a symmetric reaction, is

$$V_0^{\ddagger}(V' = 0) = \lambda/4 \tag{117}$$

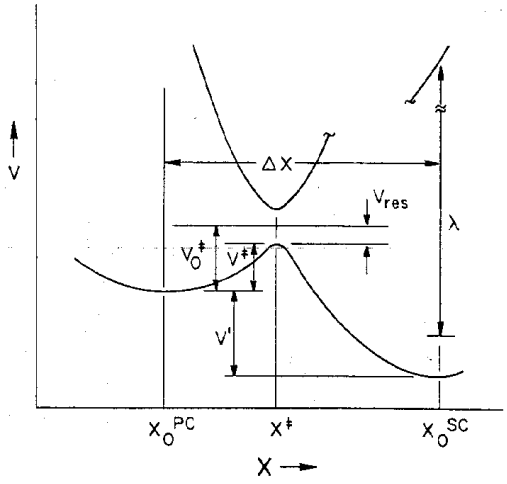

Fig. 3 A model for a derivation of the Marcus theory of electron, atom, or group transfer. To the left of the avoided crossing the lower potential curve represents $V = \frac{1}{2} f_{eff}(x - x_0^{PC})^2$ and the upper one represents $V = \frac{1}{2} f_{eff}(x - x_0^{SC})^2 + V'$. To the right of the avoided crossing the meanings of the two curves are interchanged. Note that, as drawn, V' is negative.

Next we introduce the resonance energy V_{res} resulting from the combination of the precursor valence structure and the successor valence structure at the critical configuration. In the electron transfer example it is the delocalization energy of the electron between the donor and the acceptor. The actual barrier height is given by

$$V^{\ddagger} = V_0^{\ddagger} - V_{res} \tag{118}$$

Equations (115) and (118) plus the assumption that V_{res} is small and the replacement of potential energies by free energies of activation yield Eq. (108), which was our goal. For reactions other than weak-coupling electron transfers, V_{res} is generally not small; however, if it is constant within a family of related reactions, the replacement is still approximately valid if $\lambda \gg V'$ and λ is determined empirically, via Eq. (117).

The replacement of potential energies V with free energies of activation involves the conceptual difficulties discussed in Sections 2.2.6, 2.4.4, and 4.1.1. Its validity rests primarily on the correspondence of Eqs. (107) and (108) with experimental results.

The original Marcus theory for electron transfer [183, 184] has been generalized to the case of proton and atom transfers [185, 186] and group transfers [175]. Now V_{res}, which was electronic delocalization energy for the electron transfer case, becomes the valence bond resonance energy for $A^- \cdots B\text{–}A_j \leftrightarrow A_i\text{–}B \cdots A^-$. It also includes effects due to readjustment of bond lengths along curvilinear reaction paths. Since the original theory was justified in the limit of small V_{res}, that is, small overlap or weak coupling, this extension shifts the justification for the resulting equations even farther in the empirical direction.

The discussion above shows that the physical model behind the Marcus relations is more closely related to $\Delta G^{\ddagger,0}$ than to $\Delta G^{a,0}$. Thus one might expect significant qualitative breakdown of these relations if variational-transition-state-theory optimization effects, recrossing, tunneling, internal state nonequilibrium, or solvent friction are important. However, with the introduction of the empirically determined λ, Eq. (120) may become a better approximation of $\Delta G^{CVT,0}$ than of $\Delta G^{\ddagger,0}$.

Two further points are worth noting. The two parabolas in Figure 3 do *not* refer to the donor and the acceptor, or to the A_i–B and A_j–B stretching modes. Each parabola refers to the deformation of the whole system, including both the donor and the acceptor in both cases, with appropriate contributions from their solvation shells. In the case of electron transfer, the most important contributors to x are probably the breathing modes of the inner ligand shells of the donor and acceptor. In many cases, x is not easily visualized. The second point, is that it is *not* an improvement to replace the parabolas with Morse functions of modest well depth [194], because this misrepresents the nature of x. In most cases the further extension of x, without electron transfer or covalency change, beyond the point at which such changes would normally take place, would lead to very

large potential energies, as nonbonding interactions would increase greatly.

As discussed above, an important assumption in the Marcus model is that $f_{\text{eff}}^{\text{PC}} = f_{\text{eff}}^{\text{SC}} = f_{\text{eff}}$. Another assumption is that neither f_{eff} nor Δx varies along the series of reactions being correlated. If these assumptions are not valid then the conclusions drawn about transition state structure from the Marcus formalism may need modification [175].

The generality of Eqs. (107) and (108) may be emphasized by noting that they are equivalent to

$$\Delta G^{a,0} = c_0 + c_1(\Delta G^0) + c_2(\Delta G^0)^2 \tag{119}$$

where

$$c_0 = W^{r,0} + [\lambda - (W^{r,0} - W^{p,0})]^2/(4\lambda) \tag{120}$$

$$c_1 = [1 - (W^{r,0} - W^{p,0})/\lambda]/2 \tag{121}$$

$$c_2 = 1/(4\lambda) \tag{122}$$

Equation (119) is simply a quadratic free energy relation (QFER). Since linear free energy relations (LFERs) are so widely applicable [195–197], QFERs may also have a wide validity range. The Marcus relation, Eqs. (107) and (108) or Eq. (119), can be regarded as simply an extension and explanation of the successful Brønsted catalysis law [178, 198–201]; as such, it is likely to accommodate almost any set of rate and equilibrium constants in which there is a systematic relation between the two. The accommodation of data by the formalism does not prove that the model is correct. To the extent, however, that it is, it provides us with parameters, τ and χ, that are related to transition state structure, as will be discussed in Section 5.

We now consider a system of nucleophilic displacement reactions (R4) for which rate constants are known for both symmetric variants:

$$A_i^- + B\text{–}{}^*A_i \rightarrow A_i\text{–}B + {}^*A_i^- \tag{R5}$$

and

$$A_j^- + B\text{–}{}^*A_j \rightarrow A_j\text{–}B + {}^*A_j^- \tag{R6}$$

and for which all equilibrium constants are also available. In the TS for the *ii* variant (R5) there are no A_i–B bonds if the mechanism is dissociative (upper right corner of Fig. 2), one if bond making and breaking are completely coupled (on the diagonal of Fig. 2) and two if the mechanism is associative (lower left corner of Fig. 2). In all cases there is one A_i–B bond in the reactant. The former numbers, which are identical with the τ values for these TSs, can be related to $d(\Delta G_{ii}^{a,0})/d(\Delta G_{ij}^0)$, where ΔG_{ij}^0 refers to (R4), if a convenient A_j^- is chosen and if the A_i^- form a series of structurally related nucleophiles in which both $\Delta G_{ii}^{a,0}$

and ΔG_{ij}^0 respond linearly to the bond order. A Hammett series of *m*- and *p*-substituted nucleophiles is ideal for this purpose. The result should be independent of the choice of A_j^- because, regardless of that choice, (R4) forms a full bond to A_i and removes a unit charge, and (R5) does not involve A_j^-. Since it gives acceptable values at the extremes and on the diagonal and is experimentally accessible, $d(\Delta G_{ii}^{a,0})/d(\Delta G_{ij}^0)$ is taken as the definition for $(\tau - 1)$. For the same reaction, if A_j^- were varied instead of A_i, $d(\Delta G_{ii}^{a,0})/d(\Delta G_{ij}^0)$ would give $(1 - \tau)$.

The generalized Brønsted exponent α may be defined as $d(\Delta G_{ij}^{a,0})/d(\Delta G_{ij}^0)$. This has been thought to measure the symmetry of the TS [175]. However, we note that α, so defined, will be zero for any TS with $n_{A_jB} = 0$ if only A_i is varied, and will give the fractional $B{-}A_j$ cleavage if only A_j is varied. Thus, α is not a simple measure of TS symmetry and is not likely to be single-valued if both A_i and A_j are varied.

If Equations (107) and (108) are accepted, an experimentally available, single-valued parameter, identifiable with the similarity of the TS to reactants or products, can be defined by $\Delta G_{ij}^0/(2\lambda)$. This is $\frac{1}{2} + [\partial(\Delta G_{ij}^{a,0}/\partial(\Delta G_{ij}^0)]\lambda$, which has been incorrectly identified with the experimental α [185, 191]. It is more reasonably identifiable with $(\chi - \frac{1}{2})$. The range of $\Delta G_{ij}^0/(2\lambda)$ is $-\frac{1}{2}$ (for $\Delta G_{ij}^0 = -\lambda$; $TS = A_i^- \cdots B{-}A_j$) to $+\frac{1}{2}$ (for $\Delta G_{ij}^0 = \lambda$; $TS = A_i{-}B \cdots A_j^-$) over the range of applicability of Eq. (108). A TS with $\Delta G_{ij}^0 = 0$ is modeled as having a structure equally resembling reactants and products. This is true even if $n_{A_iB} = n_{A_jB} = 0$ in the TS. In that case, $\Delta G^{a,0}$ is the same for the forward and backward directions, and the TS is found in the upper right corner of the map. A line projected from that TS, perpendicular to the diagonal from reactants to products, strikes that diagonal halfway between them, as required.

The utility of this definition is apparent when $d(\Delta G_{ij}^{a,0})/d(\Delta G_{ij}^0)$ is obtained from Eq. (119). If $\Delta G^{0\prime}$ can be equated to ΔG^0 ($W^{r,0}$ and $W^{p,0}$ assumed equal) we get

$$\frac{d(\Delta G_{ij}^{a,0})}{d(\Delta G_{ij}^0)} = \frac{1}{2} + \frac{\Delta G_{ij}^0}{2\lambda} + \frac{1}{8}\left[\frac{d\lambda_{ii}}{d(\Delta G_{ij}^0)} + \frac{d\lambda_{jj}}{d(\Delta G_{ij}^0)}\right] - \frac{\Delta G_{ij}^{02}}{8\lambda^2}\left[\frac{d\lambda_{ii}}{d(\Delta G_{ij}^0)} + \frac{d\lambda_{jj}}{d(\Delta G_{ij}^0)}\right] \tag{123}$$

which leads to

$$\alpha = \chi \pm (\tau - 1)/2 \mp (\tau - 1)[(\Delta G_{ij}^0)^2/(2\lambda^2)] \tag{124}$$

when the definitions of α, τ, and χ are appropriately substituted. The upper signs apply if i is varied. The last term in Eq. (124) will frequently be small, since $\Delta G_{ij}^0 \ll \lambda$ in many cases of practical interest. Figure 4 shows the appearance of the Brønsted plots predicted by Eq. (124) for several values of τ.

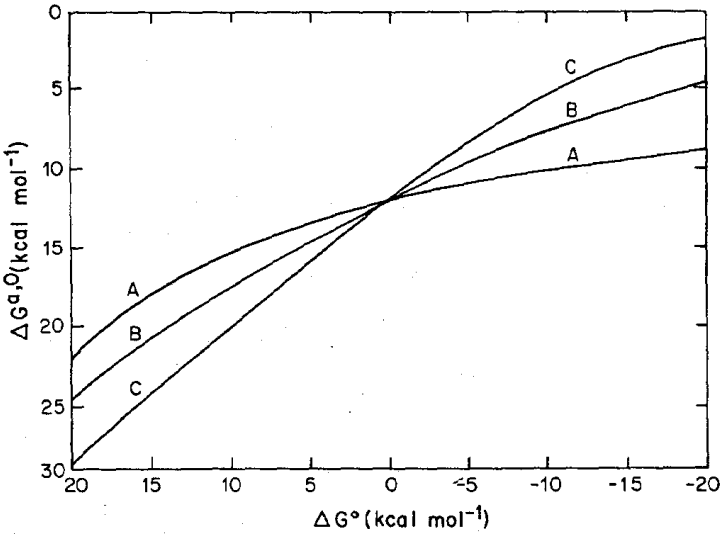

Fig. 4 Brønsted plots corresponding to $\tau = 0.5$(A), $\tau = 1.0$(B), and $\tau = 1.5$(C), with i varied and j constant. $\lambda_{ii,0} = \lambda_{jj} = 40$ kcal/mol; $\lambda_{ii} = \lambda_{ii,0} + 4(\tau - 1)\Delta G^{0}_{ij}$; $\lambda = (\lambda_{ii} + \lambda_{jj})/2$; $W^{r,0} = W^{p,0} = 2$ kcal/mol. $\Delta G^{a,0}$ was calculated according to Eqs. (119)–(122).

4.2 An Attempt at a Less Empirical Theory

In the semiempirical theory discussed above, most difficulties are circumvented by using experimental quantities. Although some structural information can be obtained by this method, much remains ambiguous. The experimental quantities implicitly contain the missing information. Levich, Dogonadze, Kuznetsov, Ulstrup (LDKU), and their co-workers have made ambitious attempts to model electron and atom transfer reactions from a less empirical perspective [202–210]. Their models have a strong emphasis on the transmission coefficient, which is treated in terms of transition probabilities along an approach coordinate, as in the (historically later) large curvature approximations [45, 47, 71–75] discussed in Section 2.2.5. We will present a highly simplified model based on their original treatments for a reaction dominated by internuclear tunneling. The LDKU model for electron transfer has roots in the original work of Gurney [211] and Libby [212], which is also the starting point for the Marcus theory. We will discuss the model for a solution phase proton transfer from an acid, AH, to a base, B.

The model to be considered in this section visualizes the reaction occurring in several stages. In the first, the reactants find one another and adopt a configuration from which tunneling will occur. This configuration is analogous to the PC of Section 4.1.2. The formation of this PC presumably brings the reactants closer than they would be at minimum potential energy, which corresponds to a hydrogen-bonded complex or other associated entity, depending on the reaction. It also requires a solvent polarization. The energy of the solvated PC with

respect to the separated reactants is ΔE^*_{PC}. The formation of the PC reduces the system's partition function from the product of the two independent partition functions Q_{AH} and Q_B to the single partition function Q^*_{PC}, which is to be computed with the distance between AH and B and their orientation confined to narrow limits. The ratio of partition functions does not appear in the work of Bruniche-Olsen and Ulstrup [207] and is not needed for the purposes to which those authors have put this theory, but we insert it to make the present treatment more realistic and more similar to our earlier discussions of TST.

The degrees of freedom of the PC, including the solvent with which it interacts, are then divided into two classes: the high frequency, quantized oscillations and the low frequency modes, which are treated classically. In the present example, for which the PC is A–H $\cdots$ B, the high frequency modes include only one mode coupled strongly to the reaction coordinate; this is the perturbed A–H stretching mode; the low frequency modes include the solvent modes that are coupled to the hydrogenic mode. This model assumes that, for reaction to occur, one of the quantized energy levels of the PC must match an energy level of the SC, which is $A^- \cdots H\text{–}B^+$. This matching cannot be achieved with high probability by progressive excitation of the A–H stretching vibration or by transfer to form a vibrational excited BH^+ because the vibrational states in which a proton motion is excited are too widely spaced. For a harmonic oscillator with a fundamental frequency of 3000 cm^{-1}, the first excited state lies above the ground state by over 8 kcal/mol. For the most part, therefore, matching is achieved by distortion of the low frequency modes and the solvent structure, treated classically. For a given quantum number n, of the A–H stretching mode, the frequency with which such structures will be achieved is given by $\nu_{eff} \exp(-\Delta E^*_S/RT)$, where ν_{eff} is the effective frequency in oscillations per unit time with which the classical modes explore the relevant domain, and ΔE^*_S is the energy which must be added to the classical modes in order to reach the isoenergetic arrangement. Thus $\exp(-\Delta E^*_S/RT)$ is the Boltzmann factor for an arrangement of the classical modes which makes the energy of quantum state n of the PC equal to that of an allowed quantum state of the SC. If the energy of the quantum state n of the A–H stretching mode is denoted ΔE_n, and the probability of crossing from a reactant structure to a product structure is denoted κ_n, then this model yields

$$k = \frac{Q^*_{PC}}{Q_{AH}Q_B} \exp\left[-\left(\frac{\Delta E^*_{PC}}{RT}\right)\right] \nu_{eff} \sum_n \kappa_n \exp\left[-\left(\frac{\Delta E^*_S + \Delta E_n}{RT}\right)\right] \quad (125)$$

For the rest of this discussion, we then simplify Eq. (125) by assuming that we are dealing with symmetric or exoergic examples.

Order-of-magnitude estimates of $Q^*_{PC}/Q_{AH}Q_B$ and ΔE^*_{PC} can be made [191, 206, 213, 214]. They also appear in the Marcus version of the theory and give rise to $W^{r,0}$ [183]. In evaluating the related quantities, ΔE^*_S, ΔE_n, κ_n, and R^*, which does not explicitly occur in Eq. (125) but is discussed next, it has generally

been assumed that the A–H mode is similar to that of the isolated molecule and is approximately harmonic, with a frequency $\bar{\nu}$ of about 3000 cm^{-1} assumed when a particular value was required [204, 206], but a Morse function has also been used. For our purposes we can regard R^* as the distance across which the proton travels in the dominant reaction path. It is determined by two countervailing effects. At large R^*, ΔE_S^* is small, but κ_0 is very small because the proton must tunnel a long way through a region of high potential energy (negative kinetic energy). At small R^*, κ_0 is high, but E_{PC}^* is high, due to the mutual repulsion of the reactants. Between these extremes a compromise is found which maximizes k. For proton transfer below the top of the barrier, which is the predominant route, κ_0 is determined in this model by an overlap factor for the vibrational wave functions of reactants and products at a distance R^*, and this factor can be estimated for particular values of R^*. R^* has also been estimated on the basis of the known structures of hydrogen bonded substances [204]. An important, qualitative point in this model is that most product is formed via the ground vibrational level of the A–H stretch, with $n = 0$ and $\Delta E_0 = \frac{1}{2}hc\bar{\nu}$, by tunneling through a barrier [207, 208]. For symmetric reactions most product would, correspondingly, be formed in the ground vibrational state.

If the A–H and H–B^+ reactant and product vibrational modes are assumed to be harmonic, ΔE_S^* is given by [183, 185, 207]

$$\Delta E_S^* = (\Delta E_{S,0} + \delta\Delta G^0)/(4\Delta E_{S,0}) \tag{126}$$

The standard free energy of acid dissociation of BH^+ less that of AH is called $\delta\Delta G^0$; the reactant-to-product solvent reorganization energy for the particular case that $\delta\Delta G^0 = 0$ is called $\Delta E_{S,0}$. We have followed the original authors here in ignoring the difference between potential energies and free energies of activation. When the value of ΔE_S^* from Eq. (126) is inserted in Eq. (125), the result is readily cast in the form of Eq. (119). The coefficients now have the values

$$c_0 = -RT \ln\left(\frac{Q_{PC}\nu_{eff}\kappa_0}{Q_{AH}Q_B}\right) + \Delta E_{PC}^* + \frac{\Delta E_{S,0}}{4} \tag{127}$$

$$c_1 = 1/2 \tag{128}$$

$$c_2 = 1/(4\Delta E_{S,0}) \tag{129}$$

Comparison with Eqs. (120)–(122) for the case that $W^{r,0} = W^{p,0}$ shows that $\Delta E_{S,0}$ can be identified with λ, and $W^{r,0}$ can be equated to $-RT \ln Q_{PC}\nu_{eff}\kappa_0/Q_{AH}Q_B + \Delta E_{PC}^*$. When it is observable, the curvature of the Brønsted plot may permit $\Delta E_{S,0}$ to be estimated, although it should be noted that κ_0, which occurs in c_0, is a function of ΔG^0 and should alter this curvature. A straightforward modification of this treatment, introducing ΔG^0, would deal with endoergic examples.

Since they are formally so similar, the same results that are consistent with

the Marcus version of the theory are also consistent with the Levich–Dogonadze–Kuznetsov–Ulstrup model. However several differences of interpretation are apparent. In the Marcus version the origin of λ is not specified, and its value is to be obtained by averaging λ for the two related symmetrical reactions. In the LDKU model, the origin of $\Delta E_{S,0}$ is specified, and in favorable cases it might be estimated. On the other hand, it is not apparent from the LDKU model for $\Delta E_{S,0}$ that the averaging procedure, which appears to work well in many cases [175, 215], should do so. Although there have been suggestions that the Marcus $W^{r,0}$ is not independent of ΔG^0 [191, 216, 217], it has usually been assumed to be constant. The LDKU equivalent of $W^{r,0}$ contains κ_0, which clearly depends on ΔG^0. Since $\kappa_0 < 1$, the way it enters the LDKU expression for $W^{r,0}$ would make that quantity larger, as would ν_{eff}, and $\Delta E_{S,0}$ could easily be small in the LDKU model. Large values of $W^{r,0}$ and correspondingly small values of λ have been hard to explain in standard interpretations of Marcus theory [191, 216]. Another attractive feature of the LDKU model is that the predicted kinetic isotope effect is not directly related to ΔG^0 and $\Delta E_{S,0}$ or to temperature, as it is in an interpretation based on the original Marcus theory, which ignores tunneling [218]. Many failures of these relations have been noted [191, 219]. An important asset of the LDKU approach for proton transfer is that it starts with a model that is explicitly consistent with our current understanding of hydrogen atom tunneling in comparable gas phase systems [45, 71–75]. In mass-scaled coordinates proton or hydrogen atom transfer between heavy moieties has an MEP with very large curvature, and for a symmetric reaction with such an MEP it was shown [74] that most of the product originates by tunneling from the ground vibrational state of the reactant channel to the product channel without reaching the saddle point, i.e., at large R*.

An important problem of the LDKU model, at least as applied so far, is its failure to take into account the modification of the hydrogenic potential as the donor and acceptor approach each other. In the terms of model we would say that the resonance of the reactant and product electron distributions, ($A–H\cdots B$ and $A^-\cdots H–B^+$), leads to a strong compression of the local vibrational energy levels. In certain, spontaneously formed, H-bonded complexes the infrared spectra demonstrate such compression [220]. The substances whose proton transfer processes are of interest typically do not form such complexes spontaneously, but it seems reasonable to believe that a similar compression is generated when they achieve comparable configurations in energetic encounters. This leads to a nontunneling zero point energy contribution to the kinetic isotope effect (although VTST calculations [45] indicate that the nontunneling KIE is often less than the conventional TST value for symmetric or nearly symmetric hydrogen atom transfers between heavy moieties). The same resonance effect that compresses the local vibrational energy levels also changes the shape of the barrier along the straight tunneling paths utilized by large curvature systems in such a way as to decrease the tunneling as compared to what would be calculated in the LDKU model. At this point it seems that further

work to establish the ranges of validity of the Marcus and LDKU models would be valuable.

4.3 Mechanistic Complications

The discussion of specific reaction mechanisms is beyond the scope of this chapter; however, a discussion of TST for one-step reactions cannot be completely separated from a discussion of mechanism because of the difficulty of unambiguously isolating an elementary reaction and especially the lack of clear criteria, either operational or theoretical, of what constitutes an intermediate [173, 221]. Short-lived arrangements of atoms may or may not correspond to a minimum on the potential surface, and minima on potential surfaces need not correspond to long-lived species. When such arrangements or minima do not meet requirements for a real intermediate, they have been called virtual intermediates [222]. In both conventional and variational TST it is formally possible to ignore intermediates or virtual intermediates, but considering them often makes it easier to model the TS and understand the observed results.

As an example, the protonation of simple nitronate anions, **1**,

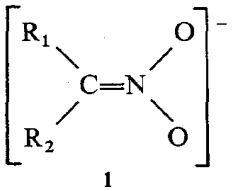

1

where R_1 and R_2 are alkyl, aryl, or hydrogen groups, by moderately strong oxygen acids in solutions containing H^+, gives rate constants many powers of ten smaller than the diffusion limit, although the reactions are strongly spontaneous [223]. In addition, when the structure of the nitronate is changed by varying R_1 or R_2, its protonation rate and equilibrium constants sometimes change in opposite directions, that is, the Brønsted exponent is negative [223, 224], although normal Brønsted behavior is observed when the structure and acidity of the oxygen acid is varied. These observations and others become more understandable when two additional facts are considered. First, deprotonation occurs on nearly every encounter between CH_3NO_2 and bases in the gas phase, even when the reactions are only slightly spontaneous [225]. This implies that the reverse reaction (which is protonation of **1** with $R_1{=}R_2{=}H$) also takes place on nearly every encounter. (However, this observation does not eliminate the possibility of a significant barrier, even in the gas phase [226].) Second, trinitromethylate anion is protonated by H^+ in *t*-butanol at nearly the diffusion-limited rate [227], although the reaction is less spontaneous than that of $CH_2NO_2^-$ with H^+ in water. Comparison of the gas phase and solution results for protonation of **1** shows that the solvent is strongly involved in the problem. The result with trinitromethylate implicates the high negative charge on the NO_2 group of simple nitronates. For static and dynamic reasons the

transition state for transfer of H^+ from H_3O^+ or ROH_2^+ to carbon

$$H^+ + R_1R_2C{=}NO_2^- \rightarrow R_1R_2CH{-}NO_2 \qquad \text{(R7)}$$

requires the reacting O–H bond to be directed toward carbon. But in **1** there is a unit negative charge on the NO_2 group, with the result that the O–H bonds of H_3O^+ or ROH_2^+ spontaneously direct themselves towards the oxygens, not the carbon. Work must be done to reorient this configuration before proton transfer can take place. When the proton acceptor is the trinitromethylate anion, the distribution of the charge over 6 oxygens makes the precursor configuration much easier to attain. It is not clear whether the effect of solvent in this case is static or dynamic (or both), in the language of Section 2.4. Apparently, solvent reorganization does not participate strongly in the reaction coordinate during the proton transfer itself, because that would substantially increase the effective reduced mass of the reaction coordinate and make the rate constant relatively insensitive to isotopic substitution, and such reactions show large hydrogen isotope effects [207]. If these reactions are to be treated in the Marcus formalism of Section 4.1.2, a substantial, structure-sensitive $W^{r,0}$ appears to be needed, and ΔE^*_{PC} would perform a similar function in the LDKU model, even though there is no evidence that the arrangement suitable for proton transfer (the PC) is metastable. Elements of such behavior also occur in other proton transfers.

Section 2.4.5 discusses another general type of system in which the decision for or against the explicit consideration of an intermediate or virtual intermediate depends on the theory being used.

One of the important benefits from the development and use of semiempirical models of reaction rates is that they can often identify the existence of very fleeting intermediates, virtual intermediates, or their absence. Ohno and coworkers [228] have proposed a three-step mechanism for hydride transfer among substituted pyridinium ions, consisting of electron transfer, followed by proton transfer, followed by another electron transfer (the EPE mechanism). This reaction is important because it is a model for a wide range of biologically important redox reactions. Marcus formalism is successful in correlating a large number of such reactions, involving a considerable range of structures and 0.4 V of redox potential (about 19 kcal/mol in ΔG^0) [229]. If the EPE mechanism were correct, the rate limiting steps and hence the TSs would be expected to be different for symmetrical and strongly unsymmetrical variants of the reaction, and such a correlation would be expected to fail. Thus the success of the correlation implies the absence of metastable intermediates. This would be true even if these intermediates were regarded as virtual intermediates, because Marcus theory depends primarily on the structure and quasithermodynamics of the TS, rather than on the dynamics by which the surface of no return is crossed. (Recent studies of kinetic isotope effects also support a one-step mechanism for hydride transfer in these reactions [230, 231].)

These examples demonstrate that the problems of TS structure and dynamics

are often inseparable from those of mechanism determination, particularly when fleeting or virtual intermediates are suggested.

5 SELECTED APPLICATIONS

5.1 Electron Transfer Reactions

Among processes of interest to chemists, electron transfer is the most extreme case of a light, fast particle moving under the influence of its interaction with much heavier, sluggish particles. The allowed energy levels of an electron are so widely spaced that only the ground electronic state is important for many nonphotochemical reactions. Here we consider ground-electronic-state electron transfer reactions. Thermal fluctuations of the reactants produce states in which the diabatic electronic energy of the donor–acceptor pair is the same as that of the donor minus one electron paired with the acceptor plus one electron. This is accomplished by distorting the structure of the reactants (including their solvent shells) in the direction of the product structures. The electron is transferred by tunneling, with an electronic transmission coefficient κ_{el} that decreases approximately exponentially with the distance between the donor and acceptor centers. Because of the small mass of the electron this is assumed to be preceded by a process in which the reactants achieve the proper separation, solvation, and, if necessary, orientation; that is, achieve the PC discussed above. This model for electron transfer is the same as the model for proton transfer in Section 4.2, and it is very similar to that used to obtain the Marcus formalism in Section 4.1.2. It leads directly to

$$k = K_A \nu_{nuc} \kappa_{el} \exp(-\Delta G^*/RT) \tag{130}$$

K_A is the formation constant for the PC, with an appropriate solvent shell, from the reactants. It is equal to $\exp(-W^{r,0}/RT)$ in the notation of Section 4.1.2, and Sutin assumes that its variation with structure depends mainly on the magnitude of the electrostatic repulsion term contained in $W^{r,0}$ [232]. (Note that Sutin [232, 233] uses the term precursor complex but we prefer precursor configuration, as discussed in Section 4.1.2.) In (130), ν_{nuc} is a frequency identified with the pseudo-lattice vibrations of the solvent and/or the lower frequency vibrations of reactants. ΔG^* has the same significance as in Section 4.1.2. Only κ_{el} is newly added, to take account of the possibility that a system may reach the TS configuration and fall back without electron transfer.

For a small number of electron transfer reactions it has been possible to evaluate the quantities required by Eq. (130) with enough reliability that k values bearing some resemblance to observed values have been obtained [133, 341]. Several bimolecular examples are shown:

$$Fe(H_2O)_6^{2+} + {}^*Fe(H_2O)_6^{3+} \rightarrow Fe(H_2O)_6^{3+} + {}^*Fe(H_2O)_6^{2+} \tag{R8}$$

$$Ru(bpy)_3^{2+} + {}^*Ru(bpy)_3^{3+} \rightarrow Ru(bpy)_3^{3+} + {}^*Ru(bpy)_3^{2+} \tag{R9}$$

$$Fe(H_2O)_6^{2+} + Ru(bpy)_3^{3+} \rightarrow Fe(H_2O)_6^{3+} + Ru(bpy)_3^{2+} \qquad (R10)$$

The partition functions in K_A were reduced to volumes [232]. The energy required to form the PC was assumed to be mostly coulombic, and it was calculated by means of a formula for electrostatic interactions. When these factors were combined for 2^+ ions reacting with 3^+ ions, values of about $10^{-1}\,M^{-1}$ were obtained for K_A. Values of $10^{12} - 10^{13}\,s^{-1}$, corresponding to spectroscopic frequencies of 30–300 cm^{-1}, were given to ν_{nuc}. For symmetrical reactions ΔG^* was evaluated by means of

$$\Delta G^* = (\lambda_{out} + \lambda_{in})/4 \qquad (131)$$

where λ_{out} is the contribution of the outer-shell (solvent) reorganization to the free energy of activation and λ_{in} is the inner-shell (intramolecular) contribution. The outer-shell contribution is the free energy that would be required to reorganize the solvent from its configuration in the PC into the configuration required by the SC if the electron remains untransferred. It was obtained from [233]

$$\lambda_{out} = e^2\left(\frac{1}{2r_D} + \frac{1}{2r_A} - \frac{1}{R}\right)\left(\frac{1}{D_{op}} - \frac{1}{D_s}\right) \qquad (132)$$

where e is the charge on the electron, r_D and r_A are the radii of donor and acceptor, respectively, R is the sum of the ionic radii of the donor and acceptor, D_{op} is the optical dielectric constant of the solvent (the square of its refractive index), and D_s is the conventional, macroscopic dielectric constant. Values of about 20–40 kcal/mol are obtained for λ_{out}. λ_{in} is the energy that would be required to distort the inner-shell structure of the PC to that of the SC, without transferring the electron. It was obtained from [234]

$$\lambda_{in} = 6f_{in}(d_D - d_A)^2 \qquad (133)$$

where f_{in} is a reduced force constant for the breathing vibrations of the donor and acceptor, given by

$$f_{in} = 2f_D f_A/(f_D + f_A) \qquad (134)$$

in terms of donor and acceptor inner-sphere force constants, and the ds are the metal–ligand bond distances in the inner ligation shells of the donor and acceptor. For (R8) a value of 0.14 Å was found for $(d_D - d_A)$ from crystallographic measurements, and f_D and f_A were obtained from donor and acceptor spectroscopic frequencies of 390 and 490 cm^{-1}, using a reduced mass of 18 amu (the mass of a water molecule) in both cases. For the unsymmetrical reaction (R10), ΔG^* was obtained according to the Marcus prescriptions (Sect. 4.1.2). For the evaluation of κ_{el}, the following variant of the Landau–Zener theory

was used:

$$\kappa_{el} = \frac{2[1 - \exp(-\nu_{el}/2\nu_{nuc})]}{2 - \exp(-\nu_{el}/2\nu_{nuc})} \tag{135}$$

where

$$\nu_{el} = \frac{2H_{AB}^2}{h}\left(\frac{\pi^3}{4RT\,\Delta G^*}\right)^{1/2} \tag{136}$$

where H_{AB} is the resonance integral. It was obtained by a highly simplified *ab initio* quantum mechanical calculation for (R8) [235, 236] and by an approximation scheme for (R9) [237], and it was taken as the geometric mean of the other two for (R10). The results are summarized in Table 1.

Although no rate constants were used in these calculations, vibration frequencies and crystallographic bond lengths were used, so it is not entirely an *ab initio* calculation. These appear to be among the most satisfactory calculations presently available for rate constants of ionic reactions in solution, even though the agreement between calculated and observed rate constants leaves room for quantitative improvement.

In contrast to the semiquantitative accuracy of the actual *calculations* of rate constants, *correlation* of rate constants for electron transfer reactions has been more successful. These correlations may illuminate TS structure, mechanism, or the structure of intermediates. For example, in the reactions (carried out in acetonitrile solution at 298 K)

$$\mathrm{RM} + \mathrm{FeL_3^{3+}} \rightarrow \mathrm{RM^+} + \mathrm{FeL_3^{2+}} \tag{R11}$$

$$\mathrm{RM^+} \rightarrow \mathrm{R} + \mathrm{M^+}$$

$$\mathrm{R} \rightarrow \text{ultimate products}$$

$$\mathrm{M^+} \rightarrow \text{ultimate products}$$

where the first step is rate limiting and the next three are fast, there are excellent

Table 1. Comparison of Calculated and Experimental Electron Transfer Rate Constants

Reaction	$K_A\nu_{nuc}$ ($M^{-1}\,s^{-1}$)	ΔG^0 (kcal/mol)	ΔG^* (kcal/mol)	κ_{el}	k_{calc} ($M^{-1}\,s^{-1}$)	k_{obs} ($M^{-1}\,s^{-1}$)
(R7)	10^{11}	0	24.6	10^{-2}	10^{-2}	4
(R8)	10^{12}	0	5.5	1	10^{9}	4×10^{8}
(R9)	10^{12}	4.7	15.1	10^{-1}	10^{8}	5×10^{6}

correlations between the standard reduction potentials E^0_{Fe} of the ferric compounds and $(\Delta G^{a,0})^{\ddagger}$, according to

$$(\Delta G^{a,0})^{\ddagger} = \lambda^{\ddagger}/2 + \mathcal{F}E^0_{RM}/(2\lambda^{\ddagger}) - \mathcal{F}E^0_{Fe}/(2\lambda^{\ddagger}) \tag{137}$$

where $\mathcal{F}$ is the Faraday and E^0_{RM} is the standard reduction potential of RM, for a variety of radical ions derived from tetralkylstannanes, tetraalkylplumbanes, and dialkylmercurials [238]. Equation (137) is simply a reorganization of Eqs. (107) and (108), with the additional assumption that the work terms are negligible, and with ΔG^0 replaced with its electrochemical equivalent, $\mathcal{F}(E^0_{RM} - E^0_{Fe})$. In the original [238], $W^{p,0}$ is actually retained, but $W^{r,0}$ is set equal to zero, and it may be more satisfactory to treat the two work terms consistently. The final outcome is essentially the same.

Plots of $\Delta G^{a,0}$ against $\mathcal{F}E^0_{Fe}$ for the oxidation of a single organometallic by a series of iron compounds are linear. The slopes, $1/(2\lambda^{\ddagger})$, of the plots of Eq. (137) are all the same, and they give a structure-independent value of 41 kcal/mol for λ. The intercepts of these plots are $[\lambda^{\ddagger}/2 + E^0_{RM}/(2\lambda^{\ddagger})]$, and since λ is available, they yield the reduction potentials E^0_{RM} of the organometallics. These cannot be directly measured because their electrode oxidations are not reversible. The existence of these correlations, with a constant value for λ, for a wide variety of alkyl groups and ligands, is a powerful argument in favor of outer-shell electron transfer between intact reactants as the rate limiting step in these reactions [238]. Any reorganization of the covalent bonds of the reactants seems likely to have been sensitive to structure.

5.2 Hydrogen Atom, Proton, and Hydride Transfer

5.2.1 Proton Transfer

Acid–base reactions are a fertile field for testing relations between rate and equilibrium constants because a large body of equilibrium constants is available, both in solution and in the dilute vapor phase, and recently many rate constants have also been measured. Proton transfer reactions resemble electron transfers in that, approximately, a light, rapidly moving particle can be considered to be moving in a field established by the heavier atoms. Tunneling is again of concern. Because of these similarities, proton transfer was one of the first reactions, after electron transfer and the work of Ref. [186], to which semiempirical rate theory like that in Section 4.1.2 was applied [213].

Many proton transfers, to and from carbon, in aqueous or partially aqueous solution, can generate the reaction series wanted for the application of semiempirical rate theories. A commonly studied example is

$$\begin{array}{l} \mathrm{O} \\ \| \\ \mathrm{A{-}C{-}CH_3} \end{array} + \mathrm{B^-} \rightarrow \begin{array}{l} \mathrm{O^-} \\ | \\ \mathrm{A{-}C{=}CH_2} \end{array} + \mathrm{HB} \tag{R12}$$

where A is an alkyl group or functionalized alkyl group, and B^- is an anionic

oxygen base. If B^- is varied with constant A, and $\log k$ values are plotted against either $pK_a(BH)$ values or $\log K$ values for the reaction itself, strongly curved Brønsted plots are obtained [216, 239]. ($pK_a(BH)$ values and $-\log K$ values are related to one another by an additive constant *provided they refer to the same solvent*. The use of $K_a(BH)$ values from water with K values measured in some other solvent deprives the theory of all its quantitative significance and much of its qualitative significance.) Rates of symmetrical reactions are unavailable, but if $W^{r,0}$ and λ are assumed to be constant and $W^{p,0} = W^{r,0}$, the coefficients c_n of Eq. (119) are constant and can be obtained, and, from these, values of $W^{r,0}$, λ, and, if it is not already known, $pK_a(ACOCH_3)$. This results in strikingly low values of $\lambda/4$, around 3 kcal/mol, and correspondingly high values of $W^{r,0}$, around 15 kcal/mol [216]. These values were obtained from data spanning about 15 units of pK_{BH} for each series. On the other hand, if the k values obtained by varying A, with B^- fixed as OH^-, are treated in the same way, a $W^{r,0}$ value of around 4 kcal/mol and $\lambda/4$ value around 10 kcal/mol are obtained [216]. The theory has been thought to require that λ and $W^{r,0}$ be independent of the position where substitution is made [213], though Eq. (124) and Fig. 4 show that this is not the case. Further work appears in order here.

Related observations have been made for the hydrolysis of diphenyldiazomethane (DDM) in 80% dimethyl sulfoxide–20% water, catalyzed by various oxygen acids, HA (carboxylic acids and phenols), covering about 8 units of pK_{HA} [191]. A very strongly curved Brønsted plot is obtained, leading to a $W^{r,0}$ of about 17 kcal/mol and a $\lambda/4$ value of about 1.5 kcal/mol. As pK_a is lowered, the rate constant plateaus at about $10\ M^{-1}\ s^{-1}$, which leads to a consistent $W^{r,0}$ value of about 18 kcal/mol; however, the rate constant remains sensitive to the introduction of substituents in the DDM. This leads to the formal conclusion that the substituents change $W^{r,0}$, rather than $\Delta G^{0\prime}$, contrary to superficial intuition at least.

There are also reactions which generate fairly straightforward results. Proton abstraction from sulfanes and cyanocarbon acids, and reprotonation of the corresponding anions, are examples [240, 241]. These reactions have $W^{r,0}$ values of about 4 kcal/mol and $\lambda/4$ values of about 3–4 kcal/mol. The strongly spontaneous reactions in these cases have proton transfer rate constants of about 10^8–$10^9\ M^{-1}\ s^{-1}$, and they have sometimes been regarded as essentially diffusion limited. However, they do not respond, as would a diffusion-limited rate, to changes in the viscosity of the solvent [242]. 1-Phenylvinylate ion has been observed to react with H^+, with a rate constant of $3 \times 10^9\ M^{-1}\ s^{-1}$ [243], a value which may be diffusion limited.

How may the apparent anomalies be resolved? We would prefer not to abandon entirely an approach which appears to represent many results with useful accuracy, so we would prefer to reconcile these anomalies without abandoning the basic framework of Section 4. Some of the sources of difficulty are easily found. From the first evaluation of $W^{r,0}$ for proton transfer reactions [213] it has been suggested that part of the origin of $W^{r,0}$ was in the desolvation of the reactants and, particularly, in the removal of the innermost, hydrogen-

bonded solvent from the oxygen acid or base. Intuition suggests [216] and experiment has shown that this desolvation energy increases with the strength of the acid or base, both in solution and in the gas phase [244–246]. Both linear [245] and nonlinear [244] relations have been reported, and, in solution, there seems to be a strong dependence on the structural type of the acid [246]. Desolvation is an example of an interaction which does vary linearly with progress along the reaction coordinate. Kresge and Keefe, in another chapter of this volume, have attributed anomalous Brønsted coefficients to such interactions.

Tunneling is probably most important for energetically symmetrical cases, decreasing in importance as the asymmetry in either direction increases. Both of these effects could increase the curvature of a Brønsted plot. For most types of proton transfers the rate constants for symmetrical reactions have not been available, so λ has been obtained from the plot of $\ln \Delta G^{a,0}$ against $\ln \Delta G^0$. The curvature of that plot is $(2\lambda)^{-1}$ if $W^{r,0}$ and λ are constant. If the curvature were increased by the variation of $W^{r,0}$ or by tunneling and this were not anticipated, the derived value of λ would be too small and the value of $W^{r,0}$ would be too large [191, 213]. Also, the solvation energy is probably different for reactants and products, making $W^{r,0}$ and $W^{p,0}$ different and $\Delta G^{0\prime}$ different from the observable ΔG^0. Potential functions other than the intersecting parabolas of the simplest Marcus theory have been suggested, and these may somewhat change the shape of the Brønsted plot [247, 248]. Another effect not explicitly included in Marcus theory or the conventional $\Delta G^{\ddagger,0}$ is that the nonequilibrium correction factor Γ of Section 2.2.5 may depend systematically on the energetics of the reaction. All of this suggests that the value of $W^{r,0}$ should not be taken too literally. The λ derived from a series of oxygen acids or bases reacting with a single carbon base or acid appears more likely to give a meaningful λ than variation of the carbon constituent, because λ is probably quite constant in the former case. This is so because proton transfer between oxygen bases in a properly aligned complex is barrierless or nearly so [249]. Thus, the λ for such a process is just half of λ_{ii} for the carbon reactant, which is constant because that reactant is not varied. Any other additive scheme for estimating λ from the properties of the individual reactants will arrive at the same conclusion. Overall, the results seem to sustain the conclusion that spontaneous proton transfer to and from carbon has a small but nonzero λ. When more substantial activation energies are found they may have origins in the details of mechanism, as discussed for nitronate reprotonation in Section 4.3.

5.2.2 Hydrogen Atom Transfer

Hydrogen atom transfer has been studied in the gas phase as well as in solution. For a small number of gas phase hydrogen atom transfers, enough data is available to make a complete test of Eqs. (108) and (119) and the cross relation. For example, the rate constants for

$$^{37}\mathrm{Cl}\cdot + \mathrm{H}^{35}\mathrm{Cl} \rightarrow \mathrm{H}^{37}\mathrm{Cl} + {}^{35}\mathrm{Cl}\cdot \qquad \text{(R13)}$$

$$H\cdot + H_2 \rightarrow H_2 + \cdot H \qquad \text{(R14)}$$

and

$$Cl\cdot + H_2 \rightarrow HCl + H\cdot \qquad \text{(R15)}$$

have been experimentally determined to be 3.1×10^6 [250], 8.5×10^5 [251], and 3.7×10^7 [252], all in units of $M^{-1}\ s^{-1}$ at 368.2 K; and (R15) has an equilibrium constant of 0.34 [253]. (Note that the rate constant given for (R14) is the distinguishable atom rate constant [254] as determined from the experimental result [251] for ortho–para conversion.) From the first two rate constants and the equilibrium constant, the third rate constant can be calculated by the model of Section 4.1.2. Assuming $W^{r,0} = W^{p,0} = 0$, the calculated value is $1.0 \times 10^6\ M^{-1}\ s^{-1}$, which is smaller than the experimental value by a factor of almost 40. The result we obtain with the deuterium analogues [250, 255, 256] is comparable. Although $W^{r,0} = W^{p,0} = 0$ has been assumed, any small, constant value gives similar results. The agreement of theory and experiment is much worse than that which has been achieved for hydride transfer and alkyl transfer reactions in solution (Sects. 5.2.3 and 5.3). These reactions involve polyatomic molecules and ions in solution. Many low frequency structural and pseudo-lattice modes probably participate in the activation process, and solvent motions may play a significant role in the reaction coordinate [257]. Marcus theory, Eq. (108), was intended for such situations, and it deals with them fairly well [258]. In the simple gas phase hydrogen atom transfers, such modes are unavailable. The activation energies of these reactions are 5–6 kcal/mol—less than the vibrational-energy-level spacing of either H_2 or HCl. A large fraction of the activation energy must be translational, rather than coming primarily from displacements in harmonic modes. The κ of Eq. (106) is also important. In spite of this failure of the cross relation, rate constants for the reactions (R13) and (R15) can be correlated [259] with rate constants for analogous $Cl\cdot + HX$ and $X\cdot + H_2$ reactions using equations very similar in effect to Eqs. (107)–(108).

Spectacular demonstrations of nuclear tunneling are obtained with hydrogen atom transfer reactions. The radical pair shown in Fig. 5 [260] was generated by irradiating a crystalline sample of dimethylglyoxime [261]; Presumably H_2 is lost in the process. The hydrogen atom transfer was identified and monitored by ESR spectroscopy. At temperatures above 100 K, the rate constant for hydrogen transfer is strongly temperature dependent, leading to an apparent activation energy of about 10 kcal/mol. At lower temperature, however, the Arrhenius plot is sharply curved, and finally becomes almost flat, so that the rate constants are almost the same at 50 K and at 4.2 K. At the lower temperatures, no reaction at all can be detected in the deuterated radical pair. A kinetic isotope effect of 10^{12} and a fantastic-appearing hydrogen tunneling correction of a factor of 10^{764} were estimated at 4.2 K by extrapolation from

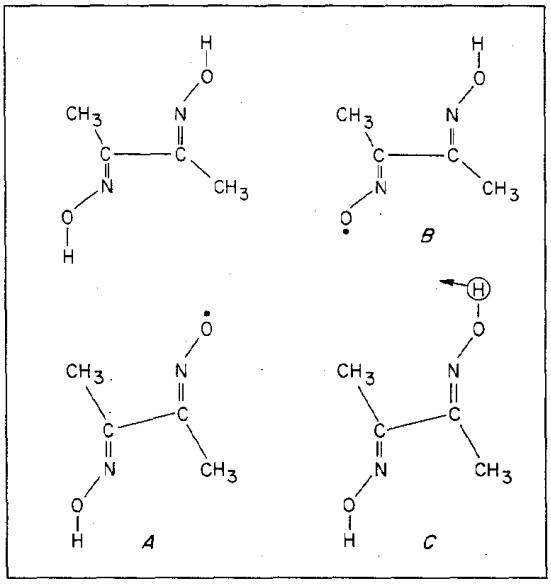

Fig. 5 The crystal structure of dimethylglyoxime [260] and the radical pair (A and B) generated by irradiation with ionizing radiation.

temperatures above 100 K [262]! The reaction

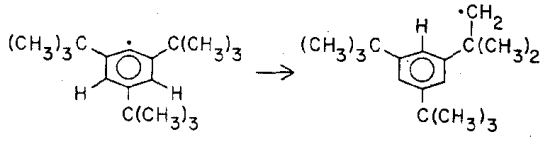

(R16)

gives a deuterium kinetic isotope effect for perdeuterated *tert*-butyl groups of 1.3×10^4 at 123 K [262, 263]. This reaction also leads to a strongly curved Arrhenius plot. The H variant has a rate constant of $10^{-2}\,s^{-1}$ at 76 K, and this is lower by only a factor of 2 at 28 K [262]. These effects have been analyzed using a one-dimensional model in which a fraction of the zero point energy in an X–H stretching vibration is used to provide a nonzero rate by tunneling, even at temperatures approaching 0 K [264, 265]. This analysis shows that tunneling is significant at all temperatures, even though its most obvious consequences can only be observed at very low temperatures. The number of systems that have been observed at temperatures below 100 K is small, and the theory is still incompletely developed (see Sect. 5.5 of this chapter). However, there is no doubt left about the reality of tunneling, and its importance appears to be general. Even at room temperature, reaction (R16) is apparently faster by a factor of about 10^2 than it would be in the absence of tunneling [263].

5.2.3 Hydride Transfer

Hydride transfer between variously substituted and elaborated pyridinium ions has recently proven to be a fruitful field for the application of semiempirical rate theory because equilibrium constants and rate constants are available for symmetrical reactions, as well as ordinary reactions. Rate constants have been obtained for four analogous, nearly symmetrical reactions of the type:

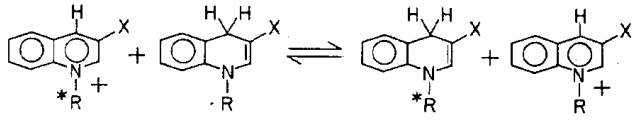

(R17)

where the R group is either a methyl group, a benzyl group, or a substituted benzyl group, X is either CN or $CONH_2$, and the star indicates some sort of labeling, and equilibrium constants have been obtained for the unsymmetrical reaction

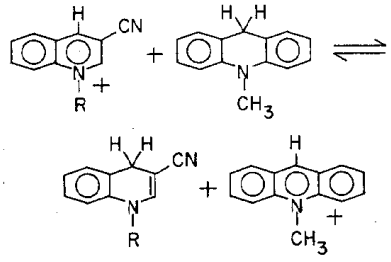

(R18)

These studies have given a τ value (Sect. 4.2.2) of 0.77 [174], indicating that bond order is not quite conserved. This value of τ and the equilibrium constants give, in Eq. (124), a value of 0.37 for the α of (R18). This is identical with the experimental value [174].

Measured equilibrium constants and rate constants for symmetrical reactions permit the calculation of fourteen rate constants for unsymmetrical reactions, using the Marcus relations [229]. The measured rate constants vary over a range of 10^7, and the average discrepancy between measured and calculated rate constants is a factor of about 1.5 [229]. In this calculation the cross relation, $\lambda_{ij} = (\lambda_{ii} + \lambda_{jj}/2)$, was used to obtain the intrinsic barriers, which were assumed to vary from one ring system to another. However, no allowance was made for the variation of λ_{ii} with substitution. That is, λ_{ii} for acridinium ion was allowed to be different from that of quinolinium ions, which, in turn, is different from that for pyridinium ions, and so on. But the systematic variation of λ_{ii} with K_{ij} was *not* taken into account and may improve the fit still further. The agreement is already far better than that described in Section 5.2.2 for gas phase hydrogen transfer and suggests that the model is more suitable for reactions in which many modes contribute to $\Delta G^{\ddagger,0}$.

In this study $W^{r,0} = W^{p,0} = 2$ kcal/mol was assumed. This raises the

question of why we can successfully assume that these quantities are small and constant in this case, when they appear to be large and structure sensitive in many examples of proton transfer. $W^{r,0}$ and $W^{p,0}$ may reasonably be substantially smaller for reactions like (R17) and (R18) than for proton transfer because no hydrogen bond has to be disrupted to reach the TS in the former cases, and also because there is a *negative* contribution from charge transfer interaction between the oxidant and the reductant. This leaves room, within the constraint of easily measured rate constants, for large values of $\Delta G^{\ddagger,0}$. $W^{r,0}$ probably remains structure sensitive, in ways that are not anticipated by the semiempirical rate theory, but the contribution to $\Delta G^{a,0}$ from well-behaved terms is now considerably larger. In addition, to the extent that the structure sensitivity of $W^{r,0}$ is an additive characteristic of the two reactants, it is taken up in λ when χ is near 0.5, as it is in these cases. The more extended systems give precursor complexes which are better stabilized by charge transfer interactions and should have less positive values of $W^{r,0}$, but since $W^{r,0}$ is held constant in the calculation, reduced values of λ_{ii} are produced instead. The combination of these effects produces the excellent results noted.

Tunneling is probably a factor in hydride transfer, as it is in proton and hydrogen atom transfer [266–268].

Semiempirical rate theory provides an insight into the general question of the mechanism of hydride transfer reactions, suggesting when they may be expected to occur in one step and when they will use the EPE mechanism (Sect. 4.3). Short-range electron transfer and proton transfer have much smaller intrinsic barriers (values of $\lambda/4$) than hydride transfer. Although the exact values are uncertain and somewhat structure-sensitive, the estimates are generally under 10 kcal/mol. Hydride transfers appear to generate $\lambda/4$ values of about 20 kcal/mol [229]. Thus, the three-step mechanism will generally be preferred when the intermediates are not extravagantly energetic. In many cases, however, ΔG^0 for the formation of radicals and radical ions from closed-shell molecules and ions is well above 20 kcal/mol. The one-electron redox potential of NADH, for example, appears to be over 1 V (24 kcal/mol) [269]. In such cases, in spite of its large λ, the hydride transfer is preferred because it leads directly to stable products, and therefore has a negative or only slightly positive ΔG^0 for cases of interest.

All of this analysis still does not answer the interesting question of why λ is so high for hydride transfer. Semiempirical rate theory cannot answer that question; in fact, it is intended to avoid it. Ultimately it will have to be answered by quantum mechanical calculations, although further experimentation, showing how λ varies with structure and solvent, may identify the particular features that are crucial.

5.3 Alkyl Transfer

Nucleophilic displacement reactions comprise one of the largest and most important classes of organic reactions [270]. They can be regarded as alkyl transfers and treated by the methods of semiempirical rate theory. In practice

this has been difficult because of the paucity of systems in which rate and equilibrium constants are both measurable, but some progress has been made, particularly for methyl transfer reactions.

A τ value 0.8 has been obtained for

$$Ar_iSO_3^- + CH_3OSO_2Ar_j \rightarrow Ar_jSO_3^- + Ar_iSO_3CH_3 \qquad (R19)$$

by studying rates of symmetrical reactions [271]. When combined with the χ value of 0.5, expected when ΔG^0 is about 0, this leads to an α value of 0.60 for variations of j (notation of Sect. 4.1.2). A value of 0.6 has been observed [271]. These results strongly support the long-held view [175, 270] that bond breaking and bond making are well coordinated in such reactions, with a small positive charge development on the central atom. A similar treatment of gas phase methyl transfer by Brauman and Pellerite [272] is also successful, but, puzzingly, their figure 2 suggests a τ value around 0.5. Intuitively, one might have expected the gas phase transition states to be tighter. The gas phase experiments require several assumptions and approximations before the "experimental" quantities are obtained, and the Marcus cross relation (Sect. 4.1.2) was assumed to evaluate barriers for symmetrical reactions, so the smallness of τ may be exaggerated, but the qualitative result seems to be sound. *Ab initio* calculations [273] support the general validity of the Marcus cross relation for potential energy barriers in this kind of reaction.

There is also some evidence that parameters which have been thought to be measures of TS structure lead to conflicting conclusions [274, 275]. This problem may be due to oversimplified interpretation of QFERs in terms of TS structure or to the influence of γ, Γ, and κ [Eq. (106)] on the rate constants; theories of TS structure will generally not anticipate the behavior of the latter parameters. More work is in order here and progress appears likely.

5.4 Other Reactions

The Marcus theory, or something very similar, can be arrived at in many different ways [190, 276, 277] so the justifications given in Sections 4.1.2 and 4.2 are not the only ones possible. When none of the available justifications of Eq. (119) appear valid, it may be regarded as a purely empirical correlation if it does fit the results. Alternatively, we may use thermochemical analogies to compute free energies of activation [278], or we may even attempt full transition-state-theory calculations based on equations like Eqs. (13)–(16) or (105)–(106). In Section 5.4.1 we give an example of how semiempirical models of the type introduced in Section 4 can be applied to a quite different class of reactions. In Section 5.4.2 we discuss cases where the solute–solvent coupling effects are more prominent and cannot be treated by this scheme.

5.4.1 Associations

Hine [279], Albery [215], and Guthrie and Cullimore [280] have applied the Marcus theory to cation–anion recombination reactions and to nucleo-

philic additions to carbonyl groups:

$$R^+ + N^{n-} \rightleftarrows RN^{(n-1)-} \tag{R20}$$

$$A{-}\overset{\displaystyle O}{\overset{\|}{C}}{-}B + N^{n-} \rightleftarrows A{-}\overset{\displaystyle O^-}{\underset{\displaystyle B}{C}}{-}N^{(n-1)-} \tag{R21}$$

where R^+ is a carbocation and N^{n-} is a nucleophile of charge n^-. These treatments rationalize a large number of rate constants; they give intuitively reasonable λ values, the differences in which (under changes in N^{n-} or the electrophile) tend to be similar, as suggested by additive theories of bond energy, with discrepancies averaging < 1 kcal/mol. The α value was calculated from an equation equivalent to

$$\alpha = 0.5\left[1 - \frac{(W^{r,0} - W^{p,0}) + RT \ln K}{\lambda}\right] \tag{138}$$

with λ obtained from the equations of Section 4.1.2. (These treatments implicitly assume that $\tau = 1.0$, and thus make α and χ identical.) Hine [279] took $W^{r,0} = 2.4$ kcal/mol and $W^{p,0} = 1.4$ kcal/mol, if the definitions of this chapter are used. Albery [215] simplified his arithmetic by taking both as zero. Experimental values of α were obtained by plotting $\log k$ against $\log K$ for homogeneous series of reactions. Two of the more extensive series are

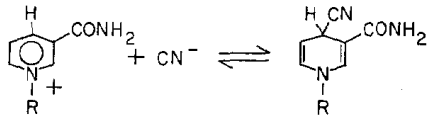

(R22)

where R is an alkyl or substituted alkyl group, and

$$\{p\text{-}[(CH_3)_2N]C_6H_4\}_2CAr^+OH^- \rightleftarrows \{p\text{-}[(CH_3)_2N]C_6H_4\}_2C(OH)AR \tag{R23}$$

where Ar is a *m*- or *p*-substituted aromatic group. The calculated values [279] were 0.48 for (R22) and 0.42 for (R23). Albery [215] gets 0.44 for (R22). The experimental values are 0.55 and 0.38, respectively [279].

Other interesting series for which data have been collected are hydroxylations of substituted quinolinium ions [281, 282]. For these the Albery-type calculations (performed by M. M. Kreevoy for the present discussion) give 0.45–0.46. The Hine values would be very similar. The experimental values are 0.46, 0.45, and 0.36 [281, 282], so the agreement is reasonably satisfactory.

Ritchie has objected to this kind of treatment [283] of recombination because the lack of symmetrical analogue reactions makes it difficult to visualize the

transformations which would generate the Marcus parabolas of Section 4.1.2. Conceptually satisfactory reactions for generating such parabolas may be written as

$$R^+ \cdots X^- \rightarrow R^+ \cdot X^- \qquad \text{(R24)}$$

$$R \cdot X \rightarrow R \cdots X \qquad \text{(R25)}$$

In (R24) the $R^+ \cdots X^-$ ion pair is compressed, without covalent bond formation, to the covalent binding distance. In (R25) the C–X bond of the covalent compound is stretched to the ionic bond length. The ΔG^0 values for these processes are not available by direct measurement although they might be estimated spectroscopically. The force constants for (R24) and (R25) are not necessarily more disparate than those of other pairs of reactions used to estimate λ values. A key consideration in formulating (R24) and (R25) is the recognition that the PC for recombination, $R^+ \cdots X^-$, is very different from the separated reactants, so that the weak forces restraining the motion of the free ions in solution do not have to be compared with the strong force restraining the lengthening of the C–Y covalent bond.

Reactions (R24) and (R25) strongly resemble the processes by which the PC and SC in an electron transfer reaction are converted to the transition state. In both cases electron transfer occurs when the appropriate structure is reached, and relaxation follows. Electron transfer differs from ion recombination in the nature of the SC and its ultimate disposition, but these factors only change the value of $W^{p,0}$. The overlap integral is probably much larger than in weak-overlap electron transfer, but this may be taken up in the experimentally determined parameters, just as it appears to be in atom and group transfer reactions.

Brønsted base reactions were also discussed in Section 5.2.1. In the cases discussed there, for which α varies widely, such reactions were shown to generate substantial, and probably structure-sensitive $W^{r,0}$ values, typically 6–10 kcal/mol. Except for the greater contribution of tunneling effects to the phenomenological $W^{r,0}$ values in the proton transfer case, $W^{r,0}$ values for the present reactions should be similar to those for proton transfers. The reason that the treatments discussed in the present section do not require nonzero $W^{r,0}$ values is that contributions to $\Delta G^{a,0}$ can be more or less arbitrarily shifted between $\lambda/4$ and $W^{r,0}$, as long as both are additive functions of reactant properties, and as long as α remains about 0.5, as it does in these cases [215, 279].

5.4.2 Isomerizations

Conformational isomerizations of hydrocarbons are useful reactions in which to look for dynamic solvent effects (Sects. 2.4.2–2.4.4) because static solvent effects should be minimized. The conformational inversion of cyclohexane has been studied in carbon disulfide, methylcyclohexane-d_{14}, and acetone-d_6 at 213–225 K, over a range of pressures up to 5000 atm [284–286].

The solvent effects on the rate constant are not large. At a single temperature and a pressure of 1 atm the total range of rate constants is about a factor of 1.5 [285]. However, the effect of pressure on the rate is quite dependent on solvent and pressure, in a way that strongly suggests dynamic solvent effects. The effect of pressure on reactivity is most conveniently discussed in terms of the volume of activation, $\Delta V^{a,0}$, given by Eq. (51b). Jonas and co-workers assume that $\Delta V^{a,0}$ can be divided into a conventional TST contribution, $\Delta V^{\ddagger,0}$, and another term, ΔV^{coll}, associated with collisions with solvent molecules. In the notation of Section 2, ΔV^{coll} is given by $-RT\partial(\ln \Gamma\gamma)/\partial P$. The mechanism of chair–chair inversion is thought to involve the twist–boat as a high energy intermediate, with two equivalent TSs resembling the two half-chair structures [287]. Such a transition state resembles cyclohexene. By correction of the molar volume difference between cyclohexane and cyclohexene for the additional two hydrogen atoms and the difference in length between a C–C single bond and a C–C double bond, $\Delta V^{\ddagger,0}$ was estimated [285] to be about $-1.5\ cm^3$. It was assumed to be solvent-independent [284, 285]. In contrast, for a pressure of 1 atm, $\Delta V^{a,0}$ varies from $-4.8\ cm^3$ in acetone-d_6 to $-1.3\ cm^3$ in methylcyclohexane-d_{14}. $\Delta V^{a,0}$ becomes less negative with increasing pressure, but is pressure derivative depends on solvent. The values of $\Delta V^{a,0}$ and their variation with pressure are in qualitative agreement with theoretical treatments [124, 134, 137, 165, 288] of Γ and γ. It has been noted that $V^{a,0}$ is generally more negative than anticipated, and not infrequently (as in the present case) more negative than ΔV^0 [289], where ΔV^0 is the molar volume of products minus that of reactants.

Other interesting examples of solvent and pressure effects on an isomerization in solution are provided by the torsional photoisomerization of electronically excited stilbene [290–294]. For example, Ladanyi and Evans [294] have discussed this in terms of a potential of mean force for the torsional coordinate. The potential of mean force includes two terms: a pressure-independent gas phase part and a pressure-dependent term calculated from the cavity distribution function. They suggested that the pressure dependence of the latter term may account for the density dependence of the observed yield of the cis isomer. Further work is required before all aspects of this interesting and well-studied case will be understood satisfactorily [293].

The factors γ, Γ, and κ may be expected to perturb the absolute value of k and its temperature derivative as well as its pressure derivative, although k will often be less sensitive than the derivatives. The rate constants have been studied for rotation about the phenyl–phenyl bond in substances of the general structure **2** [295], where X and Y are a variety of atoms and groups.

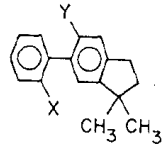

2

The two aromatic rings in **2** are not coplanar in the lowest-energy structure. Various solvents and a range of temperatures were used. There was no observable solvent effect on the rate constants, and the $\Delta G^{a,0}$ values given by Eq. (40) for 340 K are a smooth monotonic function of the van der Waals radii of X and Y [295], indicating that the $\Delta G^{a,0}$ values have approximately the significance anticipated by conventional TST. However, the $\Delta S^{a,0}$ values given by Eq. (44) vary from -11 to -30 cal/mol/K, with no recognizable pattern. Values around -10 cal/mol/K might have been anticipated from the loss of a hindered rotation in making the TS partition functions from those of the reactants [296, 297]. The variation in $\Delta S^{a,0}$ has been attributed [295] to experimental factors and some of it undoubtedly has that origin, but this does not explain the observation that the typical value of $\Delta S^{a,0}$ is considerably more negative than anticipated. The absolute values of $\Delta S^{a,0}$ suggest that γ, Γ, and κ together contribute a factor of about 10^{-2} to the rate constant in these reactions.

In reactions involving ions, large static solvent effects (Sect. 2.4.1) can be expected. The direction, and, roughly, the magnitude of these can be estimated by analogy. Even here, however, the origin of effects on thermodynamic quantities is not always well understood [298, 299], so extrapolation to the quasi-thermodynamic quantities of activation is uncertain. The conclusion we would reach is that the values of quasi-thermodynamic activation quantities for solution reactions should be interpreted with great caution, even if there are no significant experimental uncertainties. Isolated values, especially, should not be given great weight in assigning a TS structure or a reaction mechanism. Comparisons among closely related families of reactions, measured in the same solvent, are probably more reliable [296, 297].

5.5 Kinetic Isotope Effects

The structure of the variational TS often changes under isotope substitution [37, 39, 66, 67, 300]. This does not involve a breakdown of the Born–Oppenheimer approximation. It occurs because the allowed energy levels of generalized transition states shift under isotopic substitution. As an example, we will discuss the hypothetical gas phase reaction

$$*C + HC \rightarrow *CH + C \qquad \text{(R26)}$$

where the star indicates some form of labeling, and the four valence electrons of carbon are arbitrarily maintained in sp^3 hybrid orbitals. Thus, this is a three-body model of the reaction

$$*C_nH_{2n+1} + C_nH_{2n+2} \rightarrow *C_nH_{2n+2} + C_nH_{2n+1} \qquad \text{(R27)}$$

This model gives the correct (skew) angle in mass-weighted coordinates between the line of approach of the reactants and the line of retreat of products, at large separation between the reagents. At small separations, where the reagents may resemble a single molecule, the model may be much worse. The flexibility of an alkyl chain suggests that the effective mass of a reactant, for short-range inter-

actions, may be much less than its overall mass. This suggestion is reinforced by the existence of numerous characteristic functional group frequencies in infrared spectroscopy [301]. These are practically insensitive to the size of an alkyl substituent once an ethyl group has been reached [301]. Nevertheless, we proceed with this flawed model to see what insights it may give us, because full multiatom calculations have not yet been performed for (R27). For reaction (R26) CVT calculations have given two equivalent variational TSs, one on either side of the saddle point [26, 38]. Additional calculations on reaction (R26) have been performed for the present discussion (using a program described elsewhere [41, 45]). The nontunneling parts of these calculations are like those in Refs. [26] and [38] except that a LEPS-type potential energy surface [182, 302] was used. The Sato parameter [182, 302] of this surface was adjusted to give a classical barrier height of 7.17 kcal/mol. Table 2 gives some of the results of these calculations.

In the table k^{GT} denotes the hybrid rate constant, with quantized vibrations but classical reaction-coordinate motion, and $k^{GT/G}$ denotes that a large-curvature-approximation ground state transmission coefficient [45, 74] has been added to account for tunneling. For H transfer the variational TSs have a lower potential energy, but a higher total energy than the saddle point, because they have a higher, partially hydrogenic, breathing frequency. Some of the observable characteristics of the reaction will be determined by averages over the two equivalent dividing surfaces and will mimic a symmetric TS. For example, a probe of the electronic symmetry of the TS by attaching substituents at one, and then the other carbon, would indicate a symmetric TS. However, the rate constant and the kinetic isotope effect (KIE) given by the CVT TS are *not* the same as that given by conventional TST. For D transfer with $m_C = 12$, as one leaves the saddle point the ZPE does not rise as fast as the potential energy falls, so the TS is not displaced from the saddle point. Thus, for $m_C = 12$, the CVT rate constants are below the conventional TST values for H transfer, but not for D transfer. This reduces the hybrid value of the KIE by a factor of about 2, as shown. If the masses of the donor and acceptor carbons are arbitrarily increased to simulate larger donor and acceptor groups, the D transfer TS is also displaced from the saddle point and becomes very similar to the H transfer TS. However, the energy changes for D transfer remain much smaller than those for H transfer, and the hybrid KIE becomes even smaller than when $m_C = 12$ was used.

The calculated KIE is raised to a value somewhat *above* its original level, for both m_C values, by the addition of large curvature ground state tunneling. When a light atom is transferred between two heavier atoms, tunneling does not occur through the saddle-point geometry, but at a somewhat larger heavy-atom separation [45, 74]. Thus, there are two effects that lead to structural differences between isotopically different TSs: (1) CVT optimization effects and (2) large curvature tunneling. Both effects should be considered in interpreting primary and secondary KIEs. While the quantitative significance of these conclusions is reduced by the difficulties mentioned above, connected with the three-atom

Table 2. Characteristics of Reaction (R32)

m_C[a]	m_H	Theory	R_{CH}[b] (Å)	R_{CH}[b] (Å)	V[b] (kcal/mol)	$\bar{\nu}_{stretch}$[b] (cm^{-1})	$\bar{\nu}_{bend}$[b] (cm^{-1})	$10^{-5}\,k^{GT}$ ($M^{-1}\,s^{-1}$)	$k^{GT/G}$ ($M^{-1}\,s^{-1}$)	k_H^{GT}/k_D^{GT}	$k_H^{GT/G}/k_D^{GT/G}$
12	1	Conv.	1.29	1.29	7.17	562	585	8.37			
12	1	CVT	1.48	1.13	5.83	1921	522	4.15	31.8		
12	2	Conv.	1.29	1.29	7.17	562	422	1.80		4.4	
12	2	CVT	1.29	1.29	7.17	562	422	1.90	6.20	2.2	5.1
57	1	Conv.	1.29	1.29	7.17	258	576	8.79			
57	1	CVT	1.46	1.13	6.07	1835	527	1.20	25.5		
57	2	Conv.	1.29	1.29	7.17	258	409	1.85		4.7	
57	2	CVT	1.46	1.13	6.00	1306	372	0.98	4.82	1.2	5.2

[a]The masses of C and *C are the same in these examples.
[b]Properties of the conventional or the first of the two variational transition states.

model, the qualitative conclusions very likely apply to reactions of multiatomic molecules as well.

Most one-dimensional treatments of tunneling in the literature (several examples may be given [264, 265, 303, 304]) neglect the isotopic difference in TS structure and in the effective potential for tunneling. This makes barrier dimensions derived from them very unreliable. Tunneling permits $H\cdot$, H^+, or H^- to be transferred at larger C–C separations than would otherwise be the case. Although D also tunnels, the effect is significantly smaller. An obvious experimental consequence may be larger steric effects on D transfer than on H transfer. That is, unusually large kinetic isotope effects may be observed in reactions subject to steric hindrance. This effect has been observed [305, 306] although it has been explained in other ways.

Chapter VIII treats k_H/k_D and its analogues for other isotopes in some detail. Using Eq. (37) we can write this as $\exp[-\Delta G_H^{a,0} - \Delta G_D^{a,0})/RT]$, and then Eqs. (31) and (105) yield

$$k_H/k_D = (\gamma_H^{\ddagger/Y}/\gamma_D^{\ddagger/Y})(\Gamma_H/\Gamma_D)(\kappa_H^{\ddagger/Y}/\kappa_D^{\ddagger/Y})(k_H^{\ddagger}/k_D^{\ddagger}) \tag{139}$$

Most common treatments include only the last factor of Eq. (139) or the last two factors with the transmission coefficients calculated from an isotopically independent potential curve. There are several possible sources of error in such a treatment: (1) The best dividing surface does not in general pass through the saddle point, and for this reason the last factor may be a poor representation of the nontunneling equilibrium kinetic isotope effect. (2) The commonly employed treatments of tunneling may not be a good representation of the tunneling factor in the KIE, because in many cases most of the tunneling does not occur directly under the potential energy saddle, nor does it occur along the same paths for H and D. (3) and (4) Both $\gamma^{\ddagger}$ and $\Gamma^{\ddagger}$ are isotopically sensitive, although little is known in general about the effect of deuterium substitution on recrossing and reactive state depletion for reactions in solution. All of these effects are larger for hydrogen KIEs than for others because hydrogen KIEs are themselves the largest. However, it is not certain that heavier-atom kinetic isotope effects can be interpreted with any greater security. All of this suggests that KIEs should be interpreted with caution.

6 CONCLUDING REMARKS

We hope that the material presented here demonstrates the continued vitality of TST in interpreting rate constants. We have also tried to illustrate the considerable progress which has recently been made, both in improving the basic theory and in obtaining useful approximations. In several areas, notably in dealing with reactions having large reaction-path curvature, our current understanding is changing rapidly. Perhaps because of the quasi-thermodynamic formulation, there has been a tendency among some experimentalists to regard TST as an immutable part of the theoretical landscape, like equilibrium thermo-

dynamics. It is not. It is a part of dynamics, not thermodynamics. It rests on a cleverly chosen set of approximations, not on an exact derivation. It is very important that users should be aware of the nature of these approximations and their possible effects on the derived quantities. Nature provides us, in experimental results, with the output of the ultimate analogue computer, but gives no direct account of the mechanism by which this output is produced. By making a semiempirical model reproduce the experimental output at as many points as possible, we obtain an approximation to nature's "program." The goal, as in all program writing, is to find and eliminate the bugs.

ACKNOWLEDGMENTS

We thank the U.S. National Science Foundation and Department of Energy, Office of Basic Energy Sciences, for support through grant no. CHE82-15014 and contract no. DE-AC02-79ER10425, respectively. M.M.K. thanks the Henkel Corporation Research Laboratories for hospitality while this chapter was in preparation.

References

1. S. Glasstone, K. Laidler, and H. Eyring, *The Theory of Rate Processes*, McGraw-Hill, New York, 1941.
2. K. Denbigh, *The Principles of Chemical Equilibrium*, 3rd ed., Cambridge University Press, London, p. 443, (a) p. 376, (b) p. 404.
3. B. Widom, *Science*, **148**, 1555 (1965).
4. R. K. Boyd, *Chem. Rev.*, **77**, 93 (1977).
5. C. Lim and D. G. Truhlar, *J. Chem. Phys.*, **79**, 3296 (1983).
6. E. F. Greene and A. Kuppermann, *J. Chem. Educ.*, **45**, 361 (1968).
7. W. C. Gardiner, Jr., *Rates and Mechanisms of Chemical Reactions*, W. A. Benjamin, Menlo Park, CA, 1969, pp. 82ff.
8. M. A. Eliason and J. O. Hirschfelder, *J. Chem. Phys.*, **30**, 1426 (1959).
9. R. N. Porter, M. Karplus, and R. D. Sharma, *J. Chem. Phys.*, **43**, 3259 (1965).
10. R. E. Weston and H. E. Schwarz, *Chemical Kinetics*, Prentice-Hall, Englewood Cliffs, NJ, 1972, pp. 94–95, (a) pp. 95–99, (b) p. 152, (c) p. 265, (d) pp. 155ff, (e) pp. 205ff.
11. W. H. Miller, *J. Chem. Phys.*, **61**, 1823 (1974).
12. G. C. Schatz and A. Kuppermann, *J. Chem. Phys.*, **65**, 4668 (1976).
13. D. G. Truhlar and J. T. Muckerman, in R. B. Bernstein, Ed., *Atom–Molecule Collision Theory*, Plenum, New York 1979, p. 505.
14. V. Khare, D. J. Kouri, J. Jellinek, and M. Baer, in D. G. Truhlar, Ed., *Potential Energy Surfaces and Dynamics Calculations*, Plenum, New York, 1981, p. 475.
15. I. Mayer, *J. Chem. Phys.*, **59**, 2564 (1974).
16. J. B. Anderson, *J. Chem. Phys.*, **59**, 2566 (1974).
17. R. C. Tolman, *The Principles of Statistical Mechanics*, Oxford University Press, New York, 1938, pp. 48ff. See also pp. 335 ff., (a) pp. 92f.
18. H. Goldstein, *Classical Mechanics*, Addison-Wesley, Reading, MA, 1950, pp. 266ff.
19. L. D. Landau and E. M. Liftshitz, *Statistical Physics*, Part I, 3rd ed., Pergamon Press, New York, 1980, pp. 9ff., (a) p. 145.

20. D. A. McQuarrie, *Statistical Mechanics*, Harper and Row, New York, 1976, pp. 117ff., (a) p. 82, (b) p. 266, (c) pp. 456ff., (d) pp. 452ff., (e) p. 121, (f) p. 216, (g) pp. 467ff.
21. J. B. Anderson, *J. Chem. Phys.*, **58**, 4684 (1973).
22. J. B. Anderson, *J. Chem. Phys.*, **62**, 2446 (1975).
23. R. D. Present and B. M. Morris, *J. Chem. Phys.*, **50**, 151 (1969).
24. C. Lim and D. G. Truhlar, *J. Phys. Chem.*, **89**, 5 (1985).
25. E. Wigner, *Trans. Faraday Soc.*, **34**, 29, 70 (1983).
26. D. G. Truhlar and B. C. Garrett, *Acc. Chem. Res.*, **13**, 440 (1980).
27. E. Wigner, *J. Chem. Phys.*, **5**, 720 (1937).
28. J. Horiuti, *Bull. Chem. Soc. Japan*, **13**, 210 (1938).
29. J. C. Keck, *J. Chem. Phys.*, **32**, 1035 (1960).
30. J. C. Keck, *Adv. Chem. Phys.*, **13**, 85 (1967).
31. B. C. Garrett and D. G. Truhlar, *J. Phys. Chem.*, **83**, 1052, 3058 (E) (1979); **87**, 4553 (E) (1983).
32. B. H. Mahan, *J. Chem. Educ.*, **51**, 709 (1974).
33. P. Pechukas, in W. H. Miller, Ed., *Dynamics of Molecular Collisions, Part B*, Plenum, New York, 1976, p. 269.
34. T. L. Hill, *An Introduction to Statistical Thermodynamics*, Addison-Wesley, Reading, MA, 1960, p. 77, (a) p. 313, (b) p. 89.
35. D. G. Truhlar, *J. Phys. Chem.*, **83**, 188 (1979).
36. B. C. Garrett and D. G. Truhlar, *J. Chem. Phys.*, **70**, 1593 (1979).
37. B. C. Garrett and D. G. Truhlar, *J. Phys. Chem.*, **83**, 1079 (1979); **83**, 682(E) (1980); **87**, 4553(E) (1983).
38. B. C. Garrett and D. G. Truhlar, *J. Am. Chem. Soc.*, **101**, 4534 (1979).
39. B. C. Garrett and D. G. Truhlar, *J. Chem. Phys.*, **72**, 3460 (1980).
40. B. C. Garrett and D. G. Truhlar, *J. Phys. Chem.*, **84**, 805 (1980).
41. B. C. Garrett, D. G. Truhlar, R. S. Grev, and A. W. Magnuson, *J. Phys. Chem.*, **84**, 1730 (1980); **87**, 4554(E) (1983).
42. B. C. Garrett, D. G. Truhlar, and R. S. Grev, *J. Phys. Chem.*, **85**, 1569 (1981).
43. D. G. Truhlar, A. D. Isaacson, R. T. Skodje, and B. C. Garrett, *J. Phys. Chem.* **86**, 2252 (1982); **87**, 4554(E) (1983).
44. A. D. Isaacson and D. G. Truhlar, *J. Chem. Phys.*, **76**, 1380 (1982).
45. B. C. Garrett, D. G. Truhlar, A. F. Wagner, and T. H. Dunning, Jr., *J. Chem. Phys.*, **78**, 4400 (1983).
46. S. N. Rai and D. G. Truhlar, *J. Chem. Phys.*, **79**, 6046 (1983).
47. D. G. Truhlar, A. D. Isaacson, and B. C. Garrett, in M. Baer, Ed., *The Theory of Chemical Reaction Dynamics*, Vol. 4, CRC Press, Boca Raton, FL, in press.
48. D. G. Truhlar and B. C. Garrett, *Annu. Rev. Phys. Chem.*, **35**, 159 (1984).
49. D. G. Truhlar and A. Kuppermann, *J. Am. Chem. Soc.*, **93**, 1840 (1971).
50. K. Fukui, in R. Daudel and B. Pullman, Eds., *The World of Quantum Chemistry*, Dordrecht, The Netherlands, 1974, p. 113.
51. K. Fukui, S. Kato, and H. Fujimoto, *J. Am. Chem. Soc.*, **97**, 1 (1975).
52. K. Fukui, *Acc. Chem. Res.*, **14**, 363 (1981).
53. H. F. Schaefer III, *Chem. Brit.*, **11**, 227 (1975).
54. D. G. Truhlar and A. Kuppermann, *J. Chem. Phys.*, **56**, 2232 (1972).
55. L. Hofacker, *Z. Naturforsch.*, **18a**, 607 (1963).
56. R. A. Marcus, *J. Chem. Phys.*, **45**, 4493 (1966).
57. R. A. Marcus, *J. Chem. Phys.*, **46**, 959 (1967).

58. R. A. Marcus, *Discuss. Faraday Soc.*, **44**, 7, 87, 90 (1968).
59. M. S. Child, *Discuss. Faraday Soc.*, **44**, 68 (1968).
60. D. G. Truhlar and A. Kuppermann, *Chem. Phys. Lett.*, **9**, 269 (1971).
61. D. G. Truhlar, *J. Chem. Phys.*, **53**, 2041 (1970).
62. R. A. Marcus and M. E. Coltrin, *J. Chem. Phys.*, **67**, 2609 (1977).
63. B. C. Garrett and D. G. Truhlar, *J. Phys. Chem.*, **83**, 200, 3058(E) (1979).
64. W. H. Miller, N. C. Handy, and J. E. Adams, *J. Chem. Phys.*, **72**, 99 (1980).
65. B. C. Garrett, D. G. Truhlar, R. S. Grev, and R. B. Walker, *J. Chem. Phys.*, **73**, 235 (1980).
66. B. C. Garrett, D. G. Truhlar, and A. W. Magnuson, *J. Chem. Phys.*, **74**, 1029 (1981).
67. B. C. Garrett, D. G. Truhlar, and A. W. Magnuson, *J. Chem. Phys.*, **76**, 2321 (1982).
68. R. T. Skodje, D. G. Truhlar, and B. C. Garrett, *J. Phys. Chem.*, **85**, 3019 (1981).
69. R. T. Skodje, D. G. Truhlar, and B. C. Garrett, *J. Chem. Phys.*, **77**, 5955 (1982).
70. C. J. Cerjan, S. Shi, and W. H. Miller, *J. Chem. Phys.*, **76**, 2244 (1982).
71. R. A. Marcus, in S. Bruckenstein, J. D. E. McIntyre, B. Miller, and E. Yeager, Eds., *Proceedings of the Third Symposium on Electrode Processes, 1979* (Electrochemical Society, Princeton, N.J., 1980), p. 1.
72. V. K. Babamov and R. A. Marcus, *J. Chem. Phys.*, **74**, 1790 (1978).
73. V. K. Babamov, V. Lopez, and R. A. Marcus, *J. Chem. Phys.*, **78**, 5621 (1983).
74. D. K. Bondi, J. N. L. Connor, B. C. Garrett, and D. G. Truhlar, *J. Chem. Phys.*, **78**, 5981 (1983).
75. B. C. Garrett and D. G. Truhlar, *J. Chem. Phys.*, **79**, 4931 (1983).
76. A. Kupperman, J. T. Adams, and D. G. Truhlar, *Abstr. Pap. Int. Conf. Phys. Electron. Atom. Collisions, 8th*, 149 (1973).
77. A. Kupperman, *Theor. Chem. Adv. Perspect*, **6A**, 79 (1981).
78. P. J. Robinson and K. A. Holbrook, *Unimolecular Reactions*, Wiley, New York, 1972.
79. W. Forst, *Theory of Unimolecular Reactions*, Academic, New York, 1973.
80. W. L. Hase, in W. H. Miller, Ed., *Dynamics of Molecular Collisions, Part B*, Plenum, New York, 1976, p. 121.
81. M. Quack and J. Troe, in P. G. Ashmore and R. J. Donovan, Eds., *Specialist Periodical Report on Gas Kinetics and Energy Transfer*, Vol. 2, Chemical Society, London, 1977, p. 175.
82. H. M. Frey and R. Walsh, in P. G. Ashmore and R. J. Donovan, Eds., *Specialist Periodical Report on Gas Kinetics and Energy Transfer*, Vol. 3, Chemical Society, London, 1978, p. 1.
83. W. J. Chesnavich and M. T. Bowers, in M. T. Bowers, Ed., *Gas Phase Ion Chemistry*, Vol. 1, Academic, New York, 1979, p. 119.
84. M. Quack and J. Troe, *Theor. Chem. Adv. Perspect.*, **6B**, 199 (1981).
85. W. L. Hase, in D. G. Truhlar, Ed., *Potential Energy Surfaces and Dynamics Calculations*, Plenum, New York, 1981, p. 1.
86. W. L. Hase, *Acc. Chem. Res.*, **16**, 258 (1983).
87. R. A. Marcus, *J. Chem. Phys.*, **20**, 359 (1952).
88. J. L. Magee, *Proc. Natl. Acad. Sci. USA*, **38**, 764 (1952).
89. J. C. Giddings and H. Eyring, *J. Chem. Phys.*, **22**, 538 (1954).
90. M. Quack and J. Troe, *Ber. Bunsenges. Phys. Chem.*, **81**, 329 (1977).
91. M. J. Stern, W. A. van Hook, and M. Wolfsberg, *J. Chem. Phys.*, **39**, 3179 (1963).
92. S. G. Entelis, *Reaction Kinetics in the Liquid Phase*, Halsted Press, New York, 1976.
93. S. W. Benson and D. M. Golden, in H. Eyring, Ed., *Physical Chemistry, An Advanced Treatise, Volume VII, Reactions in Condensed Phases*, Academic, New York, 1975, p. 58.
94. E. Buncel and H. Wilson, *Acc. Chem. Res.*, **12**, 42 (1979).

95. E. Buncel and H. Wilson, *J. Chem. Educ.*, **57**, 629 (1980).
96. C. Reichardt, *Solvent Effects in Organic Chemistry*, Verlag Chemie, Weinheim and New York, 1979.
97. B. Perlmutter-Hayman, *Progr. Reaction Kinet.*, **6**, 239 (1971).
98. H. A. Kramers, *Physica* (The Hague), **7**, 284 (1940).
99. S. Chandrasekhar, *Rev. Mod. Phys.*, **15**, 1 (1943).
100. E. E. Nikitin, *Theory of Elementary Atomic and Molecular Processes in Gases*, Clarendon Press, Oxford, 1974, pp. 283ff., (a) pp. 305ff.
101. R. F. Grote and J. T. Hynes, *J. Chem. Phys.*, **74**, 4465 (1981).
102. R. F. Grote and J. T. Hynes, *J. Chem. Phys.*, **75**, 2191 (1981).
103. G. van der Zwan and J. T. Hynes, *J. Chem. Phys.*, **77**, 1295 (1982).
104. B. M. Ladanyi and J. T. Hynes, *J. Chem. Phys.*, **77**, 4739 (1982).
105. P. G. Wolynes, *Phys. Rev. Lett.*, **47**, 968 (1981).
106. H. Mori, *Prog. Theor. Phys.*, **33**, 423 (1965).
107. R. Kubo, *Kep. Prog. Theor. Phys.*, **29**, 255 (1966).
108. S. A. Adelman and J. D. Doll, *Acc. Chem. Res.*, **10**, 378 (1977).
109. S. A. Adelman, *Adv. Chem. Phys.*, **44**, 143 (1980).
110. J. C. Tully, *J. Chem. Phys.*, **73**, 1975 (1980).
111. G. van der Zwan and J. T. Hynes, *J. Chem. Phys.*, **78**, 4174 (1983).
112. C. Blomberg, *Physica*, **86A**, 49 (1977).
113. M. R. Pear and J. H. Weiner, *J. Chem. Phys.*, **69**, 785 (1978).
114. E. Helfand, *J. Chem. Phys.*, **54**, 4651 (1971).
115. H. C. Brinkman, *Physica (Utrecht)*, **22**, 149 (1956).
116. R. Landauer and J. A. Swanson, *Phys. Rev.*, **121**, 1668 (1961).
117. N. Takeyama, *Experientia*, **17**, 425 (1971).
118. R. F. Grote and J. T. Hynes, *J. Chem. Phys.*, **73**, 2715 (1980).
119. A. D. Osborne, H. J. V. Tyrrell, and M. Zaman, *Trans. Faraday Soc.*, **60**, 395 (1964).
120. C. -M. Hu and R. Zwanzig, *J. Chem. Phys.*, **60**, 4354 (1974).
121. M. A. Lauffer, *J. Chem. Educ.*, **58**, 250 (1981).
122. R. F. Grote, G. van der Zwan, and J. T. Hynes, *J. Phys. Chem.*, **88**, 4676 (1984).
123. J. T. Hynes, in M. Baer, Ed., *The Theory of Chemical Reaction Dynamics*, Vol. 4, CRC Press, Boca Raton, FL, in press.
124. J. L. Skinner and P. G. Wolynes, *J. Chem. Phys.*, **72**, 4913 (1980).
125. G. T. Evans, *J. Chem. Phys.*, **78**, 4963 (1983).
126. P. G. Wolynes, *Phys. Rev. Lett.*, **47**, 968 (1981).
127. J. H. Weiner and R. E. Forman, *Phys. Rev. B*, **10**, 325 (1974).
128. R. A. Harris and R. Silbey, *J. Chem. Phys.*, **78**, 7330 (1983).
129. D. G. Truhlar, W. L. Hase, and J. T. Hynes, *J. Phys. Chem.*, **87**, 2664, 5523(E) (1983).
130. V. K. Babamov, V. Lopez, and R. A. Marcus, *Chem. Phys. Lett.*, **101**, 507 (1983).
131. M. L. Dutton, D. L. Bunker, and H. H. Harris, *J. Phys. Chem.*, **76**, 2614 (1972).
132. J. Troe, in W. Jost, Ed., *Physical Chemistry: An Advanced Treatise*, *Volume VIB*, *Kinetics of Gas Reactions*, Academic, New York, p. 835.
133. J. Troe, in H. Kelm, Ed., *High Pressure Chemistry*, D. Reidel, Dordrecht, The Netherlands, 1978, p. 489.
134. D. K. Garrity and J. L. Skinner, *Chem. Phys. Lett.*, **95**, 46 (1983).
135. D. W. Oxtoby, *Adv. Chem. Phys.*, **47**, 487 (1981).

136. P. B. Visscher, *Phys. Rev. B*, **13**, 3272 (1976).
137. J. L. Skinner and P. G. Wolynes, *J. Chem. Phys.*, **69**, 2143 (1978).
138. E. F. Caldin, *Fast Reactions in Solution*, Blackwell, Oxford, 1964, pp. 10ff.
139. S. H. Lin, K. P. Li, and H. Eyring, in H. Eyring, Ed., *Physical Chemistry, An Advanced Treatise, Volume VIII, Reactions in Condensed Phases*, Academic, New York, 1975, p. 1.
140. D. G. Truhlar, *J. Chem. Educ.*, **62**, 104 (1985).
141. D. G. Truhlar and R. E. Wyatt, *Annu. Rev. Phys. Chem.*, **27**, 1 (1976).
142. D. G. Truhlar and R. E. Wyatt, *Adv. Chem. Phys.*, **36**, 141 (1977).
143. B. Liu, *J. Chem. Phys.*, **58**, 1924 (1973).
144. P. Siegbahn and B. Liu, *J. Chem. Phys.*, **68**, 2457 (1978).
145. D. G. Truhlar and C. J. Horowitz, *J. Chem. Phys.*, **68**, 2466 (1978); **71**, 1514 (E) (1979).
146. B. C. Garrett and D. G. Truhlar, *Proc. Natl. Acad. Sci. USA*, **76**, 4755 (1979).
147. B. C. Garrett and D. G. Truhlar, *J. Chem. Phys.*, **72**, 3460 (1980).
148. N. C. Blais, D. G. Truhlar, and B. C. Garrett, *J. Chem. Phys.*, **78**, 2363 (1983).
149. D. K. Bondi, D. C. Clary, J. N. L. Connor, B. C. Garrett, and D. G. Truhlar, *J. Chem. Phys.*, **76**, 4986 (1982).
150. A. A. Westenberg and N. De Haas, *J. Chem. Phys.*, **47**, 1393 (1967).
151. D. N. Mitchell and D. J. LeRoy, *J. Chem. Phys.*, **58**, 3449 (1973).
152. G. C. Schatz and A. Kuppermann, *J. Chem. Phys.*, **65**, 4668 (1976).
153. D. C. Clary, B. C. Garrett, and D. G. Truhlar, *J. Chem. Phys.*, **78**, 777 (1983).
154. B. C. Garrettt and D. G. Truhlar, *J. Am. Chem. Soc.*, **101**, 5207 (1979).
155. B. C. Garrett and D. G. Truhlar, *J. Am. Chem. Soc.*, **102**, 2559 (1980).
156. B. C. Garrett, D. G. Truhlar, and A. W. Magnuson, *J. Chem. Phys.*, **74**, 1029 (1981).
157. B. C. Garrett, D. G. Truhlar, and R. S. Grev, in D. G. Truhlar, Ed., *Potential Energy Surfaces and Dynamics Calculations*, Plenum, New York, 1981, p. 587.
158. B. C. Garrett, D. G. Truhlar, and A. W. Magnuson, *J. Chem. Phys.*, **76**, 2321 (1982).
159. T. Yamamoto, *J. Chem. Phys.*, **33**, 281 (1960).
160. S. F. Fischer and M. A. Ratner, *J. Chem. Phys.*, **57**, 2769 (1972).
161. R. A. Rosenstein, *Ber. Bunsenges. Phys. Chem.*, **77**, 493 (1973).
162. F. H. Stillinger, *Theor. Chem. Adv. Perspect.*, **3**, 178 (1978).
163. D. Chandler, *J. Chem. Phys.*, **68**, 2959 (1978).
164. R. O. Rosenberg, B. J. Berne, and D. Chandler, *Chem. Phys. Lett.*, **75**, 162 (1980).
165. J. A. Montgomery, S. L. Holmgren, and D. Chandler, *J. Chem. Phys.*, **73**, 3688 (1980).
166. S. H. Northrup and J. T. Hynes, *J. Chem. Phys.*, **73**, 2700 (1980).
167. R. Zwanzig, *Annu. Rev. Phys. Chem.*, **16**, 67 (1965).
168. M. P. Allen and P. Schofield, *Mol. Phys.*, **39**, 207 (1980).
169. M. P. Allen, *Mol. Phys.*, **40**, 1073 (1980).
170. R. W. Taft, Jr., E. Price, I. R. Fox, J. C. Lewis, K. K. Anderson, and G. T. Davis, *J. Am. Chem. Soc.*, **85**, 709 (1963).
171. W. J. Albery, *Trans. Faraday Soc.*, **63**, 200 (1967).
172. R. A. More O'Ferrall, *J. Chem. Soc. B*, **1970**, 274.
173. W. D. Jencks, *Chem. Rev.*, **72**, 705 (1972).
174. M. M. Kreevoy and I-S. H. Lee, *J. Am. Chem. Soc.*, **106**, 2550 (1984).
175. W. J. Albery and M. M. Kreevoy, *Adv. Phys. Org. Chem.*, **16**, 87 (1978).
176. K. S. Pitzer, *Quantum Chemistry*, Prentice-Hall, Englewood Cliffs, NJ, 1953, p. 143.
177. E. R. Thornton, *J. Am. Chem. Soc.*, **89**, 2915 (1967).

178. E. K. Thornton and E. R. Thornton, in R. D. Gandaur and R. L. Schowen, Eds., *Transition States in Biochemical Processes*, Plenum, New York, 1978, p. 1.
179. M. C. Evans and M. Polanyi, *Trans. Faraday Soc.*, **34**, 11 (1938).
180. J. E. Leffler, *Science*, **117**, 340 (1953).
181. G. S. Hammond, *J. Am. Chem. Soc.*, **77**, 334 (1955).
182. C. A. Parr and D. G. Truhlar, *J. Phys. Chem.*, **75**, 1844 (1971).
183. R. A. Marcus, *Annu. Rev. Phys. Chem.*, **15**, 155 (1964).
184. R. A. Marcus, *Electrochim. Acta*, **13**, 995 (1968).
185. R. A. Marcus, *J. Phys. Chem.*, **72**, 891 (1968).
186. A. O. Cohen and R. A. Marcus, *J. Chem. Phys.*, **72**, 4249 (1968).
187. W. L. Reynolds and R. A. Lumry, *Mechanisms of Electron Transfer*, Ronald Press, New York, 1966, pp. 149–151.
188. T. W. Newton, *J. Chem. Educ.*, **45**, 571 (1968).
189. W. J. Albery, *Electrode Kinetics*, Clarendon Press, Oxford, 1975, Chapt. 4.
190. J. R. Murdoch and D. E. Magnoli, *J. Am. Chem. Soc.*, **104**, 3792 (1982).
191. A. I. Hassid, M. M. Kreevoy, and T.-M. Liang, *Faraday Symp. Chem. Soc.*, **10**, 69 (1975).
192. R. A. Marcus, *Faraday Symp. Chem. Soc.*, **10**, 60 (1975).
193. N. A. Lewis, *J. Chem. Educ.*, **57**, 478 (1980).
194. W. H. Saunders, Jr., *J. Phys. Chem.*, **86**, 3321 (1982).
195. L. P. Hammett, *Physical Organic Chemistry*, 2nd ed., McGraw-Hill, New York, 1970.
196. J. E. Leffler and E. Grunwald, *Rates and Equilibria of Organic Reactions*, McGraw-Hill, New York, 1963, Chapts. 7–9.
197. J. Hine, *Physical Organic Chemistry*, 2nd ed., McGraw-Hill, New York, 1962, Chapts. 4 and 5.
198. W. P. Jencks, *Catalysis in Chemistry and Enzymology*, McGraw-Hill, New York, 1969, pp. 170ff.
199. A. J. Kresge, *Chem. Soc. Rev.*, **2**, 475 (1973).
200. A. J. Kresge, in E. Caldin and V. Gold, Eds., *Proton Transfer Reactions*, Chapman and Hall, London, 1975. Chapt. 7.
201. R. P. Bell, *Faraday Symp. Chem. Soc.*, **10**, 7 (1975).
202. V. G. Levich, *Adv. Electrochem. Electrochem. Eng.*, **4**, 249 (1966).
203. R. R. Dogonadze, A. M. Kuznetsov, and V. G. Levich, *Electrochim. Acta*, **13**, 1025 (1968).
204. R. R. Doganadze and A. M. Kuznetsov, *J. Res. Inst. Catal. Hokkaido University*, **22**, 93 (1974).
205. M. A. Vorotyntsev, R. R. Dogonadze, and A. M. Kuznetsov, *Elektrokhim.*, **10**, 867 (1974) [English transl.: *Sov. Electrochem.*, **10**, 827 (1974)].
206. R. R. Dogonadze and A. M. Kuznetsov, *Prog. Surf. Sci.*, **6**, 1 (1975).
207. N. Bruniche-Olsen, and J. Ulstrup, *J. Chem. Soc. Faraday Trans. 1*, **75**, 205 (1979).
208. J. Ulstrup, *Charge Transfer Processes in Condensed Media*, Springer-Verlag, Berlin, 1979, Chapts. 4 and 6.
209. E. D. German, A. M. Kuznetsov, and R. R. Dogonadze, *J. Chem. Soc. Faraday Trans. 2*, **76**, 1128 (1980).
210. E. D. German and A. M. Kuznetsov, *J. Chem. Soc. Faraday Trans. 1*, **77**, 397 (1981).
211. R. H. Gurney, *Proc. Roy. Soc.*, **A134**, 137 (1931).
212. W. Libby, *J. Phys. Chem.*, **56**, 863 (1952).
213. M. M. Kreevoy and D. E. Konasewich, *Adv. Chem. Phys.*, **21**, 243 (1972).
214. M. M. Kreevoy and S. Oh, *J. Am. Chem. Soc.*, **95**, 4805 (1973).

215. W. J. Albery, *Annu. Rev. Phys. Chem.*, **31**, 227 (1980).
216. D. J. Hupe and D. Wu, *J. Am. Chem. Soc.*, **99**, 7653 (1977).
217. N. Agmon, *J. Am. Chem. Soc.*, **102**, 2164 (1980).
218. M. M. Kreevoy, in E. Buncel and C. C. Lee, Eds., *Isotopes in Organic Chemistry*, Vol. 2., Elsevier Scientific Publishing Co., Amsterdam, 1976, Chapt. 1.
219. B. G. Cox, N. van Truong, and H. Schneider, *J. Chem. Soc. Perkin Trans. 2*, 515 (1983).
220. D. Hadzi, *Pure Appl. Chem.*, **11**, 435 (1965).
221. M. T. Skoog and W. P. Jencks, *J. Am. Chem. Soc.*, **106**, 7597 (1984).
222. L. Melander, *Arkiv Kimi*, **12**, 291 (1961).
223. A. J. Kresge, *Can. J. Chem.*, **52**, 1897 (1974).
224. F. G. Bordwell and W. J. Boyle, Jr., *J. Am. Chem. Soc.*, **94**, 3907 (1972).
225. G. I. Mackay and D. K. Bohme, *Int. J. Mass. Spectrom. Ion Phys.*, **26**, 327 (1978).
226. W. E. Farneth and J. I. Brauman, *J. Am. Chem. Soc.*, **98**, 7891 (1976).
227. S. A. Chaudhri and K.-D. Asmus, *J. Chem. Soc. Faraday Trans. 1*, **68**, 385 (1972).
228. A. Ohno, T. Shio, H. Yamamato, and S. Oka, *J. Am. Chem. Soc.*, **103**, 2045 (1981).
229. R. M. G. Roberts, D. Ostović, and M. M. Kreevoy, *Faraday Discuss Chem. Soc.*, **74**, 257 (1982).
230. M. F. Powell and T. C. Bruice, *J. Am. Chem. Soc.*, **105**, 7139 (1983).
231. D. Ostović, R. M. G. Roberts, and M. M. Kreevoy, *J. Am. Chem. Soc.*, **105**, 7629 (1983).
232. N. Sutin, *Acc. Chem. Res.*, **15**, 275 (1982).
233. N. Sutin, *Prog. Inorg. Chem.*, **30**, 441 (1983).
234. H. S. Brunschweig, J. Logan, M. D. Newton, and N. Sutin, *J. Am. Chem. Soc.*, **102**, 5798 (1980).
235. M. D. Newton, *Int. Quant. Chem. Symp.*, **14**, 363 (1980).
236. M. D. Newton, in D. B. Rarabacher and J. F. Endicott, Ed., *Mechanistic Aspects of Inorganic Reactions* (ACS Symp. Ser., **198**), American Chemical Society, Washington, D.C., 1982, p. 255.
237. C. Creutz and N. Sutin, in J. J. Zuckerman, Ed., *Inorganic Reactions and Methods*, Springer-Verlag, Berlin, in press.
238. S. Fukuzumi, C. L. Wang, and J. K. Kochi, *J. Am. Chem. Soc.*, **102**, 2928 (1980).
239. R. P. Bell, *The Proton in Chemistry*, 2nd ed., Cornell University Press, Ithaca, NY, 1973, p. 203.
240. F. Hibbert, F. A. Long, and E. A. Walters, *J. Am. Chem. Soc.*, **93**, 2829 (1971).
241. F. Hibbert, *J. Chem. Soc. Perkin Trans. 2*, 1289 (1973).
242. M. M. Kreevoy, J. Dolmar, and J. T. Langland, Abstracts of Papers, 166th National Meeting of the American Chemical Society, Chicago, IL, August 26–31, 1973, Abstract No. PHYS 148.
243. Y. Chiang, A. J. Kresge, and J. Wirz, *J. Am. Chem. Soc.*, **106**, 6392 (1984) and unpublished results.
244. W. R. Davidson, J. Semner, and P. Kebarle, *J. Am. Chem. Soc.*, **101**, 1675 (1979).
245. J. W. Larson and T. B. McMahon, *J. Am. Chem. Soc.*, **105**, 2944 (1983).
246. S. Y. Lam, C. Louis, and R. L. Benoit, *J. Am. Chem. Soc.*, **98**, 1156 (1976).
247. N. Agmon and R. D. Levine, *Chem. Phys. Lett.*, **52**, 197 (1977).
248. R. P. Bell, *J. Chem. Soc., Faraday Trans. 1*, **78**, 2593 (1982).
249. M. M. Kreevoy and T. M. Liang, *J. Am. Chem. Soc.*, **102**, 3315 (1980).
250. F. S. Klein, A. Persky, and R. E. Weston, Jr., *J. Chem. Phys.*, **41**, 1799 (1964).
251. W. R. Schultz and D. J. LeRoy, *J. Chem. Phys.*, **42**, 3869 (1965).

252. J. H. Lee, J. V. Michael, W. A. Payne, L. J. Stief, and D. A. Whytock, *J. Chem. Soc. Faraday Trans. 1*, **73**, 1530 (1977).
253. V. B. Parker, D. D. Wagman, and D. Garni, *Technical Report NBSIR 75-968*, N.B.S., Washington, D.C., 1976.
254. D. G. Truhlar, *J. Chem. Phys.*, **65**, 1008 (1976).
255. A. Persky and F. S. Klein, *J. Chem. Phys.*, **44**, 3617 (1966).
256. D. J. LeRoy, B. A. Ridley, and K. A. Quickert, *Discuss. Faraday Soc.*, **44**, 92 (1968).
257. J. Jaume, J. M. Lluch, A. Oliva, and J. Bertrán, *Chem. Phys. Lett.*, **106**, 232 (1984).
258. C. Langford, in D. B. Rarabacher and J. F. Endicott, Eds., *Mechanistic Aspects of Inorganic Reactions* (ACS Symp. Ser., **198**), American Chemical Society, Washington, D.C., 1982, p. 99.
259. N. Agmon and R. D. Levine, *Israel J. Chem.*, **19**, 330 (1980).
260. L. L. Merritt, Jr., and E. Lanterman, *Acta Crystallogr.*, **5**, 811 (1952).
261. K. Toriyama, K. Nunome, and M. Iwasaki, *J. Am. Chem. Soc.*, **99**, 5823 (1977).
262. G. Brunton, J. A. Gray, D. Griller, L. R. C. Barclay, and K. U. Ingold, *J. Am. Chem. Soc.*, **100**, 4197 (1978).
263. G. Brunton, D. Griller, L. R. C. Barclay, and K. U. Ingold, *J. Am. Chem. Soc.*, **98**, 6803 (1976).
264. R. J. LeRoy, H. Murai, and F. Williams, *J. Am. Chem. Soc.*, **102**, 2325 (1980).
265. R. J. LeRoy, *J. Phys. Chem.*, **84**, 3508 (1980).
266. I-S. H. Lee and D. Ostović, unpublished results.
267. J. S. Blanchard and W. W. Cleland, *Biochem.*, **19**, 3543 (1980); supplementary results by private communication.
268. W. P. Huskey and R. L. Schowen, *J. Am. Chem. Soc.*, **105**, 5704 (1983).
269. B. W. Carlson, L. L. Miller, P. Neta, and J. Grudkowski, *J. Am. Chem. Soc.*, **106**, 7233 (1984).
270. C. K. Ingold, *Structure and Mechanism in Organic Chemistry*, 2nd ed., Cornell University Press, 1969, Chapt. 7.
271. E. S. Lewis and D. D. Hu, *J. Am. Chem. Soc.*, **106**, 3292 (1984).
272. M. J. Pellerite and J. I. Brauman, *J. Am. Chem. Soc.*, **105**, 2672 (1983).
273. S. Wolfe, D. J. Mitchell, and H. B. Schlegel, *J. Am. Chem. Soc.*, **103**, 7694 (1981).
274. E. M. Arnett and R. Reich, *J. Am. Chem. Soc.*, **102**, 5892 (1980).
275. J. M. Harris, M. S. Paley, and T. W. Presthoper, *J. Am. Chem. Soc.*, **103**, 5915 (1981).
276. J. L. Kurz, *Chem. Phys. Lett.*, **57**, 243 (1978).
277. J. R. Murdoch, *J. Am. Chem. Soc.*, **105**, 2667 (1983).
278. S. W. Benson, *Thermochemical Kinetics*, 2nd ed., Wiley, New York, 1976.
279. J. Hine, *J. Am. Chem. Soc.*, **93**, 3701 (1971).
280. J. P. Guthrie and P. A. Cullimore, *Can. J. Chem.*, **58**, 1281 (1980).
281. J. W. Bunting and N. P. Fitzgerald, private communication.
282. J. W. Bunting and D. J. Norris, *J. Am. Chem. Soc.*, **99**, 1189 (1977).
283. C. D. Ritchie, C. Kubisty, and G. Y. Ting, *J. Am. Chem. Soc.*, **105**, 279 (1983).
284. D. L. Hasha, T. Eguchi, and J. Jonas, *J. Chem. Phys.*, **75**, 1571 (1981).
285. D. L. Hasha, T. Eguchi, and J. Jonas, *J. Am. Chem. Soc.*, **104**, 2290 (1982).
286. J. Jonas, in G. C. Levy, Ed., *NMR Spectroscopy: New Methods and Applications* (ACS Symp. Ser., **191**), American Chemical Society, Washington, D.C., 1982, p. 199.
287. E. L. Eliel, N. L. Allinger, S. J. Angyal, and G. A. Morrison, *Conformational Analysis*, American Chemical Society, Washington, 1981, p. 40.
288. J. A. Montgomery, Jr., D. Chandler, and B. J. Berne, *J. Chem. Phys.*, **70**, 4056 (1979).
289. T. Asano and W. J. le Noble, *Chem. Rev.*, **78**, 407 (1978).

290. L. A. Brey, G. B. Schuster, and M. G. Drickamer, *J. Am. Chem. Soc.*, **101**, 129 (1979).
291. J. R. Taylor, M. C. Adams, and W. Sibbett, *J. Photochem.*, **12**, 127 (1980).
292. R. M. Hochstrasser, *Pure Appl. Chem.*, **52**, 2683 (1980).
293. G. Rothenberger, D. K. Negus, and R. M. Hochstrasser, *J. Chem. Phys.*, **79**, 5360 (1983).
294. B. M. Ladanyi and G. T. Evans, *J. Chem. Phys.*, **79**, 944 (1983).
295. G. Bott, L. D. Field, and S. Sternhell, *J. Am. Chem. Soc.*, **102**, 5618 (1980).
296. M. M. Kreevoy, in S. L. Friess, E. S. Lewis, and A. Weissberger, Eds., *Technique of Organic Chemistry*, 2nd ed., Vol. VIII, Part II, Interscience Publishers, New York, 1963, Chapt. XXIII.
297. L. L. Schaleger and F. A. Long, *Adv. Phys. Org. Chem.*, **2**, 1 (1965).
298. R. Lumry, E. Battistel, and C. Jolicoeur, *Faraday Symp. Chem. Soc.*, **17**, 93 (1982).
299. E. S. Amis and J. F. Hinton, *Solvent Effects on Chemical Phenomena*, Vol. I, Academic Press, New York, 1973, Chapt. 5.
300. D. G. Truhlar, R. S. Grev, and B. C. Garrett, *J. Phys. Chem.*, **87**, 3415 (1983).
301. L. J. Bellamy, *The Infra-Red Spectra of Complex Molecules*, Wiley, New York, 1958.
302. I. W. M. Smith, *Kinetics and Dynamics of Elementary Gas Reactions*, Butterworths, London, 1980, pp. 43–44.
303. R. P. Bell, *The Tunnel Effect in Chemistry*, Chapman and Hall, London, 1980, Chapt. 4.
304. L. Melander and W. H. Saunders, Jr., *Reaction Rates of Isotopic Molecules*, Wiley, New York, 1980, Chapt. 5.
305. L. Funderburk and E. S. Lewis, *J. Am. Chem. Soc.*, **86**, 2531 (1964).
306. S. B. Hanna, C. Jermini, and H. Zollinger, *Tetrahedron Lett.*, **1969**, 4415.